NAVAL POSTGRADUATE SCHOOL
Monterey, California

THESIS

A260239

MODELING, SIMULATION, AND ANALYSES OF
ATTITUDE CONTROL FOR THE
CREW/EQUIPMENT RETRIEVER (CER) PROPOSED
FOR
SPACE STATION

by

Daniel L. Hansen

March 1989

Thesis Advisor Jeff B. Burl

Approved for public release; distribution is unlimited.

T241950

lassified

ity classification of this page

REPORT DOCUMENTATION PAGE

Report Security Classification Unclassified		1b Restrictive Markings	
ecurity Classification Authority		3 Distribution Availability of Report	
Declassification Downgrading Schedule		Approved for public release; distribution is unlimited.	
rforming Organization Report Number(s)		5 Monitoring Organization Report Number(s)	
ame of Performing Organization val Postgraduate School	6b Office Symbol *(if applicable)* 39	7a Name of Monitoring Organization Naval Postgraduate School	
ddress *(city, state, and ZIP code)* nterey, CA 93943-5000		7b Address *(city, state, and ZIP code)* Monterey, CA 93943-5000	
ame of Funding Sponsoring Organization	8b Office Symbol *(if applicable)*	9 Procurement Instrument Identification Number	
ddress *(city, state, and ZIP code)*		10 Source of Funding Numbers	
		Program Element No / Project No / Task No / Work Unit Accession No	

Title *(include security classification)* MODELING, SIMULATION, AND ANALYSES OF ATTITUDE CONTROL FOR E CREW EQUIPMENT RETRIEVER (CER) PROPOSED FOR SPACE STATION

Personal Author(s) Daniel L. Hansen

Type of Report	13b Time Covered	14 Date of Report *(year, month, day)*	15 Page Count
ster's Thesis	From To	March 1989	113

Supplementary Notation The views expressed in this thesis are those of the author and do not reflect the official policy or po-on of the Department of Defense or the U.S. Government.

Cosati Codes			18 Subject Terms *(continue on reverse if necessary and identify by block number)*
d	Group	Subgroup	CERS, attitude control, minimum fuel, optimal control, Three-Axis Stabilization, Space Station, Free flyer

Abstract *(continue on reverse if necessary and identify by block number)*

The Crew Equipment Retrieval System (CERS) is proposed for space station to provide the capability to rescue an EVA wman or to retrieve equipment inadvertently detached from the station. This research is directed to model, simulate, and lyze attitude control for the Crew Equipment Retriever (CER) with and without a target during autonomous attitude d. Time-optimal and weighted-time-fuel optimal control laws are derived using Pontryagin's Minimum Principle. The R baseline configuration is analyzed to accomplish some of the attitude control trade-off analyses planned for the CER liminary design phase. Optimal thruster size and placement are evaluated for three-axis stabilization. Control stability en the moment of inertia tensor changes during target capture is evaluated for several worst-case scenarios. Attitude con-l performance results are computed through computer simulation. Simulation of the CER baseline configuration shows oes not provide effective control during capture of a worst-case 850 pound target.

A new CER configuration scheme is proposed, evaluated and compared to the baseline configuration. Fuel optimal and l-of-mission performance for the new CER configuration is evaluated. Simulation of the CER proposed configuration ows it provides effective control during target capture for modified locations in the capture net.

Distribution Availability of Abstract unclassified unlimited ☐ same as report ☐ DTIC users	21 Abstract Security Classification Unclassified	
Name of Responsible Individual f B. Burl	22b Telephone *(include Area code)* (408) 646-2390	22c Office Symbol 62BL

FORM 1473,84 MAR 83 APR edition may be used until exhausted
All other editions are obsolete

security classification of this page

Unclassified

Approved for public release; distribution is unlimited.

Modeling, Simulation, and Analyses of Attitude Control for the Crew Equipment Retriever (CER) Proposed for Space Station

by

Daniel L. Hansen
Lieutenant Commander, United States Navy
B.S., United States Naval Academy, 1977

Submitted in partial fulfillment of the
requirements for the degree of

MASTER OF SCIENCE IN ELECTRICAL ENGINEERING

from the

NAVAL POSTGRADUATE SCHOOL
March 1989

ABSTRACT

The Crew Equipment Retrieval System (CERS) is proposed for space station to provide the capability to rescue an EVA crewman or to retrieve equipment inadvertently detached from the station. This research is directed to model, simulate, and analyze attitude control for the Crew Equipment Retriever (CER) with and without a target during autonomous attitude hold. Time-optimal and weighted-time-fuel optimal control laws are derived using Pontryagin's Minimum Principle. The CER baseline configuration is analyzed to accomplish some of the attitude control trade-off analyses planned for the CER preliminary design phase. Optimal thruster size and placement are evaluated for three-axis stabilization. Control stability when the moment of inertia tensor changes during target capture is evaluated for several worst-case scenarios. Attitude control performance results are computed through computer simulation. Simulation of the CER baseline configuration shows it does not provide effective control during capture of a worst-case 850 pound target.

A new CER configuration scheme is proposed, evaluated and compared to the baseline configuration. Fuel optimal and end-of-mission performance for the new CER configuration is evaluated. Simulation of the CER proposed configuration shows it provides effective control during target capture for modified locations in the capture net.

A210233
C.1

THESIS DISCLAIMER

The reader is cautioned that computer programs developed in this research may not have been exercised for all cases of interest. While every effort has been made, within the time available, to ensure that the programs are free of computational and logic errors, they cannot be considered validated. Any application of these programs without additional verification is at the risk of the user.

TABLE OF CONTENTS

I. INTRODUCTION 1
A. THESIS OBJECTIVES 1
B. CERS CONCEPT DESCRIPTION 1
1. CERS Origin and Purpose 1
2. CERS Overall Mission 1
3. CERS Capabilities 2
4. CERS Major Systems 3
5. CER Baseline Configuration 4
C. THESIS ORGANIZATION 7

II. ATTITUDE DYNAMICS FOR THE CER 9
A. ATTITUDE PARAMETERIZATION 9
1. Parameterization Discussion 9
2. Euler Angles for the CER 9
B. STATE VARIABLE REPRESENTATION 12
C. MOMENT OF INERTIA TENSOR ANALYSIS 14
1. CER Without Target Moments of Inertia 14
2. Target Moments of Inertia 14
3. CER With Target Moments of Inertia 17
D. CONTROL TORQUE ANALYSIS 20

III. ATTITUDE STABILIZATION 24
A. TIME OPTIMAL CONTROL LAW 24
B. WEIGHTED-TIME-FUEL OPTIMAL CONTROL LAW 30
C. DEADBAND CONTROL ABOUT THE ORIGIN 36
D. DISCUSSION OF CONTROL ACCELERATIONS. 38

IV. SIMULATION AND RESULTS 40
A. SIMULATION PROGRAM 40
1. Simulation Block Model 40
2. Simulation Inputs 41

3. Simulation Cases 42
B. BASELINE CONFIGURATION SIMULATION RESULTS 43
C. PROPOSED CONFIGURATION AND SIMULATION RESULTS 46
1. Proposed Configuration 46
2. Proposed Configuration Analysis and Simulation Results 48
3. Proposed Configuration With Baseline Thrusters 50
D. FUEL OPTIMAL ANALYSIS FOR THE PROPOSED CONFIGURATION 50
E. END-OF-MISSION ANALYSIS FOR THE PROPOSED CONFIGURATION 53

V. CONCLUSIONS AND RECOMMENDATIONS 56
A. CONCLUSIONS 56
B. RECOMMENDATIONS 56

APPENDIX A. TUTSIM SIMULATION PROGRAM 58

APPENDIX B. SIMULATION PLOTS 62

LIST OF REFERENCES 100

INITIAL DISTRIBUTION LIST 101

LIST OF FIGURES

Figure 1. CERS Major Components: 3
Figure 2. Mission Sequence of Events; 4
Figure 3. Major Mission Phases (with time-line); 5
Figure 4. Pictorial repesentation of the CERS Overall Mission Profile; 6
Figure 5. CER Attitude Command and Control; 7
Figure 6. CER Baseline Configuration 8
Figure 7. CER Euler Angle Parameterization 10
Figure 8. Skew-Symmetric Matrix 18
Figure 9. Target Capture Case Locations 19
Figure 10. CER Baseline Configuration Moment of Inertia Tensors for Target Capture 21
Figure 11. CER Baseline Thruster Configuration for (+)ROLL 22
Figure 12. Trajectories for U = +Uc and U = -Uc; 28
Figure 13. Trajectories for U = (+-)Uc through the origin; 29
Figure 14. Optimal Trajectories for Different Initial State Values; 30
Figure 15. Trajectories for Uc = 0; 34
Figure 16. Combined Trajectories for U(t) = 0 and U(t) = (+-)Uc; 35
Figure 17. Switching Curves for Weighted-Time-Fuel Optimal Performance; 37
Figure 18. Deadband Control around the Origin. 38
Figure 19. Simulation Block Model of the CER 41
Figure 20. Baseline Configuration Simulation Results 44
Figure 21. Baseline Configuration Simulation Results With Tx = 34, Ty = Tz = 100 (ft-lbf) 47
Figure 22. CER Proposed Configuration 48
Figure 23. CER Proposed Configuration Simulation Results 49
Figure 24. Proposed Configuration Simulation Results Using 1.0 lbf Thrusters . . . 51
Figure 25. Comparison of Minimum-Time and Optimal Fuel (Lambda = 100) Roll Axis Control for "No Target" 52
Figure 26. Fuel Optimal Analysis for Proposed Configuration 54
Figure 27. End-of-Mission Simulation Results for the Proposed Configuration . . . 55
Figure 28. TUTSIM Simulation Program (First Page) 59

Figure 29. TUTSIM Simulation Program (Second Page) 60
Figure 30. TUTSIM Simulation Program (Third Page) 61
Figure 31. Simulation Plots for Baseline No Target 62
Figure 32. Baseline No Target 63
Figure 33. Baseline Case 1A 64
Figure 34. Baseline Case 1A 65
Figure 35. Baseline Case 1B 66
Figure 36. Baseline Case 1B 67
Figure 37. Baseline Case 1C 68
Figure 38. Baseline Case 1C 69
Figure 39. Baseline Case 1D 70
Figure 40. Baseline Case 1D 71
Figure 41. Baseline Case 2 72
Figure 42. Baseline Case 2 73
Figure 43. Proposed No Target 74
Figure 44. Proposed No Target 75
Figure 45. Proposed Optimal (L = 100) No Target 76
Figure 46. Proposed Optimal (L = 100) No Target 77
Figure 47. Proposed Case 1A 78
Figure 48. Proposed Case 1A 79
Figure 49. Proposed Case 1B 80
Figure 50. Proposed Case 1B 81
Figure 51. Proposed Case 1C 82
Figure 52. Proposed Case 1C 83
Figure 53. Proposed Case 1C.1 84
Figure 54. Proposed Case 1C.1 85
Figure 55. Proposed Case 1D 86
Figure 56. Proposed Case 1D 87
Figure 57. Proposed Case 2 88
Figure 58. Proposed Case 2 89
Figure 59. Proposed Case 1A End of mission 90
Figure 60. Proposed Case 1A End of Mission 91
Figure 61. Proposed Case 1B End of Mission 92
Figure 62. Proposed Case 1B End of Mission 93
Figure 63. Proposed Case 1C.1 End of Mission 94

Figure 64. Proposed Case 1C.1 End of Mission 95
Figure 65. Proposed Case 1D End of Mission 96
Figure 66. Proposed Case 1D End of Mission 97
Figure 67. Proposed Case 2 End of Mission 98
Figure 68. Proposed Case 2 End of Mission 99

ACKNOWLEDGEMENTS

I would like to thank John Harduvel of McDonnell Douglas Astronautics Company Space Station Division for his knowledgable support of this research and for sending the data on the CER. I give special thanks to Professor Jeff Burl, for his patience and instructive guidance as my thesis advisor. I would also like to thank CAPT Terry Lackey, USN, for his support of my endeavors to become the first "Air Boss" on Space Station. To Sherry, Jason, Bill and Matt, thank you for understanding the many hours we were apart and for all your love and support. I dedicate this thesis to you.

I. INTRODUCTION

A. THESIS OBJECTIVES

The overall objective of this thesis is to model, simulate, and analyze attitude control for the Crew Equipment Retriever or "CER" with and without a target during autonomous attitude hold for all mission phases [Ref. 1: p. 1].

Specifically, the CER baseline configuration is analyzed and the following trade analyses are accomplished:

- Optimal thruster size and placement.
- Control stability when the moment of inertia tensor changes for the total system during capture of a target (maximum 850 pounds).
- Optimal fuel performance.
- End of mission control performance.

B. CERS CONCEPT DESCRIPTION

1. CERS Origin and Purpose

In May 1987 the National Aeronautics and Space Administration (NASA), Johnson Space Center Space Station Projects Office sent out a "Request for Proposal" (RFP) as part of Space Station Work Package 2.[Ref. 2 : p. L-2-14a] The RFP (including an added Amendment 7) defined requirements to provide the capability to rescue an incapacitated EVA (external-vehicular activity) crewman and to retrieve equipment inadvertantly detached from Space Station.

McDonnell Douglas Astronautics Company (MDAC) responded to the RFP with the Crew Equipment Retrieval System or "CERS", a practical, low cost retriever concept in September 1987.[Ref. 1: p. i] Funding for CERS is predicted for Spring 1989 and the conclusions and recommendations of this research will hopefully assist Johnson Space Center and MDAC in completing some of the attitude control trade-off analyses planned for the CERS preliminary design phase.

2. CERS Overall Mission

The CERS includes the following components:

1. A crew and equipment retriever (CER) vehicle.
2. A retriever support station (RSS).
3. A retriever berthing station (RBS).

4. Supporting Space Station capabilities.

The major components of the system are shown in Figure 1 on page 3. [Ref. 1: p. 15] The CER is remotely commanded from inside Space Station by the retriever operator or the Station Traffic Management System depending on the mission phase.

The mission sequence of events is shown in Figure 2 on page 4 [Ref. 1 : p. 8]. The major mission events are further subdivided into nine phases:

1. Pre-mission Phase (Storage and Standby Mode)
2. Mission Phase-1 (Target Departure and Acquisition)
3. Mission Phase-2 (CER Deployment and Rendezvous Initiation)
4. Mission Phase-3 (Target Rendezvous Completion)
5. Mission Phase-4 (Target Capture and Station Rendezvous Initiation)
6. Mission Phase-5 (Station Rendezvous Completion)
7. Mission Phase-6 (Terminal CER Operations)
8. Mission Phase-7 (Airlock Ingress)
9. Post-Mission Phase (CER Refurbishment)

The major mission phases are shown with a time-line in Figure 3 on page 5 and a pictorial representation of the overall mission profile is shown in Figure 4 on page 6. [Ref. 1: pp. 5-6,17]

3. CERS Capabilities

CERS was proposed as a quick-response design and a summary of its more important capabilities are listed as follows:[Ref. 1: p. 9]

- Retrieve an 850 pound target (includes a 10% safety margin), defined as a lost crewmember or equipment.
- Retrieve and deposit target into airlock within 120 minutes of deployment.
- Retriever can be activated and deployed without the assistance of an EVA crewman.
- Retriever senses own attitude, range and range rate to target, and relays information to station.
- Retriever can be remotely controlled from any command and control station in the Space Station.
- Accomodates a worst-case target separation of 3.5 ft/sec.
- Retriever senses and controls its own attitude with and without a target.
- Has attitude hold and three-axis translation capability.

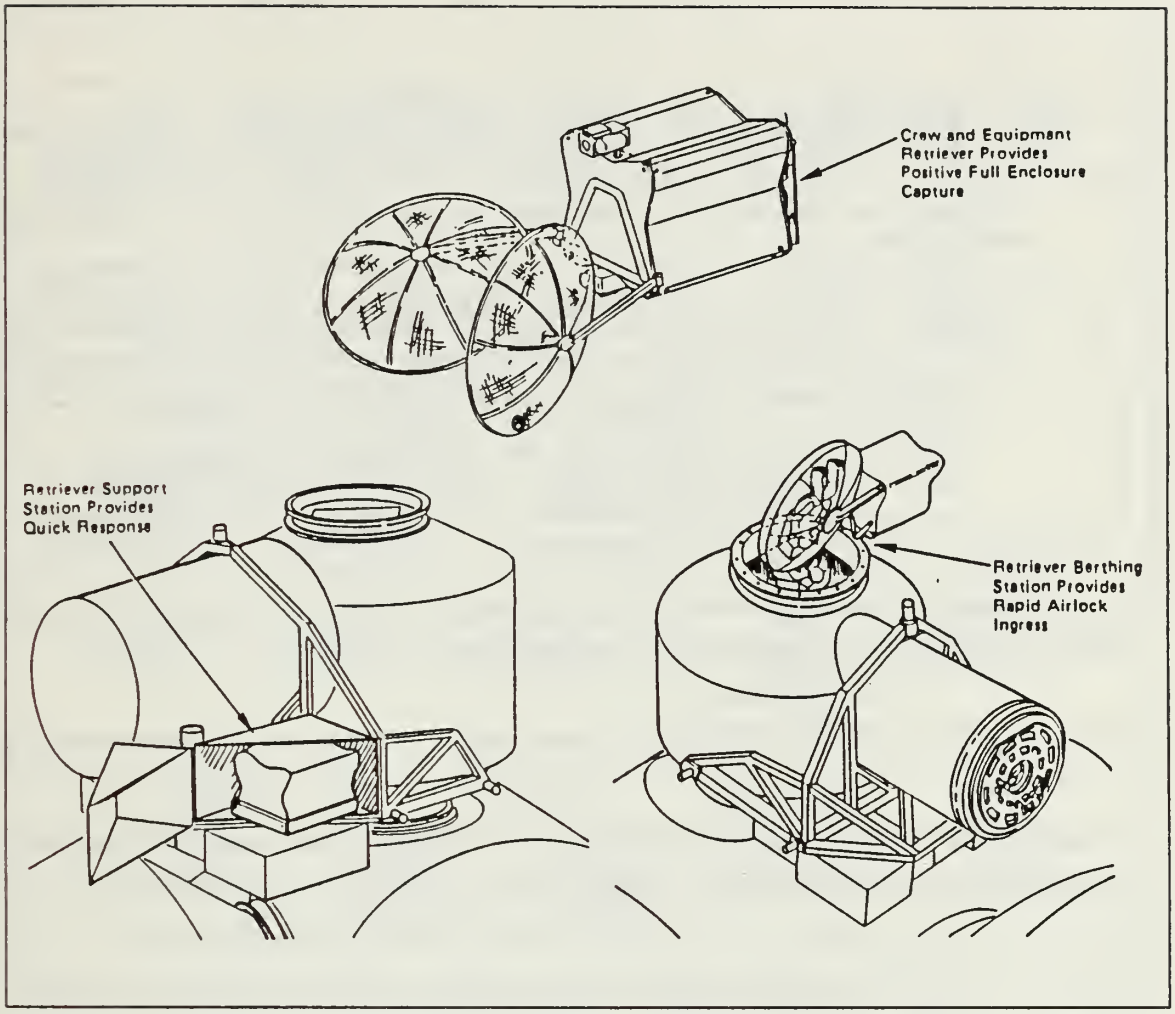

Figure 1. CERS Major Components; From [Ref. 1 : p. 15]

4. CERS Major Systems

CERS major systems are described in detail in Ref. 1 (pp. 20-68). The Avionics system is of particular interest as it contains hardware and software required to perform attitude control, attitude determination and command, control and monitoring functions (among other important functions). Attitude reference determination for CERS is well established and detailed in Ref. 1 (p. 25) and will not be discussed further.

Attitude control of the Crew/Equipment Retriever (CER) is based on a simple switchline control system that maintains the attitude within a specified deadband about the commanded attitude. Once the target is acquired, the control system uses a closed loop television tracking processor along with tele-operator commands to orient the CER

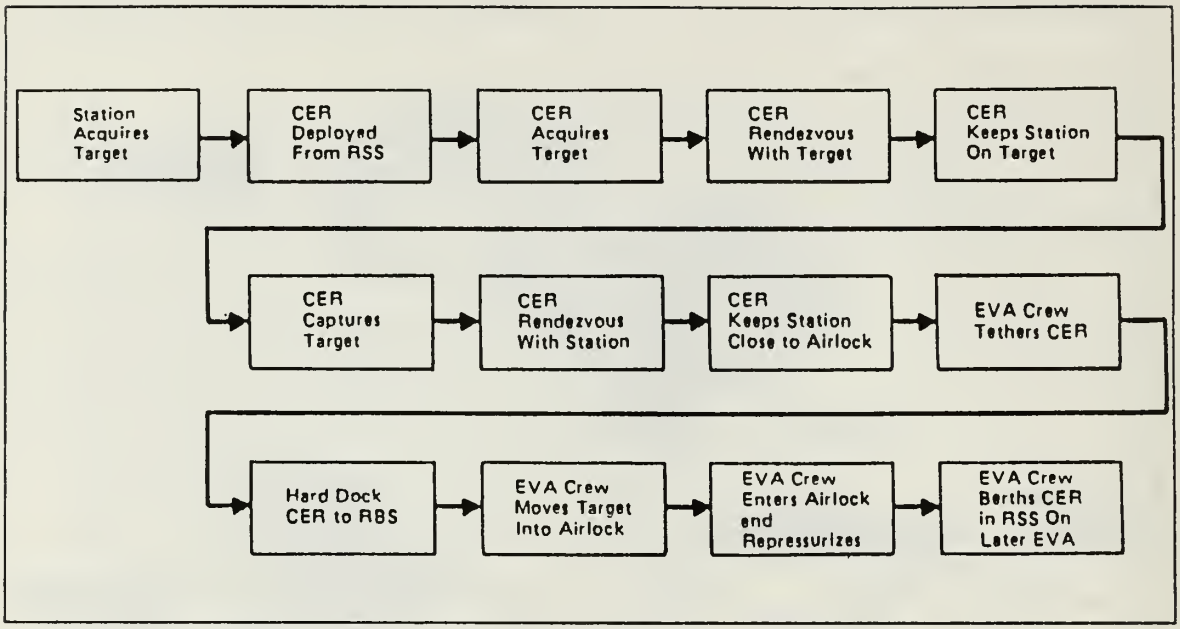
Station Acquires Target
CER Deployed From RSS
CER Acquires Target
CER Rendezvous With Target
CER Keeps Station On Target
CER Captures Target
CER Rendezvous With Station
CER Keeps Station Close to Airlock
EVA Crew Tethers CER
Hard Dock CER to RBS
EVA Crew Moves Target Into Airlock
EVA Crew Enters Airlock and Repressurizes
EVA Crew Berths CER in RSS On Later EVA

Figure 2. Mission Sequence of Events; From [Ref. 1 : p. 8]

as needed for the specific mission phase. The control system approach is shown in Figure 5 on page 7.

Velocity control required for the CER to complete rendezvous with the target, to zero relative velocity when approaching close to the target, and to rendezvous with the Station is commanded by the Station Traffic Management System [Ref. 1: p. 28]. Discussion of the CER velocity adjustments required to initiate and maintain *translation* to achieve rendezvous are *not* included in this research.

5. CER Baseline Configuration

The initial CER baseline configuration proposed to provide the desired performance characteristics during all mission phases is represented by Figure 6 on page 8. This simple box shape representation of the CER will be used to simplify the calculations describing its attitude dynamics.

The characteristics of the baseline configuration that will be used in the analysis of the CER attitude control performance are listed as follows: [Ref. 1: p. 24]

- 850 pounds total weight (combined weight of capture arms and nets assumed negligible for computation purposes).
- Three-axis (six degrees of freedom) stabilized remote tele-operated free flyer.
- Uses 24 cold Nitrogen gas (N_2) jet thrusters (two separate redundant systems) rated at 1.0 lbf.

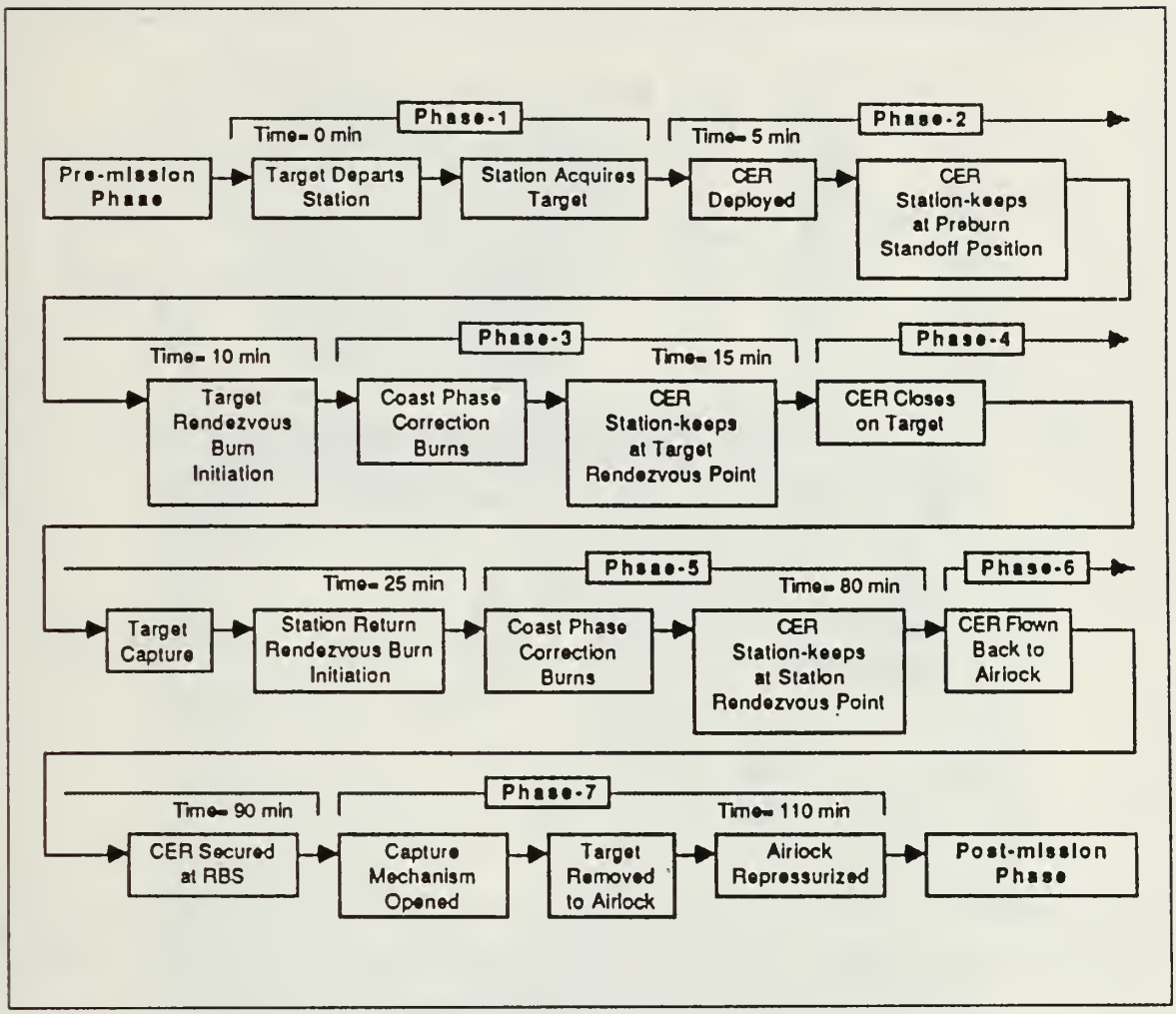

Figure 3. Major Mission Phases (with time-line); From [Ref. 1 : p. 17]

- Attitude control accomplished by firing thrusters in pairs to produce couples about any of the three orthogonal axes.
- Summation of control torques ($T = \vec{r} \times F$):

$$(+\text{-})\text{ROLL} \sum T_x = 3 \text{ (ft-lbf)} \tag{1.1}$$

$$(+\text{-})\text{PITCH} \sum T_y = 3 \text{ (ft-lbf)} \tag{1.2}$$

$$(+\text{-})\text{YAW} \sum T_z = 4 \text{ (ft-lbf)} \tag{1.3}$$

- Moment of Inertia Tensor $[I_{TOT}]$ (No Target):

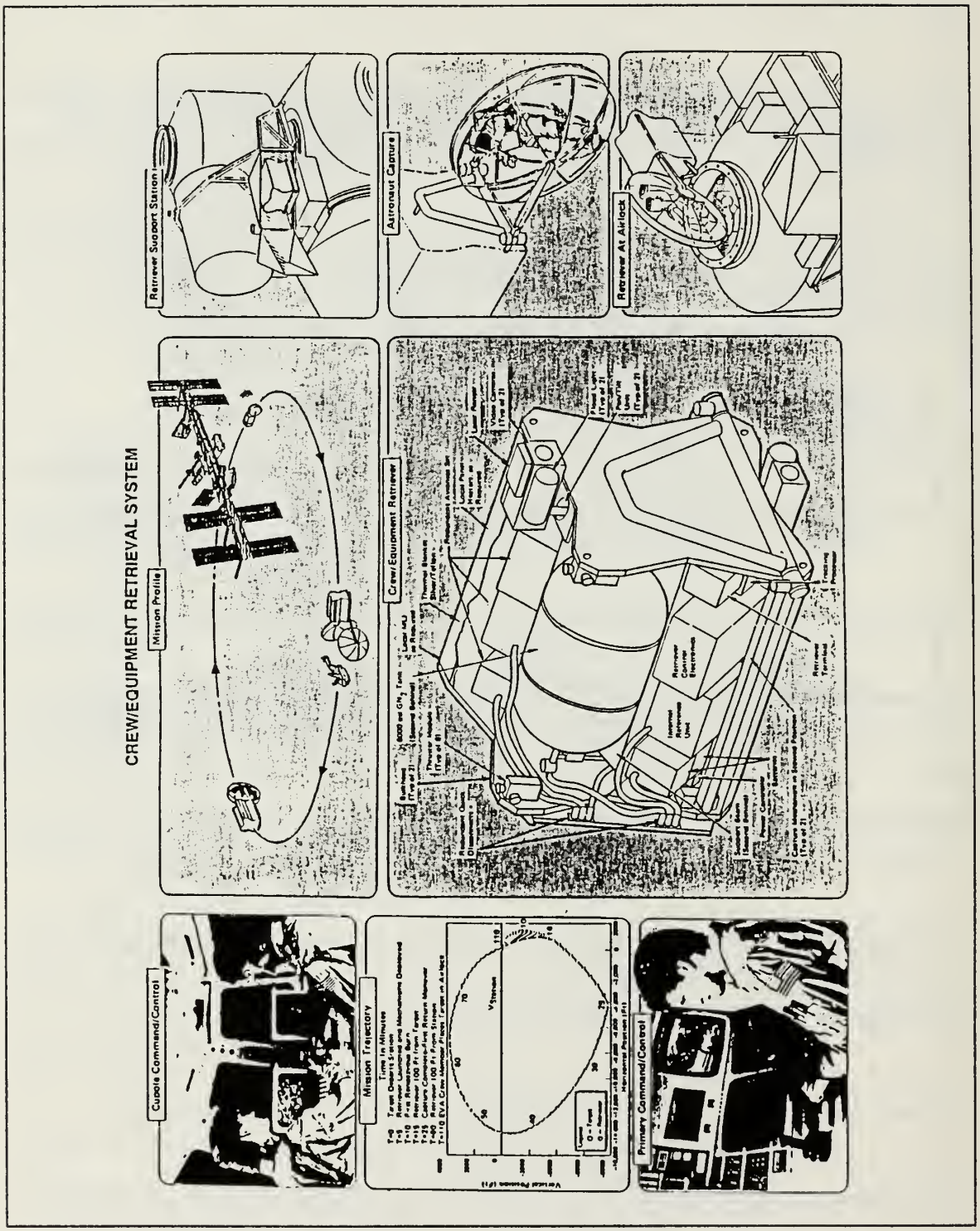

Figure 4. Pictorial repesentation of the CERS Overall Mission Profile; From [Ref. 1 : pp. 5-6]

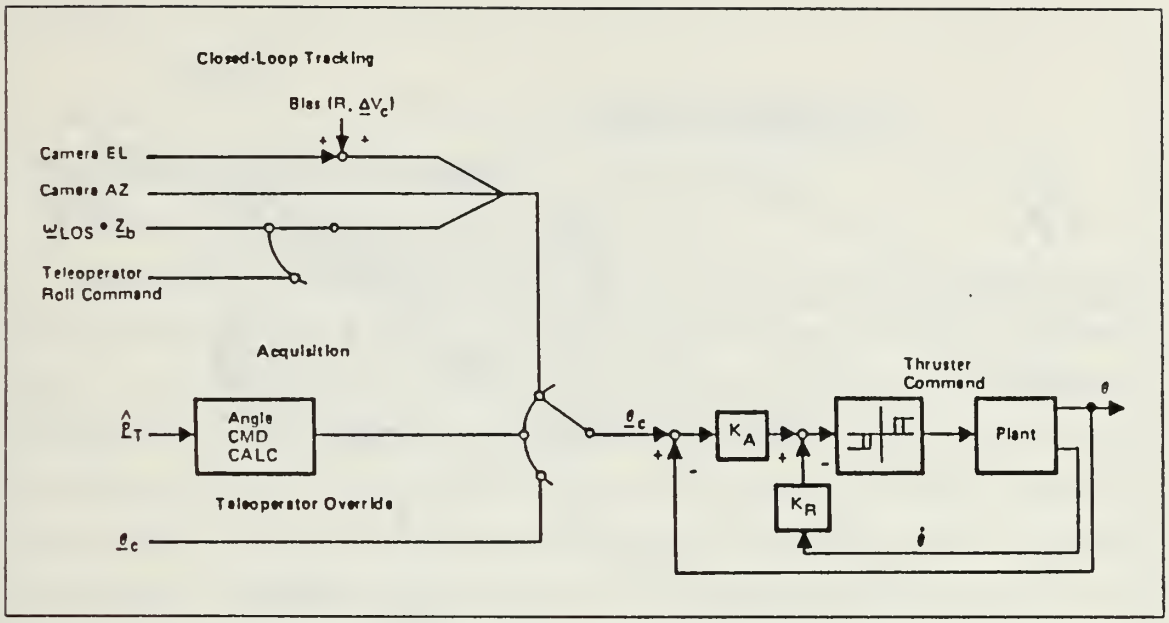

Figure 5. CER Attitude Command and Control; From [Ref. 1 : p. 27]

$$I_{TOT} = \begin{bmatrix} I_{xx} & I_{xy} & I_{xz} \\ I_{yx} & I_{yy} & I_{yz} \\ I_{zx} & I_{zy} & I_{zz} \end{bmatrix} = \begin{bmatrix} 39.6 & 0 & 0 \\ 0 & 55 & 0 \\ 0 & 0 & 55 \end{bmatrix} \text{ (in slug-}ft^2\text{)} \qquad (1.4)$$

The moment of inertia tensor data for the CER with no target was calculated by the author assuming an 850 pound total system weight symmetrically distributed about the center of gravity (weight of the capture mechanism assumed negligible).

C. THESIS ORGANIZATION

In Chapter II the CER attitude dynamics are modeled and described by deriving Euler's moment equations for the retriever with target and representing them using state variables. The moment of inertia tensors for the CER with and without a target are calculated for different worst-case target capture scenarios. Control torques summed about the shifting center of gravity are calculated for the CER with and without a target.

Chapter III describes the attitude stabilization of the CER by deriving the time optimal and fuel optimal control laws that will be used in the model simulation. State space plots of the corresponding switching curves are illustrated, and a deadband control scheme about the origin is also implemented.

In Chapter IV the CER model is simulated for the different worst-case target capture scenarios. The CER baseline configuration simulation results are tabulated and

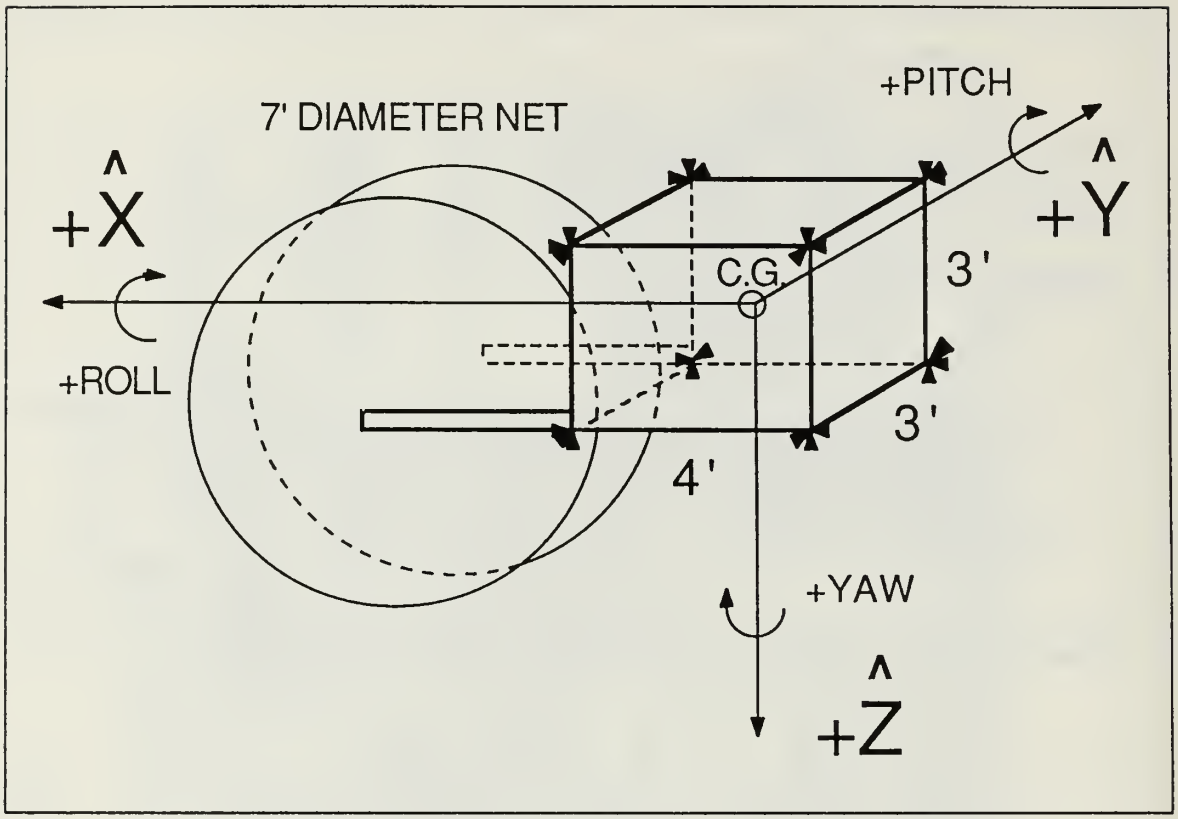

Figure 6. CER Baseline Configuration

analyzed to yield attitude control performance. A *new* CER configuration is proposed and the new model is simulated. The results are tabulated and compared to the CER baseline configuration. Fuel optimal analysis of the proposed model concludes Chapter IV.

Conclusions based on the simulation results are presented in Chapter V, as well as recommendations to improve the design and operational performance of the CER.

II. ATTITUDE DYNAMICS FOR THE CER

A. ATTITUDE PARAMETERIZATION

1. Parameterization Discussion

Several representations of the rigid body rotations about the coordinate axes for the CER were considered, including the use of quaternions as formulated by Hamilton in Ref. 3. The *direction cosine matrix* is well known as a nine parameter coordinate transformation between the body or spacecraft axes and the selected reference frame axes, and is considered to be the basic quantity specifying the orientation of a rigid body in space. [Ref. 4: pp. 410-420] Parameterizing the direction cosine matrix in terms of *Euler Symmetric parameters* incorporates the use of quaternions, requires only four parameters and does not involve trigonometric functions. However, the geometrical visualization of the rigid body rotations using Euler Symmetric parameters is not readily apparent.

The author decided to use *Euler angle* parameterization of the CER rigid body rotations. Euler angles are in terms of three rotation angles about coordinate axes, rotated in a specific sequence to describe the rigid body orientation in space. They are not computed as easily as Euler Symmetric parameters but are easy to visualize and small angle approximations can be used.

2. Euler Angles for the CER

The CER baseline configuration shown in Figure 6 on page 8 illustrates three orthogonal coordinate axes with origin at the CER center of gravity. Euler angle rotation (θ, ψ, ϕ) for the CER is shown in Figure 7 on page 10 and the dynamic elements shown are defined as follows: [Ref. 4: pp. 516-523]

- θ is the roll angle (in radians) about $\hat{X}$.
- ψ is the pitch angle (in radians) about $\hat{Y}$.
- ϕ is the yaw angle (in radians) about $\hat{Z}$.
- $\vec{L} = L_x + L_y + L_z$ is the angular momentum vector.
- $\vec{\omega} = \omega_x + \omega_y + \omega_z = \dot{\theta} + \dot{\psi} + \dot{\phi}$ is the angular velocity vector (in radians/second).

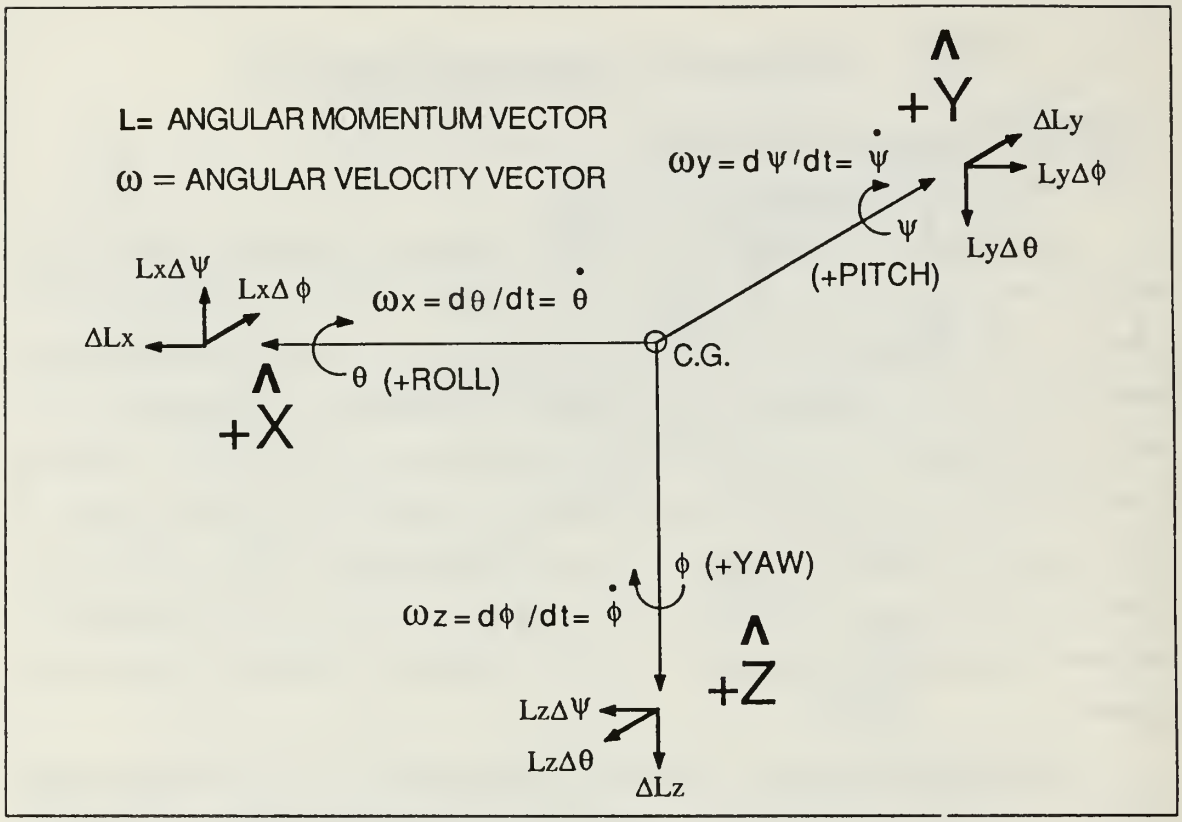

Figure 7. CER Euler Angle Parameterization

Note the coupling between the angular momentum vector components as shown by the small vector groups at the end of the coordinate axes. Since the rate of change of the angular momentum vector is equal to the sum of the applied torques, or

$$\sum T = \frac{\Delta \vec{L}}{\Delta t} = \dot{\vec{L}} \tag{2.1}$$

then the sum of the applied torques about each axis yields

$$T_x = \frac{\Delta L_x}{\Delta t} - \frac{L_y \Delta \phi}{\Delta t} + \frac{L_z \Delta \psi}{\Delta t} \tag{2.2}$$

$$T_y = \frac{\Delta L_y}{\Delta t} - \frac{L_z \Delta \theta}{\Delta t} + \frac{L_x \Delta \phi}{\Delta t} \tag{2.3}$$

$$T_z = \frac{\Delta L_z}{\Delta t} - \frac{L_x \Delta \psi}{\Delta t} + \frac{L_y \Delta \theta}{\Delta t} \tag{2.4}$$

The angular momentum vector is also defined as

$$\vec{L} = [I]\vec{\omega} \tag{2.5}$$

where $\vec{\omega}$ is the angular velocity vector and $[I]$ is the moment of inertia tensor given by

$$\mathrm{I} = \begin{bmatrix} I_{xx} & I_{xy} & I_{xz} \\ I_{yx} & I_{yy} & I_{yz} \\ I_{zx} & I_{zy} & I_{zz} \end{bmatrix} \quad (I_{ij} = I_{ji})$$

It follows that the rate of change of the angular momentum vector is

$$\dot{\vec{L}} = [T]\dot{\vec{\omega}} \tag{2.6}$$

Now taking the limit

$$\lim_{t \to 0} \{ \frac{\Delta \vec{L}}{\Delta t} \} = \dot{\vec{L}}$$

for equations (2.2), (2.3), and (2.4) and also substituting equation (2.6) yields Euler's moment equations

$$T_x = I_x \dot{\vec{\omega}} - \omega_z L_y + \omega_y L_z \tag{2.7}$$

$$T_y = I_y \dot{\vec{\omega}} - \omega_x L_z + \omega_z L_x \tag{2.8}$$

$$T_z + I_z \dot{\vec{\omega}} - \omega_y L_x + \omega_x L_y \tag{2.9}$$

Combining terms and expanding $\dot{\vec{\omega}}$ and $[I]$ while substituting equation (2.5) into equations (2.7), (2.8), and (2.9) yields

$$T_x = I_{xx}\dot{\omega}_x + I_{xy}\dot{\omega}_y + I_{xz}\dot{\omega}_z - (\omega_z\omega_y)(I_{yy} - I_{zz}) - (\omega_z\omega_x)I_{xy} - (\omega_z\omega_z)I_{yz} + (\omega_y\omega_x)I_{xz} + (\omega_y\omega_y)I_{yz} \tag{2.10}$$

$$T_y = I_{xy}\dot{\omega}_x + I_{yy}\dot{\omega}_y + I_{yz}\dot{\omega}_z - (\omega_x\omega_z)(I_{zz} - I_{xx}) - (\omega_x\omega_x)I_{xz} - (\omega_x\omega_y)I_{yz} + (\omega_z\omega_y)T_{xy} + (\omega_z\omega_z)I_{xz} \tag{2.11}$$

$$T_z = I_{xz}\dot{\omega}_x + I_{yz}\dot{\omega}_y + I_{zz}\dot{\omega}_z - (\omega_y\omega_x)(I_{xx} - I_{yy}) - (\omega_y\omega_y)I_{xy} - (\omega_y\omega_z)I_{xz} + (\omega_x\omega_x)I_{xy} + (\omega_x\omega_z)I_{yz} \tag{2.12}$$

Assuming small angular velocities, the terms containing angular velocity *products* in equations (2.10), (2.11), and (2.12) can be dropped, leaving

$$T_x = I_{xx}\dot{\omega}_x + I_{xy}\dot{\omega}_y + I_{xz}\dot{\omega}_z \tag{2.13}$$

$$T_y = I_{xy}\dot{\omega}_x + I_{yy}\dot{\omega}_y + I_{yz}\dot{\omega}_z \tag{2.14}$$

$$T_z = I_{xz}\dot{\omega}_x + I_{yz}\dot{\omega}_y + I_{zz}\dot{\omega}_z \tag{2.15}$$

Summarizing equations (2.13), (2.14), and (2.15) yields

$$\sum T = [I]\dot{\vec{\omega}} \tag{2.16}$$

or

$$\dot{\vec{\omega}} = [I]^{-1}\sum T \tag{2.17}$$

Equation (2.17) gives the angular acceleration vector $\vec{\omega}$ for the CER in terms of its inverse moment of inertia tensor values and the sum of all torques that act on it.

B. STATE VARIABLE REPRESENTATION

The angular acceleration vector components given by equation (2.17) can be used as control accelerations about their respective coordinate axes. To effectively demonstrate this, equation (2.17) is modeled in state variable form as follows:

$$\begin{array}{lll} X_1 = \theta & \dot{X}_1 = \dot{\theta} & \ddot{X}_1 = \ddot{\theta}\ (= \dot{\omega}_x) \\ X_2 = \psi & \dot{X}_2 = \dot{\psi} & \ddot{X}_2 = \ddot{\psi}\ (= \dot{\omega}_y) \\ X_3 = \phi & \dot{X}_3 = \dot{\phi} & \ddot{X}_3 = \ddot{\phi}\ (= \dot{\omega}_z) \end{array}$$

The inverse moment of inertia tensor is given by

$$[I]^{-1} = \frac{\text{adj}[I]}{\det[I]} \tag{2.18}$$

and using only the matrix component subscripts

$$[I]^{-1} = \frac{\begin{bmatrix} (yzz - yzy) & -(xzz - xzy) & (xyz - xzy) \\ -(yxz - yzx) & (xxz - xzx) & -(xxz - xzx) \\ (yxy - yyx) & -(xxy - xyx) & (xxy - xyy) \end{bmatrix}}{[\,(xxyzz) - (xxyzy) - (xyyxz) + (xyyzx) + (xzyxy) - (xzyyx)\,]} \tag{2.19}$$

To simplify equation (2.19), the following variables are defined:

$a = (yzz - yzy)$ $\quad f = (xxz - xzx)$
$b = (xzz - xzy)$ $\quad g = (yxy - yyx)$
$c = (xyz - xzy)$ $\quad h = (xxy - xyx)$
$d = (yxz - yzx)$ $\quad i = (xxy - xyy)$
$e = (xxz - xzx)$ $\quad j =$ Denominator

The matrix representation of the state equations is given by

$$\begin{bmatrix} \dot{X}_1 \\ \dot{X}_2 \\ \dot{X}_3 \\ \ddot{X}_1 \\ \ddot{X}_2 \\ \ddot{X}_3 \end{bmatrix} = \begin{bmatrix} 0 & 0 & 0 & 1 & 0 & 0 \\ 0 & 0 & 0 & 0 & 1 & 0 \\ 0 & 0 & 0 & 0 & 0 & 1 \\ 0 & 0 & 0 & 0 & 0 & 0 \\ 0 & 0 & 0 & 0 & 0 & 0 \\ 0 & 0 & 0 & 0 & 0 & 0 \end{bmatrix} \begin{bmatrix} X_1 \\ X_2 \\ X_3 \\ \dot{X}_1 \\ \dot{X}_2 \\ \dot{X}_3 \end{bmatrix} + \begin{bmatrix} 0 & 0 & 0 \\ 0 & 0 & 0 \\ 0 & 0 & 0 \\ \frac{a}{j} & \frac{-b}{j} & \frac{c}{j} \\ \frac{-d}{j} & \frac{e}{j} & \frac{-f}{j} \\ \frac{g}{j} & \frac{-h}{j} & \frac{i}{j} \end{bmatrix} \begin{bmatrix} T_x \\ T_y \\ T_z \end{bmatrix}$$

The last three state equations are meaningful and are given as

$$(\ddot{\theta} =)\ \ddot{X}_1 = \frac{a}{j} T_x - \frac{b}{j} T_y + \frac{c}{j} T_z \tag{2.20}$$

$$(\ddot{\psi} =)\ \ddot{X}_2 = -\frac{d}{j} T_x + \frac{e}{j} T_y - \frac{f}{j} T_z \tag{2.21}$$

$$(\ddot{\phi} =)\ \ddot{X}_3 = \frac{g}{j} T_x - \frac{h}{j} T_y + \frac{i}{j} T_z \tag{2.22}$$

Equations (2.20), (2.21), and (2.22) represent the CER angular acceleration components for three-axis attitude control. The following sections will yield the moment of inertia tensors and control torque values needed in the equations.

C. MOMENT OF INERTIA TENSOR ANALYSIS

1. CER Without Target Moments of Inertia

The CER moment of inertia tensor (without a target), was listed in equation (1.4) on page 7 and is repeated here

$$[I_{TOT}] = \begin{bmatrix} 39.6 & 0 & 0 \\ 0 & 55 & 0 \\ 0 & 0 & 55 \end{bmatrix} \text{ (slug-}ft^2\text{)} \tag{2.23}$$

Notice the cross-products of inertia are zero due to the symmetrical distribution of mass around the CER coordinate axes. The moment of inertia tensor was approximated by the author using

$$[I] = \sum M_i(||\vec{r}_i||^2 \mathrm{I} - \vec{r}_i\vec{r}_i^T) = \sum M_i(\mathrm{Tr}(\vec{r}_i\vec{r}_i^T)\mathrm{I} - \vec{r}_i\vec{r}_i^T) \tag{2.24}$$

where $\mathrm{Tr}(x) \equiv$ Trace of x, "I" is the identity matrix, and

$$\sum M_i = \int\int\int \rho \, dx \, dy \, dz \tag{2.25}$$

where ρ is the density in slugs/ft^3. [Ref. 5: pp. 236-240] As an example, I_{xx} is calculated using

$$I_{xx} = \int_{-1.5}^{1.5}\int_{-1.5}^{1.5}\int_{-2}^{2} (y^2 + z^2)\rho \, dx \, dy \, dz$$
$$\text{where } \rho = \frac{\text{mass}}{\text{vol}} = \frac{850/32.2}{36} \quad \frac{\text{slugs}}{ft^3} \tag{2.26}$$

resulting in

$$I_{xx} = 39.6 \text{ slug-}ft^2 \tag{2.27}$$

2. Target Moments of Inertia

The CER will be used to capture various targets with different mass and moment of inertia properties. The flexible capture net will provide a compliant capture

while maintaining sufficient rigidity to secure the target and maintain its center of gravity location [Ref. 1: p. 53].

A *point mass* with no moment of inertia properties is used to represent targets such as small tools or equipment. The *primary* target of interest, however, is an EVA crewman which includes the combined mass of the man, his environment suit or EMU (extra-vehicular mobility unit), and the MMU (manned manuevering unit). [Ref. 6] For a worst-case target capture, an EVA crewman would have the following approximate mass and moment of inertia properties:

226	100 percentile male
258	EMU
338	MMU (full propellant)
16	Ancillary equipment
12	1.5% safety margin
850	pounds

$$[I_{\underset{TARGET}{PRIMARY}}] = \begin{bmatrix} 27.21 & 0 & 0 \\ 0 & 44.78 & 0 \\ 0 & 0 & 41.62 \end{bmatrix} \text{ (slug-}ft^2\text{)} \tag{2.28}$$

The moment of inertia tensor calculated in equation (2.28) assumes the target axes would be aligned with the CER coordinate axes during target capture. For a more realistic analysis, the target is rotated about its center of gravity to give a new moment of inertia tensor which is found by using the coordinate transformation theory detailed in Ref. 4 (pp. 761-765). To summarize

$$\vec{r}' = [T]\vec{r} \tag{2.29}$$

$$\vec{r}'^{T} = \vec{r}^{T}[T]^{T} \tag{2.30}$$

where

$\vec{r}$ = cartesian vector for target
$[T]$ = transformation matrix or direction cosine matrix
$\vec{r}'$ = cartesian vector for rotated target

and from equations (2.24) and (2.25)

$$[I] = \int (\mathrm{Tr}(\vec{r}_i \vec{r}_i^T)\mathrm{I} - \vec{r}_i \vec{r}_i^T) dm \tag{2.31}$$

Multiplying both sides of equation (2.31) by $[T]$ and $[T]^T$

$$[T][I][T]^T = \int ([T](\mathrm{Tr}(\vec{r}_i \vec{r}_i^T))\mathrm{I}[T]^T - [T]\vec{r}_i \vec{r}_i^T [T]^T) dm \tag{2.32}$$

moving the T's inside the trace and substituting from equations (2.29) and (2.30) yields

$$[T][I][T]^T = \int (\mathrm{Tr}(\vec{r}_i' \vec{r}_i'^T)\mathrm{I} - \vec{r}_i' \vec{r}_i'^T) dm$$

and since

$$\mathrm{Tr}(\vec{r}_i' \vec{r}_i'^T) = ||\vec{r}_i'||^2$$

then

$$[T][I][T]^T = \int (||\vec{r}_i'||^2 \mathrm{I} - \vec{r}_i' r_i'^T) dm$$

or

$$[I]' = [T][I][T]^T \tag{2.33}$$

From equation (2.33), the original moment of inertia tensor for the target is multiplied by the transformation matrix (direction cosine matrix) and its transpose to yield the rotated target's tensor. The general direction cosine matrix for a 3-1-2 Euler angle rotation is given by

$$[T_{312}(\phi,\theta,\psi)] = \begin{bmatrix} \cos\psi\cos\phi - \sin\theta\sin\psi\sin\phi & \cos\psi\sin\phi + \sin\theta\sin\psi\cos\phi & -\cos\theta\sin\psi \\ -\cos\theta\sin\phi & \cos\theta\cos\phi & \sin\theta \\ \sin\psi\cos\theta + \sin\theta\cos\psi\sin\phi & \sin\psi\sin\phi - \sin\theta\cos\psi\cos\phi & \cos\theta\cos\psi \end{bmatrix} \tag{2.34}$$

where

3 – (Yaw) rotation by ϕ about $\hat{z}$

1 – (Roll) rotation by θ about $\hat{x}'$

2 – (Pitch) rotation by ψ about $\hat{y}''$

Using equations (2.33) and (2.34) for a 3-1-2 rotation angle sequence of

$\phi = 45°$
$\theta = 45°$
$\psi = 45°$

yields

$$[I]' = \begin{bmatrix} 43.6 & 2.4 & -1.4 \\ 2.4 & 38.8 & 6.4 \\ -1.4 & 6.4 & 31.2 \end{bmatrix} \tag{2.35}$$

Out of several different combinations of rotation angles calculated, equation (2.35) represents the worst-case moment of inertia tensor for a rotated primary target.

3. CER With Target Moments of Inertia

The CER with target moment of inertia tensor is calculated using the parallel-axis theorem

$$[I_{TOT}] = [I_{CER}] + [I_{TARGET}] - \frac{M_1 M_2}{M_1 + M_2}[R_2]^2 \tag{2.36}$$

where $[R_2]$ is the *skew-symmetric matrix* derived from the vector $\vec{r}_2$ between the center of gravities of the CER (mass M_1) and the target (mass M_2) and is illustrated in Figure 8 on page 18. [Ref. 7]

During target capture the total moment of inertia tensor changes accordingly, depending on the target's moments of inertia and location in the capture net. To provide the worst-case (largest), moment of inertia tensors for input into equations (2.20), (2.21), and (2.22), the following cases were analyzed:

- CASE 1A ($\hat{X}_{max}$) - 850 pound point mass captured on $\hat{X}_{max}$ net edge located at $\vec{r}_2 = 9(i) + 0(j) + 1.5(k)$ from CER center of gravity.
- CASE 1B ($\hat{Y}_{max}$) - 850 pound point mass captured on $\hat{Y}_{max}$ net edge located at $\vec{r}_2 = 5.583(i) + 1.5(j) + 1.5(k)$ from CER center of gravity.
- CASE 1C ($\hat{Z}_{max}$) - 850 pound point mass captured on $\hat{Z}_{max}$ net edge located at $\vec{r}_2 = 5.583(i) + 0(j) + 5(k)$ from CER center of gravity.

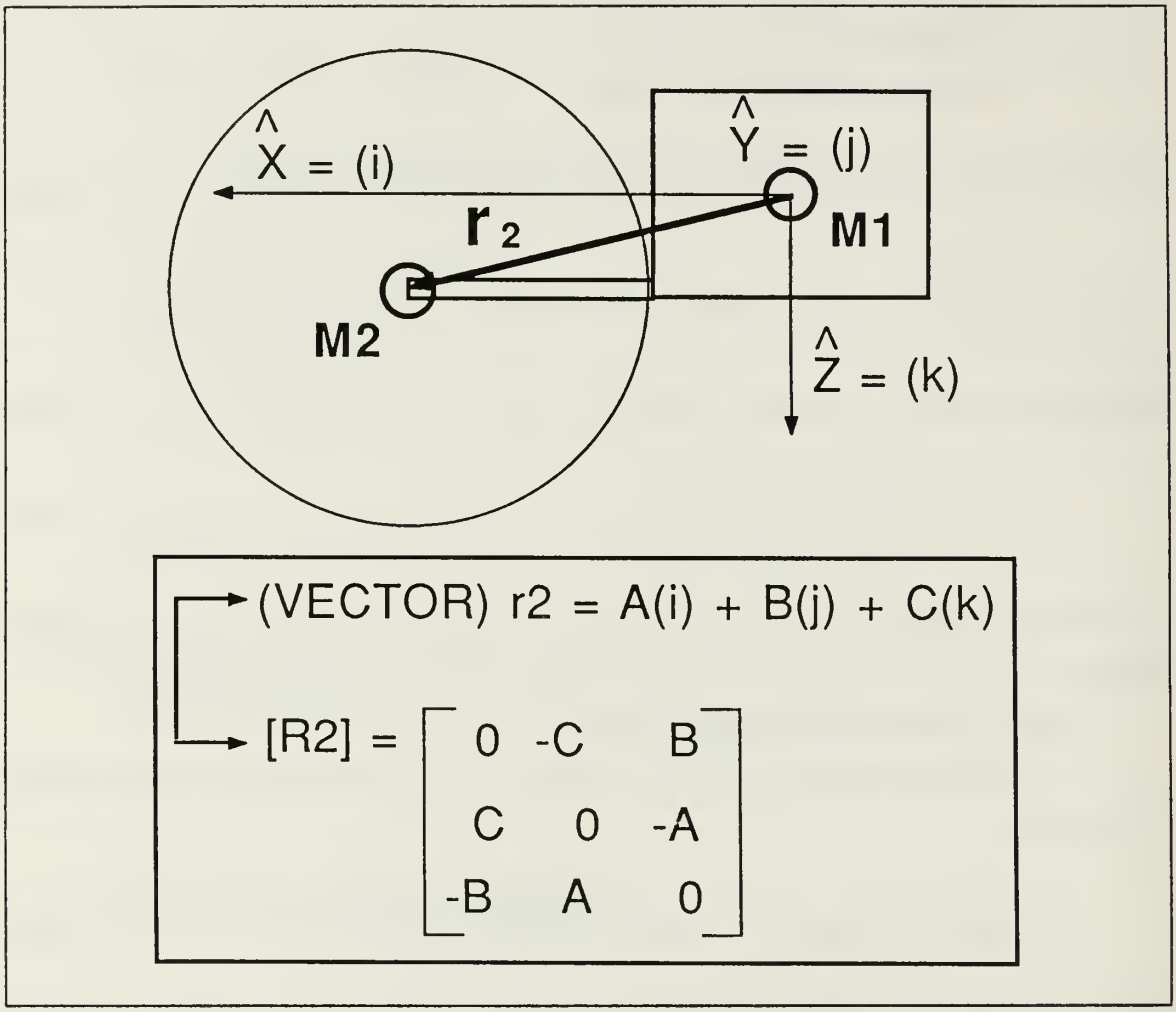

Figure 8. Skew-Symmetric Matrix

- CASE 1D ($\hat{X} = \hat{Z}, \hat{Y} = 1$) - 850 pound point mass captured at $\hat{X} = \hat{Z}, \hat{Y} = 1$ from net center, located at $\vec{r}_2 = 7.097(i) + 1(j) + 3.014(k)$ from CER center of gravity.
- CASE 2 (man & mmu) - 850 pound primary target (man & mmu rotated $\phi = \theta = \psi = 45°$) captured at net center, located at $\vec{r}_2 = 5.583(i) + 0(j) + 1.5(k)$ from CER center of gravity.

The target capture cases are illustrated in Figure 9 on page 19.

An example calculation of the total moment of inertia tensor for CASE 2 (man & mmu) is in order. The following values are used in equation (2.36):

$$\vec{r}_2 = 5.583(i) + 0(j) + 1.5(k) \rightarrow [R_2]$$

where

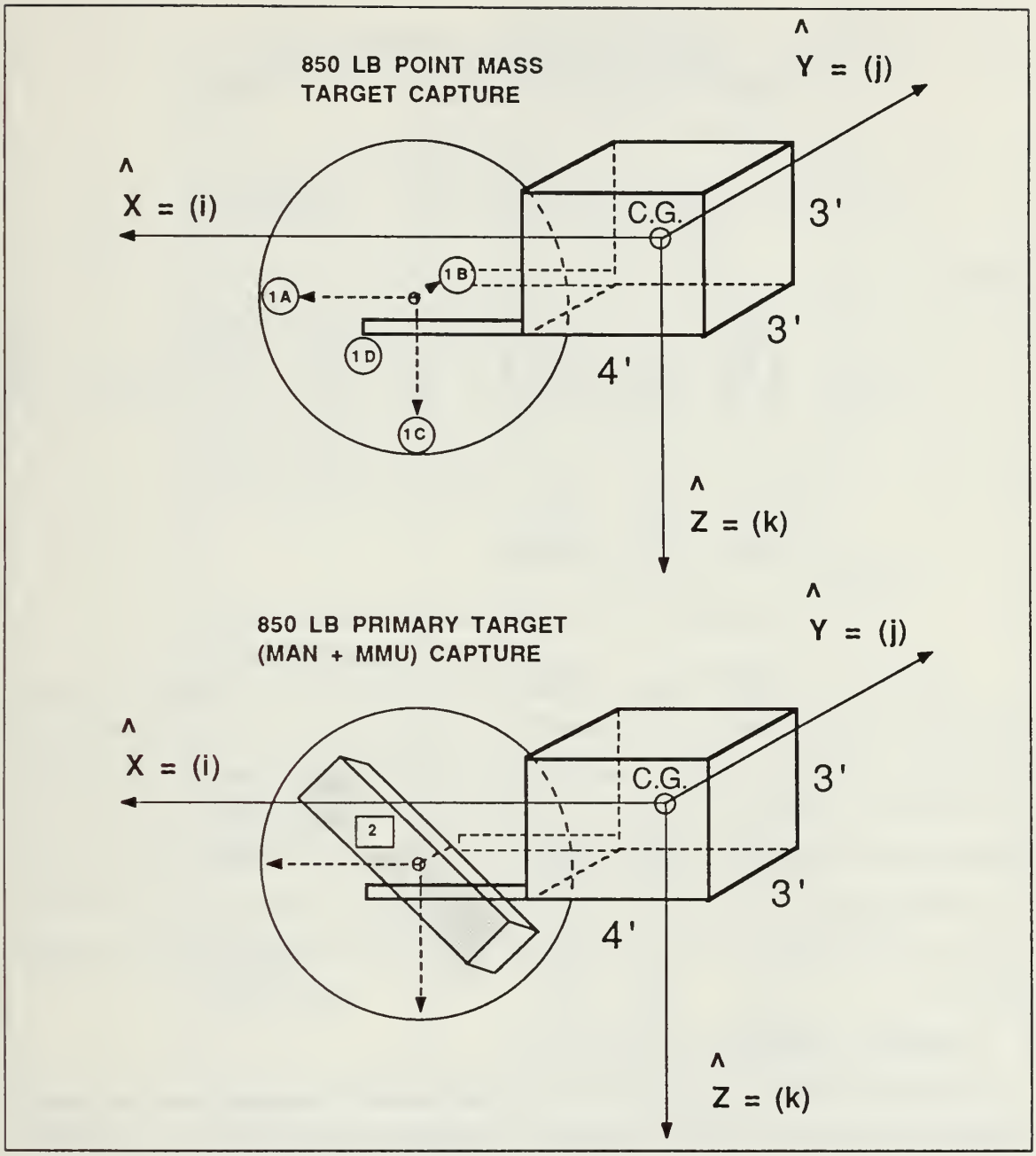

Figure 9. Target Capture Case Locations

$$[R_2]^2 = \begin{bmatrix} 0 & -1.5 & 0 \\ 1.5 & 0 & -5.583 \\ 0 & 5.583 & 0 \end{bmatrix} \begin{bmatrix} 0 & -1.5 & 0 \\ 1.5 & 0 & -5.583 \\ 0 & 5.583 & 0 \end{bmatrix}$$

$$\frac{M_1 M_2}{M_1 + M_2} = \frac{(26.3975)(26.3975)}{(26.3975) + (26.3975)} = 13.19875 \text{ (slugs)}$$

$[I_{CER}]$ = equation (2.23)

$[I_{TARGET}]$ = equation (2.35)

to yield

$$[T_{TOT}] = \begin{bmatrix} 39.6 & 0 & 0 \\ 0 & 55 & 0 \\ 0 & 0 & 55 \end{bmatrix} + \begin{bmatrix} 43.6 & 2.4 & -1.4 \\ 2.4 & 38.8 & 6.4 \\ -1.4 & 6.4 & 31.2 \end{bmatrix} - \begin{bmatrix} -29.7 & 0 & 110.5 \\ 0 & -441.1 & 0 \\ 110.5 & 0 & -411.4 \end{bmatrix}$$

or

$$[I_{TOT}] = \begin{bmatrix} 112.9 & 2.4 & -111.9 \\ 2.4 & 534.9 & 6.4 \\ -111.9 & 6.4 & 497.6 \end{bmatrix}$$

All of the moment of inertia tensors for the CER baseline configuration during target capture were calculated as in the previous example and are shown in Figure 10 on page 21. A quick comparison shows that the 850 pound point mass (with no *internal* cross-products of inertia), induces *larger* cross-products of inertia when captured at the edges of the net than does the primary target (850 pound man & mmu), when captured in a rotated position at the center of the net. The ability to reduce the cross-products of inertia for the CER (with target) will prove to be a critical factor for attitude control stability.

D. CONTROL TORQUE ANALYSIS

The CER baseline configuration was listed in Section I.5 on page 4 as having 24 cold gas jet thrusters rated at 1.0 lbf to make up two separate redundant systems. Also listed were the summation of control torques based on the thruster size and locations from the CER center of gravity. The thrusters are fired in pairs to produce couples about any of the three orthogonal axes. An example of a thruster pair firing to produce a positive roll about $\hat{X}$ is shown in Figure 11 on page 22. The corresponding calculations of the control torques summed about the center of gravity are as follows:

$$\vec{F}_1 = 0(i) + 0(j) + 1(k) \tag{2.37}$$

CASE	MOMENT OF INERTIA TENSOR (SLUG-FT ^{2})
NO TARGET	$[I] = \begin{bmatrix} 39.6 & 0 & 0 \\ 0 & 55 & 0 \\ 0 & 0 & 55 \end{bmatrix}$
CASE 1A (Xmax)	$[I] = \begin{bmatrix} 69.3 & 0 & -178.2 \\ 0 & 1153.8 & 0 \\ -178.2 & 0 & 1124.1 \end{bmatrix}$
CASE 1B(Ymax)	$[I] = \begin{bmatrix} 98.9 & -110.5 & -110.5 \\ -110.5 & 496.1 & -29.7 \\ -110.5 & -29.7 & 496.1 \end{bmatrix}$
CASE 1C(Zmax)	$[I] = \begin{bmatrix} 369.5 & 0 & -368.4 \\ 0 & 796.4 & 0 \\ -368.4 & 0 & 503.6 \end{bmatrix}$
CASE 1D (X=Z,Y=1)	$[I] = \begin{bmatrix} 172.7 & -93.7 & -282.3 \\ -93.7 & 839.7 & -39.8 \\ -282.3 & -39.8 & 732.9 \end{bmatrix}$
CASE 2 (MAN+MMU)	$[I] = \begin{bmatrix} 112.9 & 2.4 & -111.9 \\ 2.4 & 534.9 & 6.4 \\ -111.9 & 6.4 & 497.6 \end{bmatrix}$

Figure 10. CER Baseline Configuration Moment of Inertia Tensors for Target Capture

$$\vec{r}_1 = -2(i) + 1.5(j) - 1.5(k) \tag{2.38}$$

$$\vec{F}_2 = 0(i) + 0(j) - 1(k) \tag{2.39}$$

$$\vec{r}_2 = -2(i) - 1.5(j) + 1.5(k) \tag{2.40}$$

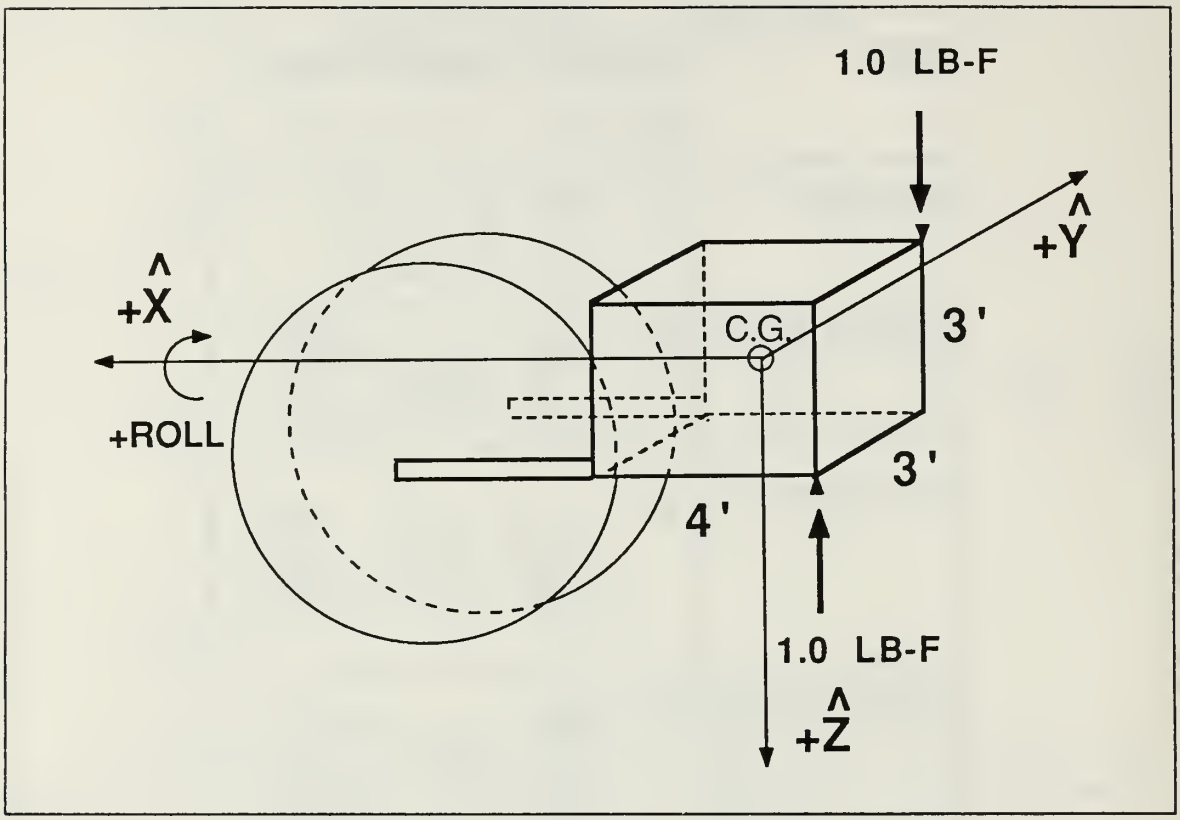

Figure 11. CER Baseline Thruster Configuration for (+)ROLL

Substituting equations (2.37) thru (2.40) into

$$T_i = \vec{r}_i \times \vec{F}_i \tag{2.41}$$

and summing the torques

$$\sum T = T_1 + T_2 = (1.5(i) + 2(j) + 0(k)) + (1.5(i) - 2(j) + 0(k)) \tag{2.42}$$

or

$$\sum T_x = 3(i) \text{ (ft-lbf)} \tag{2.43}$$

Equations (2.17), (2.43), and the moment of inertia I_{xx} value from equation (2.23) for the CER with no target are used as follows to find the normalized control acceleration if no cross-products of inertia exist:

$$\dot{\omega}_x = [I_{xx}]^{-1} T_x = \frac{3}{39.6} = .07575 \quad \frac{\text{(ft-lbf)}}{\text{(slug-}ft^2\text{)}} = \frac{\text{rad}}{\text{sec}^2} \tag{2.44}$$

Equation (2.44) reveals the relatively small magnitude of the control acceleration generated by the 1.0 lbf baseline thrusters acting on the CER with no target.

During target capture the moment of inertia tensor changes and the center of gravity shifts accordingly. Since the thrusters are fired in pairs to produce couples about any of the orthogonal axes, *the shift in center of gravity has no effect on the summation of control torque calculations.* To change the control torques, either the location of the thrusters must change to increase or decrease the distance between the thruster pairs, or the thruster size must be increased or decreased as desired. The ability to change the control torques (and subsequently the control accelerations), will prove to be beneficial to the attitude control stability of the CER with and without a target.

III. ATTITUDE STABILIZATION

The CER will provide an autonomous attitude hold capability at all times and will also respond to commanded rotations as required for the mission. Since the CER will operate in close proximity to the Space Station and must be precisely oriented during target capture, a *minimum-time* control response is desired to maintain strict attitude control during all mission phases. However, maintaining strict attitude control while coasting between orbits is not critical, especially without a target, and a *minimum-fuel* control response could be used. The following sections will derive the *optimal control laws* to obtain a minimum-time and a minimum-fuel control response. The optimal control laws will be used in combination to define switching curves for a *weighted-time-fuel optimal* control response that can be used to support a specific CER mission phase.

A. TIME OPTIMAL CONTROL LAW

The objective of minimum-time control is to transfer a system from an arbitrary initial state to a specified final state as quickly as possible. The optimal control system to achieve a minimum-time response is normally referred to as a *bang-bang* system, where the optimal control switches between its maximum and minimum magnitudes. [Ref. 8: p. 259]

The control acceleration for each axis will be calculated, as in equation (2.44), for the CER. Each acceleration ($\dot{\omega}_i$) will be used to drive its respective angular position and velocity from arbitrary initial conditions to final states of zero. An example problem formulated by Kirk in Ref. 8 : pp. 249-254, of deriving the optimal control law and corresponding switching curves can be used for the CER system to find the optimal control to accomplish this in minimum-time. To summarize the derivation to follow, the underlying optimal control principles must first be presented.

The optimal control (u^*), is defined as the control acceleration that minimizes the designated performance function $J_{(u)}$. The minimum time performance function is:

$$J_{(u)} = \int_{t_0}^{t_f} dt = t_f - t_0 \tag{3.1}$$

where it is assumed that the final time is free (not specified), and the final state is fixed (specified at zero). These boundary conditions are used to help specify the *necessary conditions* for optimal control.

The necessary conditions consist of a set of 2n, first-order differential equations referred to as the *state* and *costate* equations, and a set of algebraic relations that must be satisfied during the control interval. The costate $p^*(t)$, is described using lagrange multipliers and the state $x^*(t)$, is from the state variable representation of the system. The solution of the state and costate equations contain 2n constants of integration that are evaluated by using (2n + 1) equations since the final time t_f is not specified [Ref. 8: p. 200]. It will be convenient to use the function $\mathcal{H}$, called the *Hamiltonian*, defined as

$$\mathcal{H}(x(t),u(t),p(t)(t),t) \equiv g(x(t),u(t),t) + p^T(t)[a(x(t),u(t).t)] \tag{3.2}$$

The two variables in equation (3.2) not yet described are g, which is the integrand of the performance function, and a, which represents the state equations. The necessary conditions, for all $t \in [t_0,t_f]$, are [Ref. 8 : p. 188]

$$\dot{x}^*(t) = \frac{\hat{c}\mathcal{H}}{\hat{c}p}(x^*(t),u^*(t),p^*(t),t) \tag{3.3}$$

$$\dot{p}^*(t) = -\frac{\hat{c}\mathcal{H}}{\hat{c}x}(x^*(t),u^*(t),p^*(t),t) \tag{3.4}$$

$$0 = \frac{\hat{c}\mathcal{H}}{\hat{c}u}(x^*(t),u^*(t),p^*(t),t) \tag{3.5}$$

and

$$\left[\frac{\hat{c}h}{\hat{c}x}(x^*(t_f),t_f) - p^*(t_f)\right]^T \delta x_f + \left[\mathcal{H}(x^*(t_f),u^*(t_f),p^*(t_f),t_f) + \frac{\hat{c}h}{\hat{c}t}(x^*(t_f),t_f)\right]\delta t_f = 0 \tag{3.6}$$

Since the final time (t_f) is arbitrary and the final state is fixed at zero, then $\delta x_f = 0$ and equation (3.6) yields

$$\mathcal{H}(x^*(t_f),u^*(t_f),p^*(t_f),t_f) + \frac{\hat{c}h}{\hat{c}t}(x^*(t_f),t_f) = 0 \tag{3.7}$$

In addition to the necessary conditions discussed above, an optimal control must satisfy *Pontryagin's minimum principle* which states that an optimal control must minimize the Hamiltonian. [Ref. 8: pp. 227-234] The minimum principle is appropriate to use

when the admissible controls are *constrained* by certain maximum values (in this case the thrusters are limited by their maximum force settings).

Applying Pontryagin's minimum principle modifies equation (3.5) to yield

$$\mathcal{H}(x^*(t),u^*(t),p^*(t),t) \leq \mathcal{H}(x^*(t),u(t),p^*(t),t) \quad \text{(for all admissible } u(t)\text{)} \tag{3.8}$$

where $u^*(t)$ is a control that causes $\mathcal{H}(x^*(t),u(t),p^*(t),t)$ to assume its absolute minimum.

To find the optimal control law and corresponding switching curves for minimum-time control about one axis of the CER, the system is defined by the state equations

$$\begin{aligned} \dot{x}_1(t) &= x_2(t) \\ \dot{x}_2(t) &= u_c(t) \end{aligned} \tag{3.9}$$

which will be transferred from initial conditions to final states at the origin in minimum-time by the optimal control constrained by

$$|u_a(t)| \leq u_c(t) \tag{3.10}$$

where $u_c(t)$ is the control acceleration previously calculated in equation (2.44), and $u_a(t)$ is defined as an admissible control. The system is assumed to be completely controllable and normal (no singular intervals exist). The applicable necessary conditions to be used are from equations (3.3), (3.4), (3.5), (3.8), and (3.7). The performance function to be used is from equation (3.1).

The Hamiltonian for the CER system is

$$\mathcal{H}(x(t),u(t),p(t)) = 1 + p_1(t)x_2(t) + p_2(t)u_a(t) \tag{3.11}$$

and the minimum principle produces

$$1 + p_1^*(t)x_2^*(t) + p_2^*(t)u^*(t) \leq 1 + p_1^*(t)x_2^*(t) + p_2^*(t)u_a(t) \tag{3.12}$$

or

$$p_2^*(t)u^*(t) \leq p_2^*(t)u_a(t) \tag{3.13}$$

or from equations (3.13) and (3.10) the optimal control must be

$$u^*(t) = \begin{bmatrix} -u_c(t), & \text{for } p_2^*(t) > 0 \\ +u_c(t), & \text{for } p_2^*(t) < 0 \end{bmatrix} \tag{3.14}$$

Using the Hamiltonian in the necessary condition, equation (3.4), yields the costate equations

$$\dot{p}_1^*(t) = -\frac{\partial \mathcal{H}}{\partial x_1} = 0 \tag{3.15}$$

$$\dot{p}_2^*(t) = -\frac{\partial \mathcal{H}}{\partial x_2} = -p_1^*(t) \tag{3.16}$$

The costate equation solutions are found by integrating both sides of equations (3.15) and (3.16) to yield

$$p_1^*(t) = c_1 \tag{3.17}$$

$$p_2^*(t) = -c_1 t + c_2 \tag{3.18}$$

Equation (3.18) indicates that $p_2^*(t)$, and therefore from equation (3.14), $u^*(t)$ can change signs at most *one* time.

Segments of the optimal trajectories can be found by integrating the state equations defined in equation (3.9), and after a few manipulations the result is

$$x_1(t) = \frac{x_2^2(t)}{2u_c(t)} + c_5 \quad (u = +u_c(t)) \tag{3.19}$$

$$x_1(t) = -\frac{x_2^2(t)}{2u_c(t)} + c_6 \quad (u = -u_c(t)) \tag{3.20}$$

Equations (3.19) and (3.20) each define a family of parabolas and are shown on a state space plot in Figure 12 on page 28 with the arrows indicating direction as time increases. [Ref. 8: pp. 252-253] By setting c_5 and c_6 equal to zero in equations (3.19) and (3.20), to satisfy the final time condition on the state, the state space plot shows one continuous curve through the origin as shown in Figure 13 on page 29.

Since one switching can occur at most, the optimal control found in equation (3.14) can be one of the following:

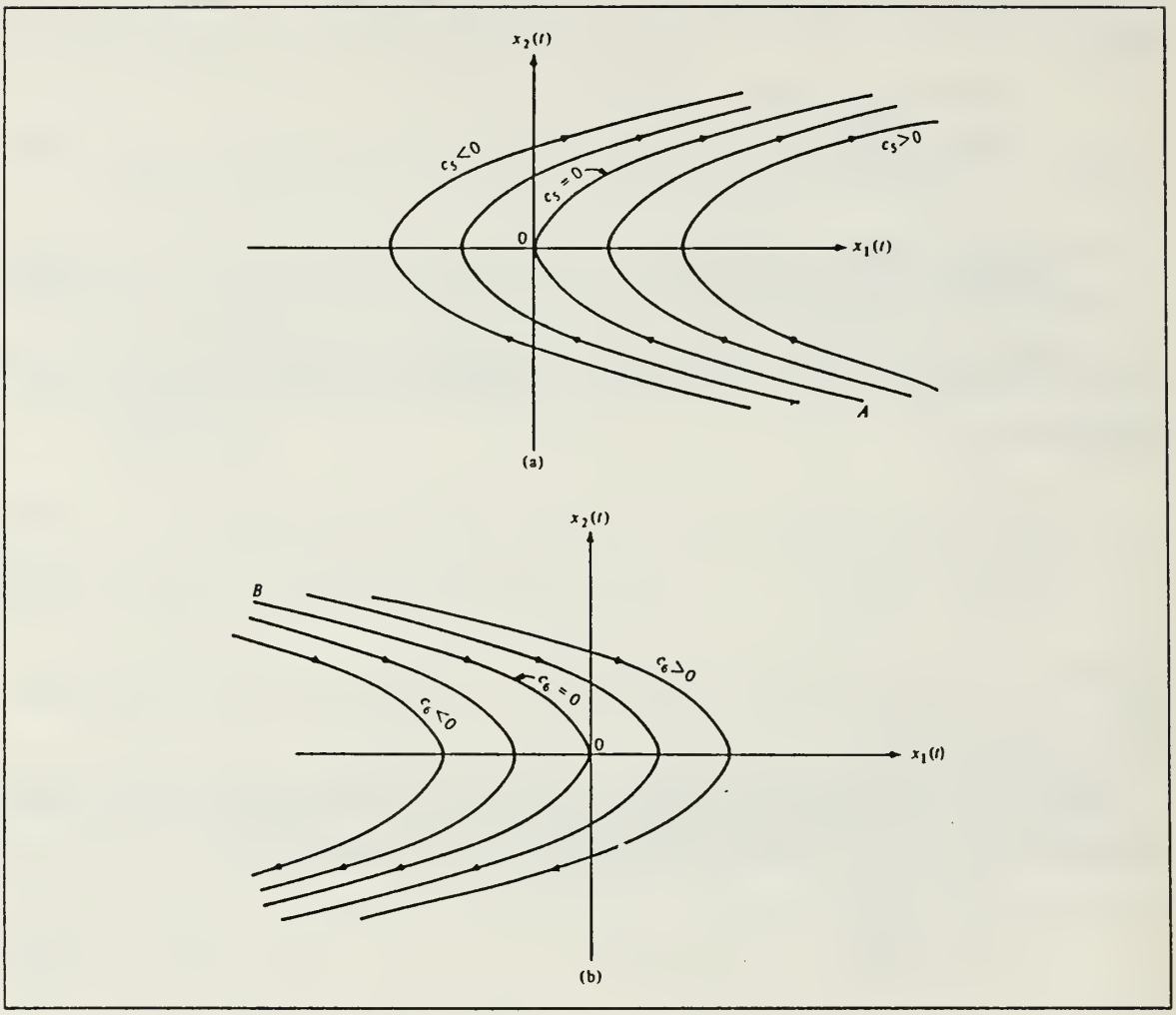

Figure 12. Trajectories for U = + Uc and U = -Uc; From [Ref. 8 : p. 252]

$$u^*(t) = \begin{bmatrix} \text{(Form 1)} & +u_c(t), & t \in [t_0, t^*], \text{ or} \\ \text{(Form 2)} & -u_c(t), & t \in [t_0, t^*], \text{ or} \\ \text{(Form 3)} & +u_c(t), & t \in [t_0, t_1) \text{ and } -u_c(t), \quad t \in [t_1, t^*), \text{ or} \\ \text{(Form 4)} & -u_c(t), & t \in [t_0, t_1) \text{ and } +u_c(t), \quad t \in [t_1, t^*) \end{bmatrix} \tag{3.21}$$

Direct minimization of the performance function yields the optimal controls for different initial conditions

- Form 1 -- Initial states lie on segment $A \rightarrow O$ with $u^*(t) = +u_c$.
- Form 2 -- Initial states lie on segment $B \rightarrow O$ with $u^*(t) = -u_c$.

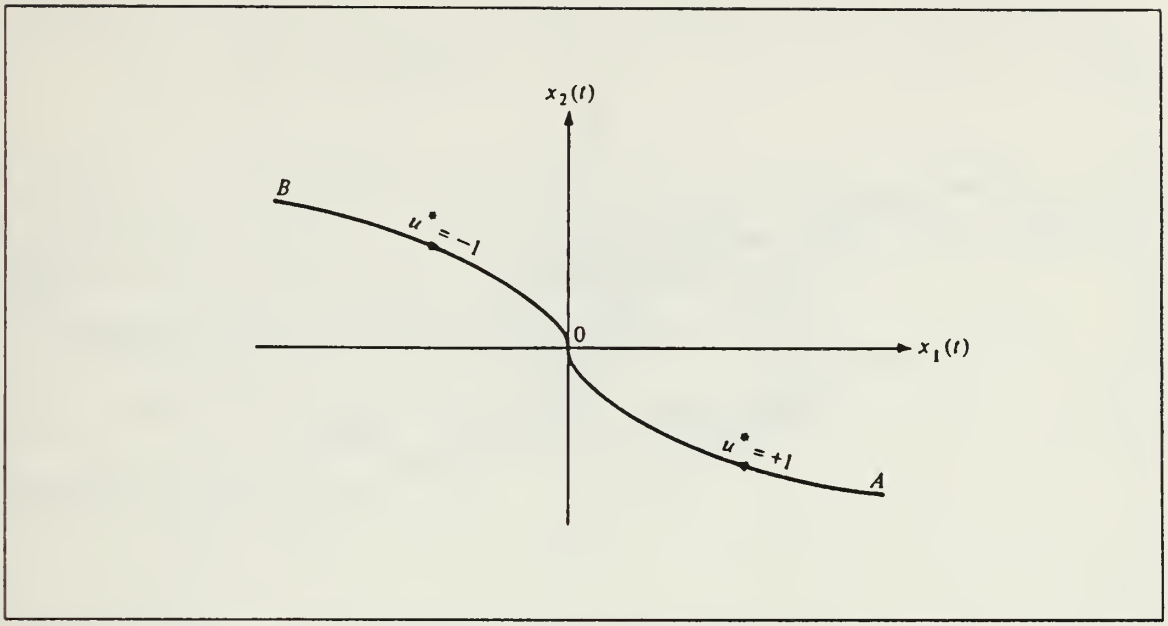

Figure 13. Trajectories for U=(+-)Uc through the origin; From [Ref. 8 : p. 253]

- Form 3 -- Initial states lying below both segments $A \rightarrow O$ and $B \rightarrow O$ will have $u^*(t) = +u_c$ until $B \rightarrow O$ is reached, then $u^*(t) = -u_c$ thereafter.
- Form 4 -- Initial states lying above both segments $A \rightarrow O$ and $B \rightarrow O$ will have $u^*(t) = -u_c$ until $A \rightarrow O$ is reached, then $u^*(t) = +u_c$ thereafter.

Optimal trajectories for several initial state values are shown in Figure 14 on page 30. The continuous curve represents the locus of points where control switches from $+-u_c(t)$ to $-+u_c(t)$ and is known as a *switching curve*. The equation describing the curve also defines the *optimal control law* for minimum-time control and is given by

$$x_1(t) = -\frac{x_2(t)|x_2(t)|}{2u_c(t)} \tag{3.22}$$

To simplify the use of equation (3.22), a switching function $s(\mathbf{x}(t))$ is defined

$$s(\mathbf{x}(t)) \equiv x_1(t) + \frac{x_2(t)|x_2(t)|}{2u_c(t)} \tag{3.23}$$

and implies that for

- $s(\mathbf{x}(t)) > 0$ $x(t)$ lies above A-O-B.
- $s(\mathbf{x}(t)) < 0$ $x(t)$ lies below A-O-B.
- $s(\mathbf{x}(t)) = 0$ $x(t)$ lies on A-O-B.

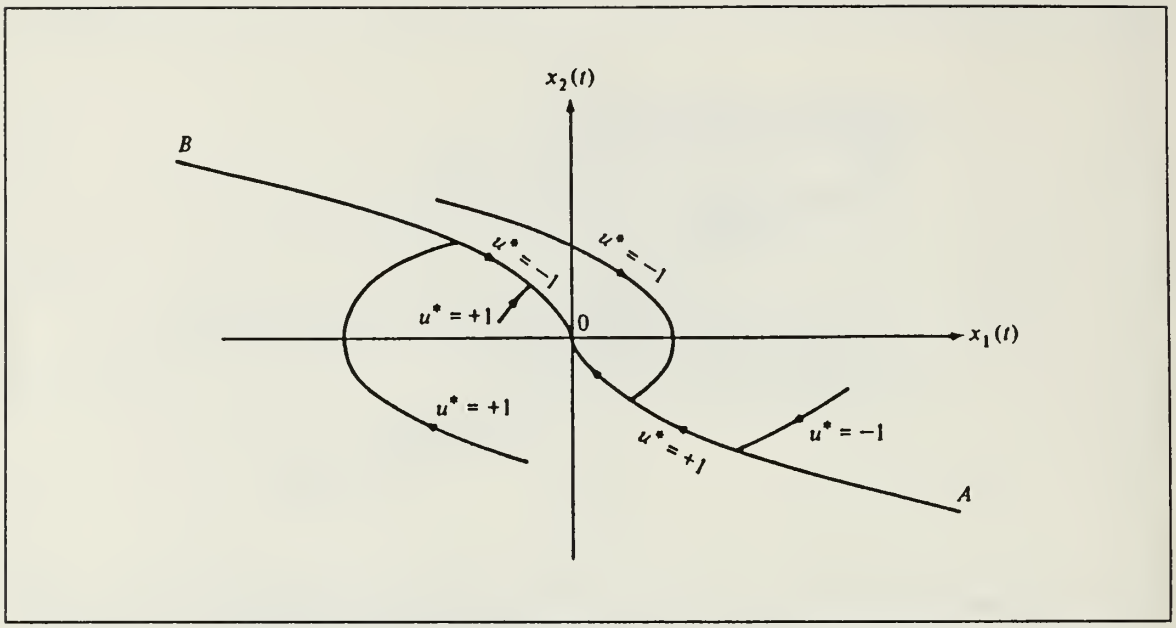

Figure 14. Optimal Trajectories for Different Initial State Values; From [Ref. 8 : p. 253]

The switching function is used in the simulation program discussed in the next chapter.

B. WEIGHTED-TIME-FUEL OPTIMAL CONTROL LAW

The CER may have an opportunity to relax its control response time while coasting between orbits, consequently conserving fuel. *Minimum-fuel* control response, however, is not desired since the final time t_f is not specified and the system would virtually take an infinite amount of time to reach the desired final state at the origin. Using a *weighted-time-fuel performance function* would allow the CER to use a minimum-time control response or to conserve fuel while maintaining a satisfactory time response as required for the mission phase.

The same method that described the minimum-time control law will be used to find the optimal control law and corresponding switching curves for a weighted-time-fuel control response. The state equations for the CER defined in equation (3.9) will be used and the control is again constrained as in equation (3.10). The final time t_f is not specified and the system is to be transferred to a final state $x(t_f) = 0$ while minimizing the following performance function:

$$J(u) = \int_{t_0}^{t_f} \left[1 + \lambda \left| u_a(t) \right| \right] dt \tag{3.24}$$

Note that for $\lambda = 0$, equation (3.24) becomes the minimum-time performance function as in equation (3.1). For $\lambda = \infty$, equation (3.24) becomes a minimum-fuel performance function corresponding to an infinite time to reach the final state.

Beginning the derivation, the Hamiltonian is

$$\mathcal{H}(x(t),u(t),p(t)) = 1 + \lambda \left| u_a(t) \right| + p_1(t)x_2(t) + p_2(t)u_a(t) \tag{3.25}$$

The costate equations are

$$\dot{p}_1^*(t) = 0 \tag{3.26}$$

$$\dot{p}_2^*(t) = - p_1^*(t) \tag{3.27}$$

and equations (3.26) and (3.27) have solutions of

$$p_1^*(t) = c_1 \tag{3.28}$$

$$p_2^*(t) = - c_1 t + c_2 \tag{3.29}$$

Pontryagin's minimum principle yields

$$\lambda \left| u^*(t) \right| + p_2^*(t)u^*(t) \leq \lambda \left| u_a(t) \right| + p_2^*(t)u_a(t) \tag{3.30}$$

or

$$(\lambda + p_2^*(t)) \left| u^*(t) \right| \leq \left| u_a(t) \right| (\lambda + p_2^*(t)) \tag{3.31}$$

From equations (3.30) and (3.10) the optimal control must be

$$u^*(t) = \begin{bmatrix} + u_c(t) \text{ for } p_2^*(t) < - \lambda \\ 0 \text{ for } - \lambda < p_2^*(t) < \lambda \\ - u_c(t) \text{ for } \lambda < p_2^*(t) \\ \text{undetermined, but } \geq 0 \text{ for } p_2^*(t) = - \lambda \\ \text{undetermined, but } \leq 0 \text{ for } p_2^*(t) = + \lambda \end{bmatrix} \tag{3.32}$$

Equations (3.28) and (3.29) for the costate solutions show that $p_2^*(t)$ can change sign at most once, so the optimal control must be one of the following:

$$u^*(t) = \begin{bmatrix} 0 \\ +u_c(t) \\ -u_c(t) \\ (0, +u_c(t)) \\ (0, -u_c(t)) \\ (+u_c(t), 0) \\ (-u_c(t), 0) \\ (+u_c(t), 0, -u_c(t)) \\ (-u_c(t), 0, +u_c(t)) \end{bmatrix} \tag{3.33}$$

The control intervals that end with $u^*(t) = 0$ cannot be optimal since the final condition cannot be achieved without the application of a control. Therefore

$$u^*(t) = \begin{bmatrix} +u_c(t) \\ -u_c(t) \\ (0, +u_c(t)) \\ (0, -u_c(t)) \\ (+u_c(t), 0, -u_c(t)) \\ (-u_c(t), 0, +u_c(t)) \end{bmatrix} \tag{3.34}$$

and for the controls

$$u^*(t) = \begin{bmatrix} -u_c(t) \\ (0, -u_c(t)) \\ (+u_c(t), 0, -u_c(t)) \end{bmatrix} \tag{3.35}$$

the trajectories resulting must terminate at the origin with an interval of $u^*(t) = -u_c(t)$ control, therefore, the terminal segments of these trajectories all lie on curve $B \rightarrow O$ as shown in Figure 14 on page 30. When $u_c(t) = 0$, the state equations become

$$\dot{x}_1(t) = x_2(t) \tag{3.36}$$

$$\dot{x}_2(t) = 0 \tag{3.37}$$

which implies

$$x_2(t) = c_3 \tag{3.38}$$

$$x_1(t) = c_3 t + c_4 \tag{3.39}$$

Time increases and $x_1(t)$ increases or decreases depending on if $x_2(t)$ is greater than or less than zero when control switches to $u_c(t) = 0$, and the trajectories are shown in Figure 15 on page 34.

The trajectories for $u^*(t) = (+-)u_c(t)$ are the same as shown before in Figure 13 on page 29. The two types of trajectories are combined in Figure 16 on page 35. Noting the labels in Figure 16 on page 35, the optimal control laws are derived as follows:

t_1 = time optimal control switches from +1 to 0 (somewhere on C-K)
t_2 = time optimal control switches from 0 to -1 (somewhere on K-O)

On segment K-O

$$x_1^*(t_2) = -\frac{x_2^{*2}(t_2)}{2u_c(t)} \tag{3.40}$$

and integrating

$$\dot{x}_1(t) = x_2(t) \tag{3.41}$$

yields

$$x_1^*(t_2) = x_1^*(t_1) + x_2^*(t_1)[t_2 - t_1] \tag{3.42}$$

Equations (3.29) and (3.32) indicate

$$p_2^*(t_1) = -c_1 t_1 + c_2 = -\lambda \tag{3.43}$$

$$p_2^*(t_2) = -c_1 t_2 + c_2 = +\lambda \tag{3.44}$$

Because

$p_2^*(t_1) = -\lambda$ and
$p_2^*(t_2) = +\lambda$

the necessary condition stated in equation (3.5) requires that for times $t = t_1$ and $t = t_2$:

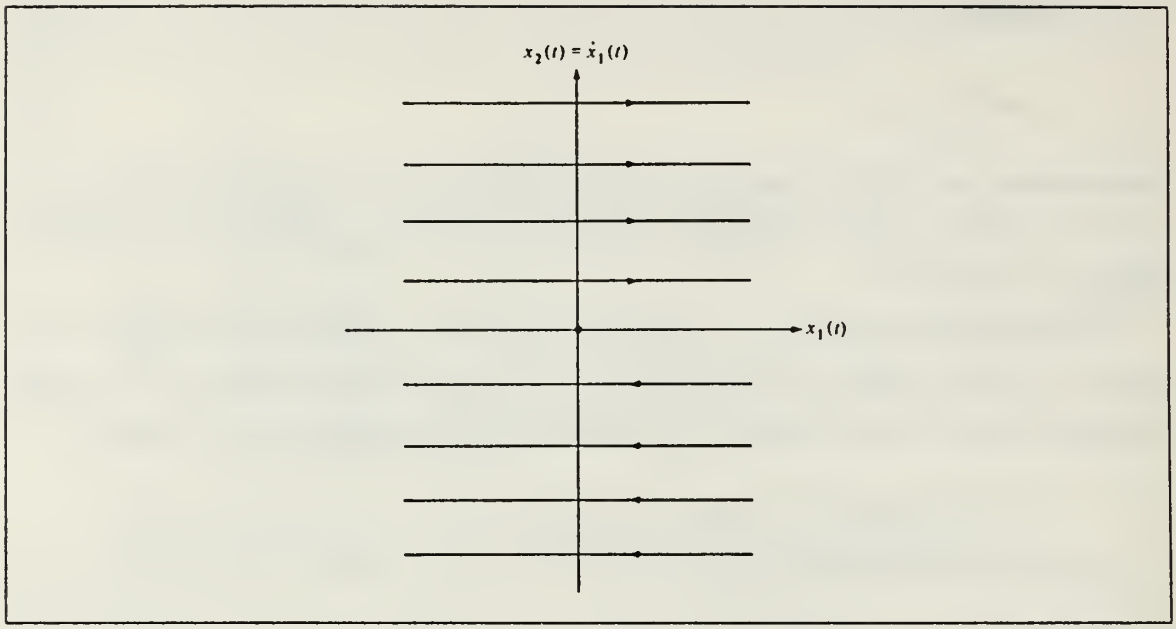

Figure 15. Trajectories for Uc = 0; From [Ref. 8 : p. 280]

$$0 = 1 + \lambda |u_a(t)| + p_1^*(t)x_2^*(t) + p_2^*(t)u_a(t) \tag{3.45}$$

Substituting equations (3.28) and (3.43) into equation (3.45) for time t_1 yields

$$0 = 1 + \lambda |u_a(t_1)| + c_1 x_2^*(t_1) + (-\lambda)u_a(t_1) \tag{3.46}$$

Substituting equations (3.28) and (3.44) into equation (3.45) for time t_2 yields

$$0 = 1 + \lambda |u_a(t_2)| + c_1 x_2^*(t_2) + (+\lambda)u_a(t_2) \tag{3.47}$$

Substituting $u^*(t) = 0$ into equations (3.46) for $t = t_1$ and equation (3.47) for $t = t_2$ yields

$$-1 = c_1 x_2^*(t_1) \tag{3.48}$$

$$-1 = c_1 x_2^*(t_2) \tag{3.49}$$

Now solve equations (3.40) through (3.49) for $x_1^*(t_1)$. Equations (3.48) and (3.49) imply

$$x_2^*(t_1) = x_2^*(t_2) \tag{3.50}$$

Subtracting equation (3.44) from equation (3.43) results in

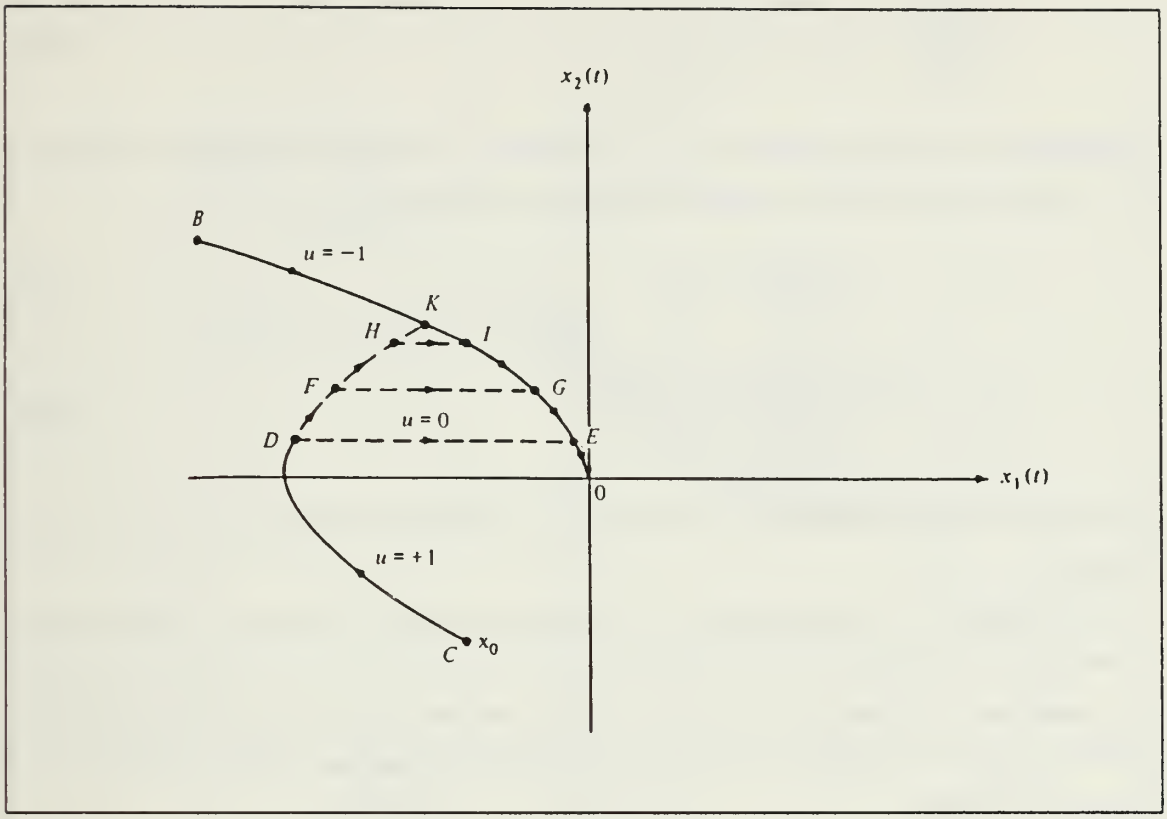

Figure 16. Combined Trajectories for U(t) = 0 and U(t) = (+-)Uc; From [Ref. 8 : p. 281]

$$[t_2 - t_1] = -\frac{2\lambda}{c_1} \tag{3.51}$$

Substituting for c_1 from equation (3.48) into equation (3.51)

$$[t_2 - t_1] = 2\lambda x_2^*(t_1) \tag{3.52}$$

Substitute $[t_2 - t_1]$ from equation (3.52) into equation (3.42) to yield

$$x_1^*(t_2) = x_1^*(t_1) + 2\lambda x_2^{*2}(t_1) \tag{3.53}$$

Equation (3.40) also defines $x_1^*(t_2)$, so equating it with equation (3.53) yields

$$-\frac{x_2^{*2}(t_2)}{2u_c(t_1)} = x_1^2(t_2) + 2\lambda x_2^{*2}(t_1) \tag{3.54}$$

Substituting for $x_2^*(t_2)$ from equation (3.51) into equation (3.54)

$$-\frac{x_2^{*2}(t_1)}{2u_c(t_1)} = x_1^*(t_1) + 2\lambda x_2^{*2}(t_1) \tag{3.55}$$

Combining terms and solving for $x_1^*(t_1)$ in equation (3.55) yields *the equations making up the optimal control law for a weighted-time-fuel control response*

$$x_1^*(t_1) = -\frac{1 + 4\lambda u_c(t_1)}{2u_c(t_1)} x_2^{*2}(t_1) \tag{3.56}$$

$$x_1^*(t_1') = +\frac{1 + 4\lambda u_c(t_1')}{2u_c(t_1')} x_2^{*2}(t_1') \tag{3.57}$$

and equation (3.40) for minimum-time control completes the optimal control law set of equations.

The trajectories corresponding to the optimal control law define the switching curves for weighted-time-fuel optimal performance and are shown for various λ values and initial conditions in Figure 17 on page 37. The weighted-time-fuel optimal trajectories shown in Figure 17 on page 37 also illustrate the *bang-dead zone-bang* characteristic of this type of control.

Using the switching function again, equations (3.56) and (3.57) can be represented by

$$s(x(t)) \equiv x_1^*(t_1) - \frac{1 + 4\lambda u_c(t_1)}{2u_c(t_1)} x_2^*(t_1)|x_2^*(t_1)| \tag{3.58}$$

The switching functions derived in this chapter will be used to implement the optimal control law into the simulation program discussed in the next chapter.

C. DEADBAND CONTROL ABOUT THE ORIGIN

A control deadband about the origin is needed in addition to the weighted-time-fuel optimal control law and corresponding switching curves to implement attitude control for the CER. The deadband allows for the CER attitude to be maintained within a limit cycle bounded by a displacement of $+/-1.25^\circ$ and a a rate of $+/-0.05^\circ$ sec. In addition to the limit cycle deadband, an inner deadband bounded by a displacement of $+/-0.01^\circ$ and a rate of $+/-0.02^\circ$ sec is installed around the origin. When the attitude controller drives the system to within this inner, or *zero* deadband, the simulation or actual logic software shuts off the control acceleration. Without deadbands about the

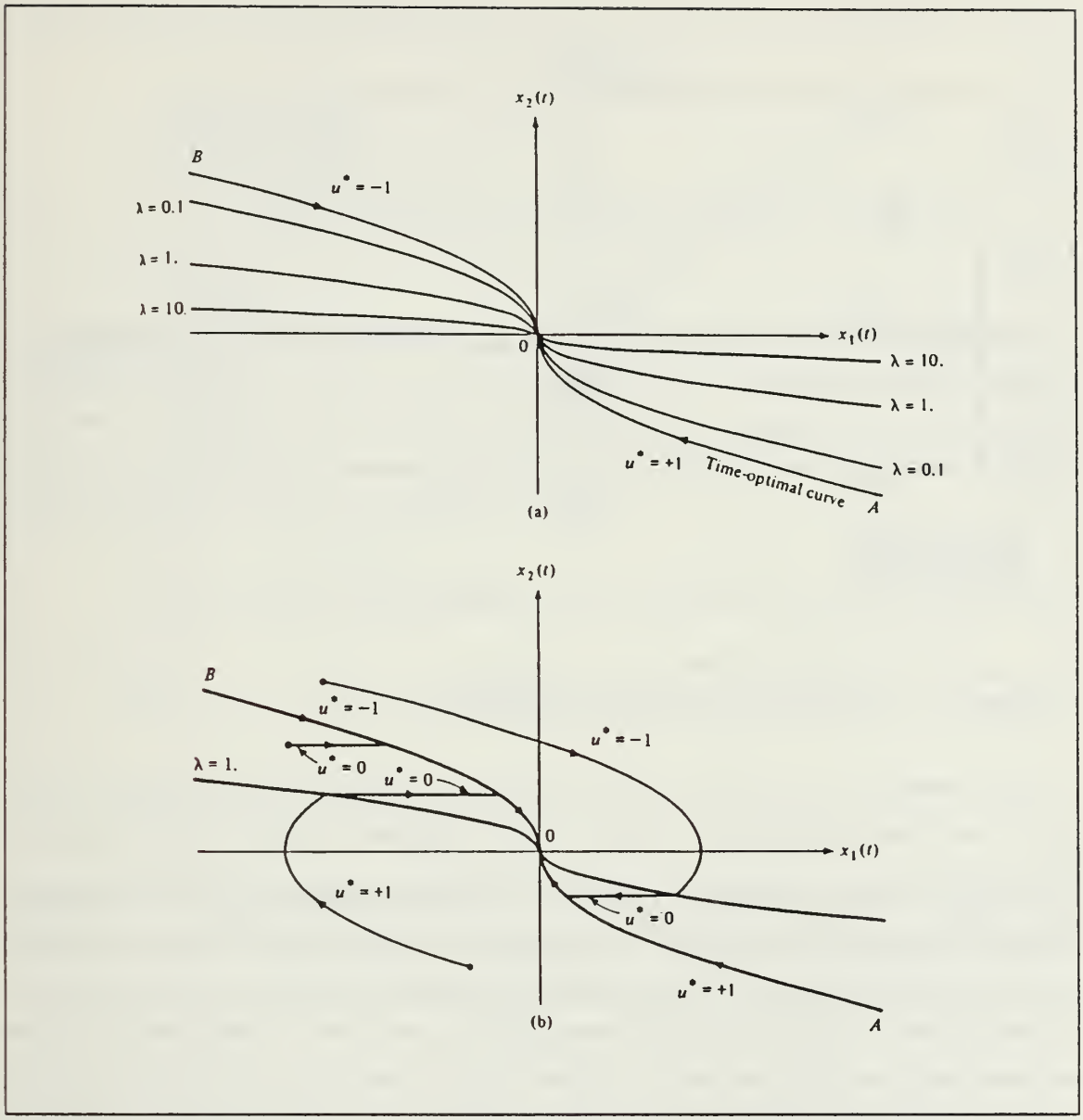

Figure 17. Switching Curves for Weighted-Time-Fuel Optimal Performance; After [Ref. 8 : p. 283]

origin, the controller would *chatter* back and forth around the origin, cycling between positive and negative control accelerations. The residual velocity or any external disturbance torques will eventually drive the system back out to the outer or limit cycle deadband and the control process repeats. An illustration of the two-deadband control scheme is shown in Figure 18 on page 38.

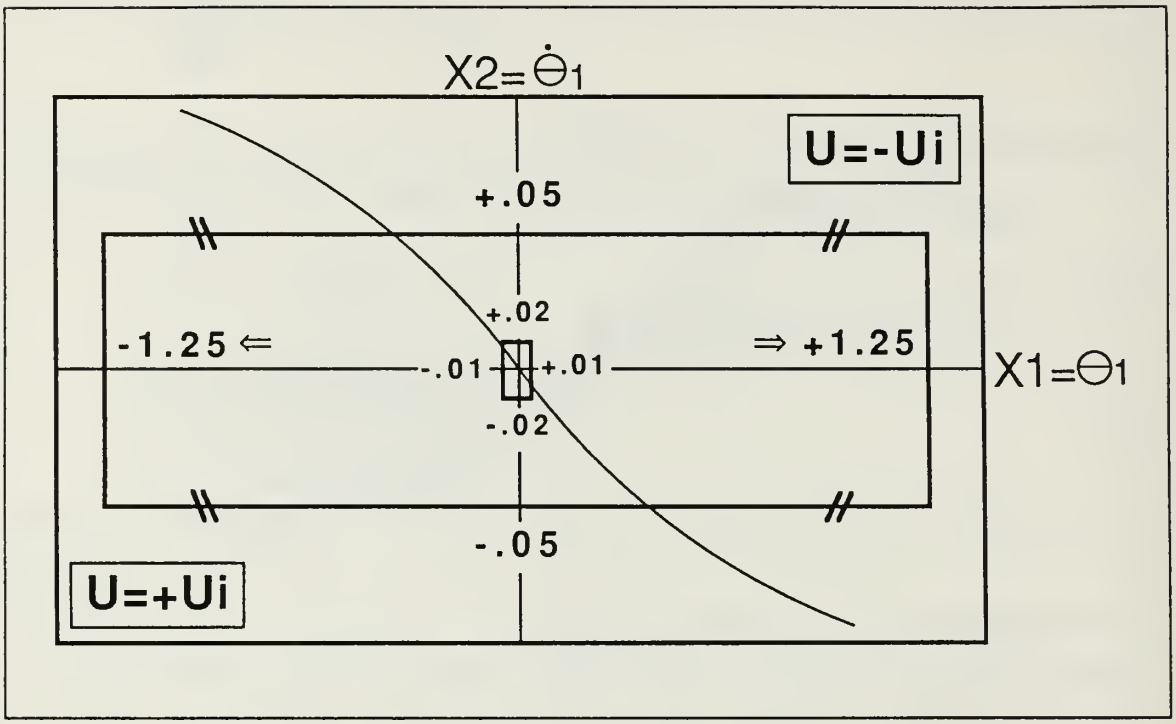

Figure 18. Deadband Control around the Origin.

The *simulation step-size* has a major effect on setting the boundary limits for the inner or zero deadband around the origin. If the step-size is larger than the boundaries, it completely steps over the zero deadband and chatters back and forth, cycling across the deadband without shutting off. For actual operation of the CER, the simulation step-size could be thought of as the minimum impulse specification of the jet thruster. If the minimum impulse time (corresponding to the step-size) is greater than the zero or inner deadband limits, then the controller will not be able to shut down the thruster before the system is already back out of the dead zone. The *rate* boundary limits are more critical due to the switching curves used. The minimum-time curves approach the origin parabolically and the rate changes faster than the displacement as the system is driven along the switching curve.

D. DISCUSSION OF CONTROL ACCELERATIONS.

The normalized control accelerations to be used for each axis are generated by the applied torques for each axis acting on the principal moments of inertia for each axis and are listed as follows:

$$u_{cx}(t) = \dot{\omega}_x = [I_{xx}]^{-1} T_x = \frac{a}{j} T_x \tag{3.59}$$

$$u_{cy}(t) = \dot{\omega}_y = [I_{yy}]^{-1} T_y = \frac{e}{j} T_y \tag{3.60}$$

$$u_{cz}(t) = \dot{\omega}_z = [I_{zz}]^{-1} T_z = \frac{i}{j} T_z \tag{3.61}$$

The normalized control accelerations are also components of the total amount of acceleration acting on all three axes, which includes the cross-coupling effects between axes due to the cross-products of inertia. The sum of the accelerations acting on each of the axes are listed in equations (2.20), (2.21), and (2.22), and are listed below with the control accelerations displayed in bold face:

$$(\ddot{\theta} =)\ \ddot{x}_1 = \frac{\mathbf{a}}{\mathbf{j}} \mathbf{T}_x - \frac{b}{j} T_y + \frac{c}{j} T_z \tag{3.62}$$

$$(\ddot{\psi} =)\ \ddot{x}_2 = -\frac{d}{j} T_x + \frac{\mathbf{e}}{\mathbf{j}} \mathbf{T}_y - \frac{f}{j} T_z \tag{3.63}$$

$$(\ddot{\phi} =)\ \ddot{x}_3 = \frac{g}{j} T_x - \frac{h}{j} T_y + \frac{\mathbf{i}}{\mathbf{j}} \mathbf{T}_z \tag{3.64}$$

The bold face control accelerations above are the *only* components used in the optimal control laws derived in this chapter. Using only the acceleration components generated by the principal moments of inertia to drive the respective states (angular position and velocity), of each axis to zero, *decouples* each axis attitude control from the other axes. It will be shown in the next chapter that, if the sum of the acceleration components (for each axis) generated by the cross-products of inertia is *greater* than the control acceleration component for that axis, then the final state of zero is never reached.

IV. SIMULATION AND RESULTS

A. SIMULATION PROGRAM

Attitude control performance for the CER baseline configuration is computed through computer simulation of a model describing the CER in terms of its equations of motion, total moment of inertia tensor, summation of applied torques, selected initial conditions, and optimal-fuel weighting factors. The equations of motion used in the simulation are represented by equation (2.17), which is presented in component form by equations (3.62), (3.63), and (3.64). The inverse moment of inertia tensor values included in these equations were calculated by substituting the moment of inertia components for *each target capture case* listed in Figure 9 on page 19 into equation (2.19). The baseline configuration control torques included in the equations are listed in Section I.5 on page 4.

1. Simulation Block Model

The simulation program was written using the TUTSIM computer simulation language to accomplish a dynamic simulation of the block model shown in Figure 19 on page 41 [Ref. 9: pp. 1.1-1.3]. Note that the angular acceleration components are integrated twice in succession to yield angular velocity and angular position for each axis. The switching curves and the deadbands about the origin described in Chapter three are used to determine the control acceleration required to drive the system to the desired final state of zero for each axis. The angular velocity and position yielded by the integrators define the *location* of the system on the state-space plot for each axis as previously shown in Figure 17 on page 37. The control acceleration components applied to drive the system to zero help define the switching curves and are listed bold face in equations (3.62), (3.63), and (3.64). The acceleration components (for each axis) generated by the cross-products of inertia act as disturbance accelerations driving the system. They are input through the integrators and subsequently affect the systems location on the state space plots. From Figure 19 on page 41 it is easy to see that if the sum of the acceleration components for an axis generated by the cross-products of inertia is greater than the control acceleration for that axis, then the final state of zero may not be reached. The simulation runs displaying unstable control are expected to have control accelerations less than the cross-product generated acceleration term sums.

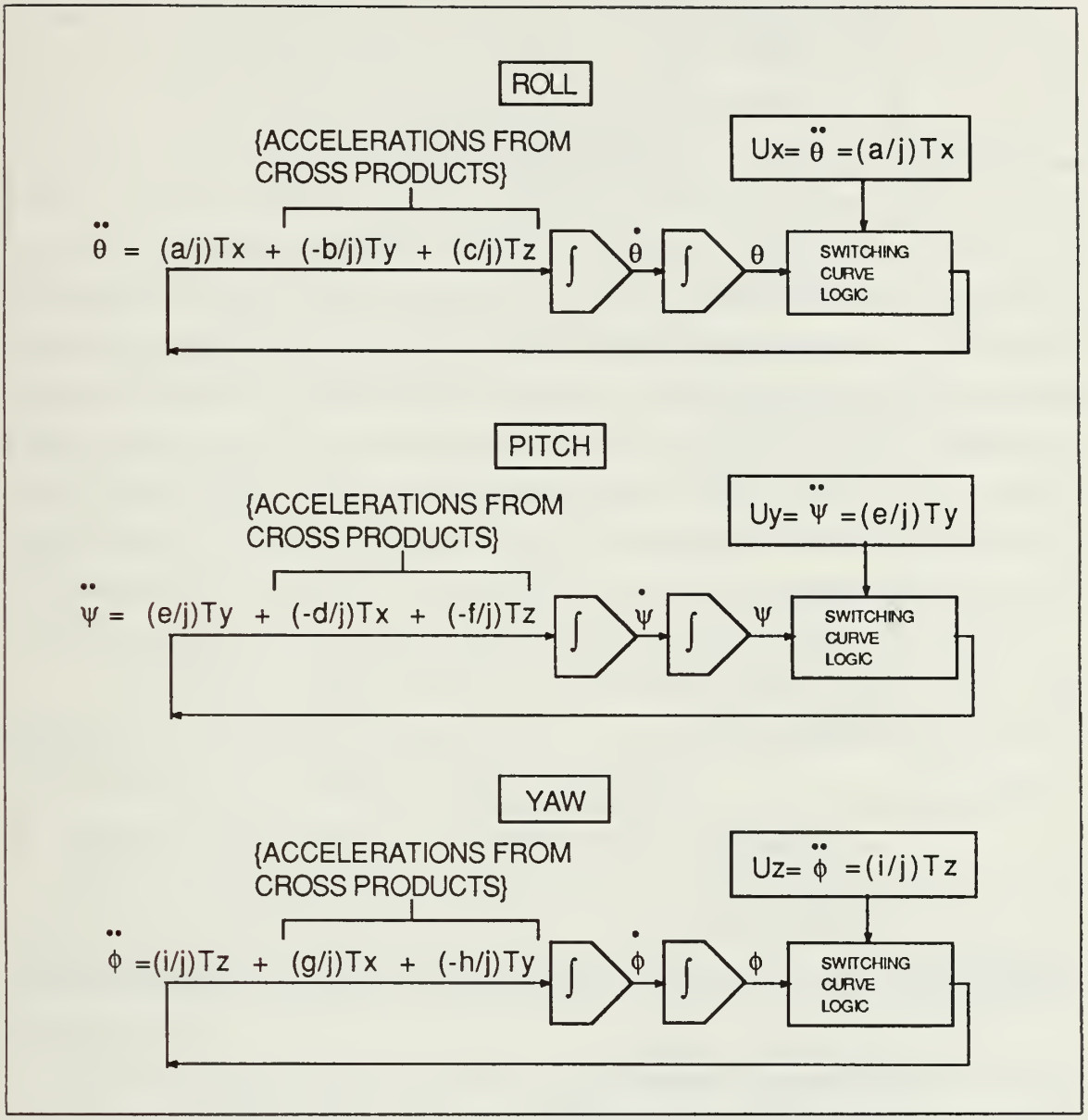

Figure 19. Simulation Block Model of the CER

2. Simulation Inputs

The simulation program is listed in "APPENDIX A. TUTSIM SIMULATION PROGRAM" on page 58 and requires the following inputs to dynamically simulate three-axis attitude control for the CER:

- Three control torques (*ft-lbf*):

$\sum T_x \rightarrow$ (Block 73)

$\sum T_y \rightarrow$ (Block 249)

$\sum T_z \rightarrow$ (Block 450 >

- Nine inverse moment of inertia values $[I]^{-1}$ (*ft-lbf*):

$\frac{a}{j} \rightarrow$ (Block 70)

$\frac{b}{j} \rightarrow$ (Block 240)

$\frac{c}{j} \rightarrow$ (Block 439)

$\frac{d}{j} \rightarrow$ (Block 68)

$\frac{e}{j} \rightarrow$ (Block 239)

$\frac{f}{j} \rightarrow$ (Block 443)

$\frac{g}{j} \rightarrow$ (Block 71)

$\frac{h}{j} \rightarrow$ (Block 243)

$\frac{i}{j} \rightarrow$ (Block 44)

- Three lambda values ($\lambda = 0$ for minimum-time):

$\lambda_x \rightarrow$ (Block 15)
$\lambda_y \rightarrow$ (Block 213)
$\lambda_z \rightarrow$ (Block 413)

- Initial conditions for each axis of angular position in radians and angular velocity in radians second:

Roll position → (Block 1)
Roll velocity → (Block 2)
Pitch position → (Block 201)
Pitch velocity → (Block 200)
Yaw position → (Block 401)
Yaw velocity → (Block 400)

A detailed description of the different types of blocks used in the simulation program can be found in Ref. 9: pp. 6.1-6.83.

3. Simulation Cases

The CER baseline configuration was simulated without a target and with a target captured in different net locations as shown previously in Figure 9 on page 19. The

radian equivalents for the initial conditions of 2° angular position and 0.2°/sec angular velocity are assigned to each axis for all the simulation runs for comparison to allow for easy visualization of the dynamic movement. The initial conditions correspond to the system state values after being offset from the desired reference frame by some disturbance impulse. The angular velocities were assumed to be small and the angular velocity products were dropped from equations (2.13), (2.14), and (2.15). The simulation model is now only applicable to manuevers using small angular velocities. The model is ideal for autonomous attitude-hold simulation since only small position and velocity initial condition offsets are used. The model is not applicable to simulation of commanded rotations (slewing) for minimum-time control of the CER other than making small angle position adjustments since the corresponding maximum angular velocities attained during the manuevers are too large. A weighted-time-fuel optimal control could be used for slewing manuevers since the maximum angular velocities attained would be minimized by the deadzone characteristic of the control. This results in a slower time response to drive the states to zero. A more detailed discussion will follow later in this chapter.

To determine control stability for the selected target capture cases, only minimum-time simulations were initially run. The optimal-fuel weighting factor lambda (λ) for each axis was accordingly assigned a zero value.

B. BASELINE CONFIGURATION SIMULATION RESULTS

The angular position and velocity for each axis were driven to zero from the selected initial conditions using minimum-time control. Of main interest is the *maximum overshoot* attained by the states while being driven to zero and the time it took to initially arrive near zero.

The CER baseline configuration using 1.0 lbf thrusters was simulated for all target-capture cases and the results are shown in Figure 20 on page 44 along with the moment of inertia tensors corresponding to each case. The left-handed arrows indicate the axes where the desired final state of zero was never reached and the unstable overshoots are indicated by the infinity (∞) symbols. The five case/axis combinations experiencing unstable control are from the 850 pound point mass target capture cases. The absolute value of the control acceleration component for each axis experiencing unstable control is less than the absolute value of the sum of the acceleration components generated from the cross-products of inertia.

CASE	MAX OVERSHOOT FROM I.C. = 2°/0.2 °/sec & TIME TO ZERO (sec)	MOMENT OF INERTIA TENSOR
NO TARGET	R 2.1 / 2.9 / 1.5 P 2.1 / 2.3 / 1.5 Y 2.1 / 2.9 / 1.5	$[I] = \begin{bmatrix} 39.6 & 0 & 0 \\ 0 & 55 & 0 \\ 0 & 0 & 55 \end{bmatrix}$
CASE1A (Xmax)	R 2.1 / 2.5 / 1.4 P 2.2 / 0.6 / 8.3 Y ∞ ⇐	$[I] = \begin{bmatrix} 69.3 & 0 & -178.2 \\ 0 & 1153.8 & 0 \\ -178.2 & 0 & 1124.1 \end{bmatrix}$
CASE1B(Ymax)	R 2.0 / 2.1 / 1.9 P ∞ ⇐ Y ∞ ⇐	$[I] = \begin{bmatrix} 98.9 & -110.5 & -110.5 \\ -110.5 & 496.1 & -29.7 \\ -110.5 & -29.7 & 496.1 \end{bmatrix}$
CASE1C(Zmax)	R 2.5 / 0.5 / 15.6 P 2.2 / 0.7 / 6.6 Y 2.1 / 1.2 / 3.8	$[I] = \begin{bmatrix} 369.5 & 0 & -368.4 \\ 0 & 796.4 & 0 \\ -368.4 & 0 & 503.6 \end{bmatrix}$
CASE1D (X=Z,Y=1)	R 2.0 / 2.0 / 2.2 P ∞ ⇐ Y ∞ ⇐	$[I] = \begin{bmatrix} 172.7 & -93.7 & -282.3 \\ -93.7 & 839.7 & -39.8 \\ -282.3 & -39.8 & 732.9 \end{bmatrix}$
CASE2 (MAN+MMU)	R 2.0 / 1.9 / 2.2 P 2.1 / 0.9 / 4.9 Y 2.1 / 0.8 / 6.6	$[I] = \begin{bmatrix} 112.9 & 2.4 & -111.9 \\ 2.4 & 534.9 & 6.4 \\ -111.9 & 6.4 & 497.6 \end{bmatrix}$

Figure 20. Baseline Configuration Simulation Results

The "No Target" case and "Case 1A" angular acceleration components were hand-calculated using equations (3.62), (3.63), and (3.64) to gain further insight into the simulation. The control acceleration magnitude is shown bold face as follows:

- No Target:

$$\ddot{\theta} = \frac{a}{j} T_x - \frac{b}{j} T_y + \frac{c}{j} T_z$$
$$\ddot{\theta} = (.02526)(3) - (0)(3) + (0)(4)$$
$$\ddot{\theta} = .07578 + (0) \quad \text{(stable)}$$
$$\ddot{\psi} = \frac{e}{j} T_y - \frac{d}{j} T_x - \frac{f}{j} T_z$$
$$\ddot{\psi} = (.01818)(3) - (0)(3) - (0)(4)$$
$$\ddot{\psi} = .05454 - (0) \quad \text{(stable)}$$
$$\ddot{\phi} = \frac{i}{j} T_z + \frac{g}{j} T_x - \frac{h}{j} T_y$$
$$\ddot{\phi} = (.01818)(4) + (0)(3) - (0)(3)$$
$$\ddot{\phi} = .07272 + (0) \quad \text{(stable)}$$

- Case 1A:

$$\ddot{\theta} = \frac{a}{j} T_x - \frac{b}{j} T_y + \frac{c}{j} T_z$$
$$\ddot{\theta} = (.02437)(3) - (0)(3) + (.00386)(4)$$
$$\ddot{\theta} = .07311 + .01545 \quad \text{(stable)}$$
$$\ddot{\psi} = \frac{e}{j} T_y - \frac{d}{j} T_x - \frac{f}{j} T_z$$
$$\ddot{\psi} = (.00087)(3) - (0)(3) - (0)(4)$$
$$\ddot{\psi} = .0026 - (0) \quad \text{(stable)}$$
$$\ddot{\phi} = \frac{i}{j} T_z + \frac{g}{j} T_x - \frac{h}{j} T_y$$
$$\ddot{\phi} = (.0015)(4) + (.00386)(3) - (0)(3)$$
$$\ddot{\phi} = .006 + (.01158) \quad \text{(unstable)}$$

Similar calculations for the rest of the cases were completed by the author and for every case of unstable control, the absolute value of the control acceleration magnitude was less than the absolute value of the sum of the acceleration components generated from the cross-products of inertia.

The maximum overshoot values displayed in Figure 20 on page 44 were taken from the simulation runs in state space plot form for each of the axes of every case. The times to initially arrive to zero were taken off the simulation runs of the angular positions versus time plots for every case. The simulation plots are found in "APPENDIX B. SIMULATION PLOTS" on page 62 and the angular positions and velocities are displayed in radians and radians/second respectively. Note that some of the simulations were allowed to run long enough to show the limit cycle resulting from the inner and outer deadband regions.

The author tried various combinations of torque summation values for the three axes in an attempt to reduce the number of unstable cases without changing the CER structure or thruster location. The best combination found after many iterations was

$$\sum T_x = 34 \text{ (ft-lbf)} \tag{4.1}$$

$$\sum T_y = 100 \text{ (ft-lbf)} \tag{4.2}$$

$$\sum T_z = 100 \text{ (ft-lbf)} \tag{4.3}$$

which yielded unstable control about four case/axis combinations as shown in Figure 21 on page 47. The simulation plots are *not* displayed in Appendix B to avoid confusion.

C. PROPOSED CONFIGURATION AND SIMULATION RESULTS

1. Proposed Configuration

The cross-products of inertia must be *reduced* and the summation of control torques about the axes may have to be increased to achieve stable control about all axes of every target capture case. The target capture mechanism can be raised up to center on the $\hat{X}$ axis to reduce the cross-products of inertia. This enables the target to be captured closer to the CER center of gravity, resulting in a reduction of the magnitude of the vector $\mathbf{r}_2$ and the corresponding skew-symmetric matrix as shown previously in Figure 8 on page 18. Equation (2.36) shows that a reduction in the skew-symmetric matrix reduces the total moment of inertia tensor. The following thruster sizes are proposed to be used at the original baseline locations since the torque combination from equations (4.1), (4.2), and (4.3) reduced the number of unstable control axes for the baseline configuration:

$$F_x = 11.3 \text{ lbf} \tag{4.4}$$

$$F_y = 33.33 \text{ lbf} \tag{4.5}$$

$$F_z = 25 \text{ lbf} \tag{4.6}$$

CASE	MAX OVERSHOOT FROM I.C. = 2°/0.2 °/sec & TIME TO ZERO (sec)	MOMENT OF INERTIA TENSOR
NO TARGET	R 2.0 / 9.9 / 0.3 P 2.0 / 14.3 / 0.3 Y 2.0 / 14.3 / 0.3	$[I] = \begin{bmatrix} 39.6 & 0 & 0 \\ 0 & 55 & 0 \\ 0 & 0 & 55 \end{bmatrix}$
CASE1A (Xmax)	R 2.0 / 8.0 / 0.5 P 2.0 / 2.6 / 1.2 Y 2.1 / 2.0 / 2.1	$[I] = \begin{bmatrix} 69.3 & 0 & -178.2 \\ 0 & 1153.8 & 0 \\ -178.2 & 0 & 1124.1 \end{bmatrix}$
CASE1B(Ymax)	R ∞ ⇐ P 2.0 / 2.3 / 2.0 Y 2.0 / 2.3 / 2.0	$[I] = \begin{bmatrix} 98.9 & -110.5 & -110.5 \\ -110.5 & 496.1 & -29.7 \\ -110.5 & -29.7 & 496.1 \end{bmatrix}$
CASE1C(Zmax)	R ∞ ⇐ P 2.0 / 3.9 / 1.0 Y 2.0 / 8.0 / 0.45	$[I] = \begin{bmatrix} 369.5 & 0 & \\ 0 & 796.4 & 0 \\ -368.4 & 0 & 503.6 \end{bmatrix}$
CASE1D (X=Z,Y=1)	R ∞ ⇐ P ∞ ⇐ Y 2.0 / 3.8 / 1.1	$[I] = \begin{bmatrix} 172.7 & -93.7 & -282.3 \\ -93.7 & 839.7 & -39.8 \\ -282.3 & -39.8 & 732.9 \end{bmatrix}$
CASE2 (MAN+MMU)	R 2.0 / 4.8 / 0.8 P 2.0 / 4.7 / 0.8 Y 2.0 / 4.9 / 0.8	$[I] = \begin{bmatrix} 112.9 & 2.4 & -111.9 \\ 2.4 & 534.9 & 6.4 \\ -111.9 & 6.4 & 497.6 \end{bmatrix}$

Figure 21. Baseline Configuration Simulation Results With Tx = 34, Ty = Tz = 100 (ft-lbf)

The CER proposed configuration is illustrated in Figure 22 on page 48, and shows an example of a thruster pair firing to produce a positive roll about $\hat{X}$. Note the capture mechanism is now attached so as to be centered on $\hat{X}$.

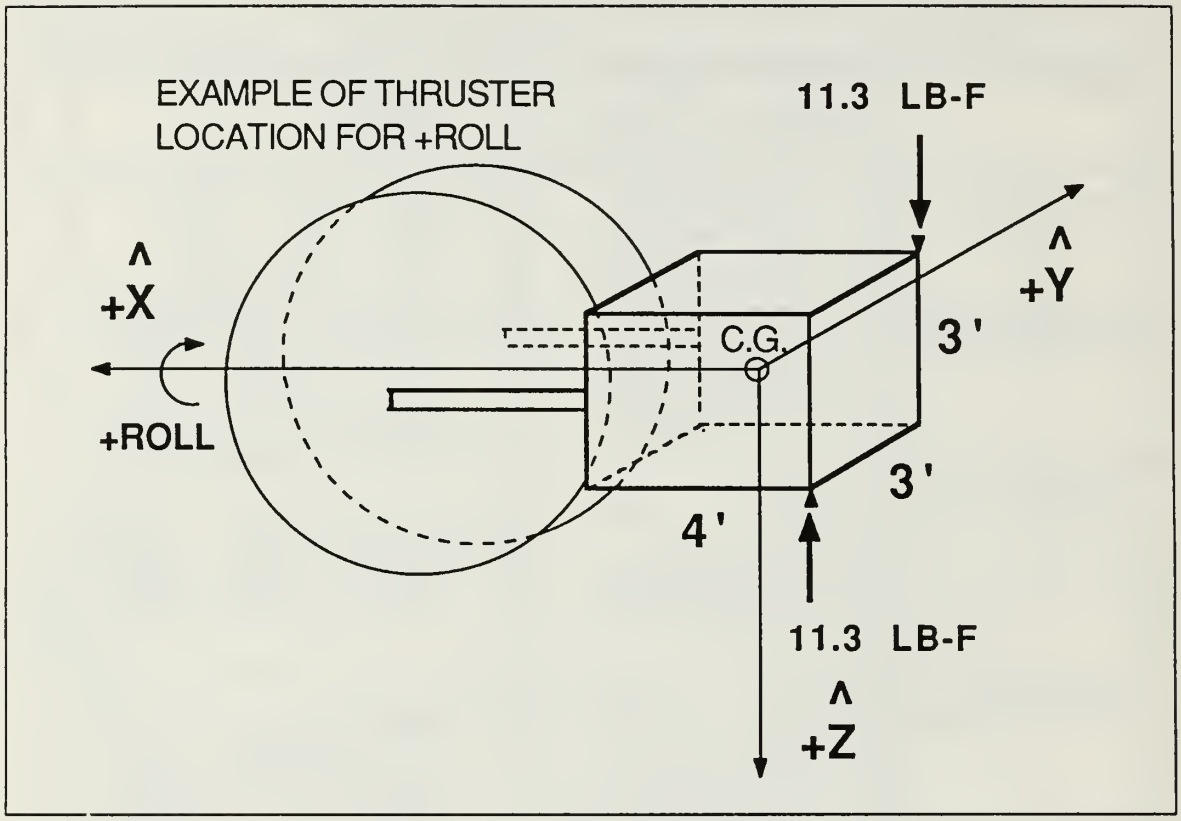

Figure 22. CER Proposed Configuration

2. Proposed Configuration Analysis and Simulation Results

The methods described in Chapter Two for computing the moment of inertia tensors for the selected target capture cases were used to generate the tensors for the proposed configuration. The CER proposed configuration was simulated for all target capture cases and the results are shown in Figure 23 on page 49 along with the moment of inertia tensors corresponding to each case. The left-handed arrow indicates unstable control about the $\hat{X}$ axis for Case 1C target capture. All the other target capture cases have stable control with satisfactory maximum overshoot values.

Case 1C is the 850 pound point mass captured at the bottom of the capture net. The target was brought closer to the center of the net until the simulation produced stable control. Satisfactory stable control occurred with the target located + 2 feet from the net center in the $\hat{Z}$ direction, and is represented by Case 1C.1 in Figure 23 on page 49.

CASE	MAX OVERSHOOT FROM I.C. = 2 °/0.2 °/sec & TIME TO ZERO (sec)	MOMENT OF INERTIA TENSOR
NO TARGET	R 2.0 / 9.9 / 0.3 P 2.0 / 14.3 / 0.4 Y 2.0 / 14.3 / 0.4	$[I] = \begin{bmatrix} 39.6 & 0 & \\ 0 & 55 & 0 \\ 0 & 0 & 55 \end{bmatrix}$
CASE1A (Xmax)	R 2.0 / 9.9 / 0.4 P 2.0 / 2.9 / 1.2 Y 2.0 / 2.9 / 1.2	$[I] = \begin{bmatrix} 39.6 & 0 & 0 \\ 0 & 1124 & 0 \\ 0 & 0 & 1124 \end{bmatrix}$
CASE1B(Ymax)	R 2.0 / 6.4 / 0.6 P 2.0 / 5.1 / 0.77 Y 2.0 / 9.5 / 0.77	$[I] = \begin{bmatrix} 69.3 & -110.5 & 0 \\ -110.5 & 466.4 & 0 \\ 0 & 0 & 496 \end{bmatrix}$
CASE1C (Zmax=3.5')	R ∞ ⇐ P 2.0 / 4.4 / 0.9 Y 2.0 / 7.8 / 0.5	$[I] = \begin{bmatrix} 201.3 & 0 & -257.9 \\ 0 & 628.1 & 0 \\ -257.9 & 0 & 466.4 \end{bmatrix}$
CASE1D (X=Z,Y=1)	R 2.0 / 2.6 / 1.7 P 2.1 / 1.2 / 3.8 Y 2.1 / 1.4 / 3.5	$[I] = \begin{bmatrix} 83 & -93.7 & -141.8 \\ -93.7 & 750 & -19.9 \\ -141.8 & -19.9 & 732.9 \end{bmatrix}$
CASE2 (MAN+MMU)	R 2.0 / 2.9 / 0.8 P 2.0 / 4.7 / 0.8 Y 2.0 / 4.7 / 0.8	$[I] = \begin{bmatrix} 110.4 & 2.4 & -1.4 \\ 2.4 & 549.9 & 6.4 \\ -1.4 & 6.4 & 539.2 \end{bmatrix}$
CASE1C.1 (Zmax=2')	R 2.0 / 3.4 / 1.2 P 2.0 / 4.8 / 0.8 Y 2.0 / 5.6 / 0.7	$[I] = \begin{bmatrix} 92.4 & 0 & -147.4 \\ 0 & 519.2 & 0 \\ -147.4 & 0 & 466.4 \end{bmatrix}$

Figure 23. CER Proposed Configuration Simulation Results

All of the moment of inertia tensors in Figure 23 on page 49 have smaller component magnitudes than the baseline configuration tensors shown in Figure 20 on page 44. The time response to initially drive the system to zero is satisfactory. The simulation plots for the proposed configuration are shown in Appendix B.

3. Proposed Configuration With Baseline Thrusters

The proposed configuration was simulated using 1.0 lbf thrusters in the original baseline locations to minimize changes to the baseline configuration. The simulation results are shown in Figure 24 on page 51 and the left-handed arrows indicate unstable control about 2 axes of Case 1D and 1 axis of Case 1B. The simulation plots are not included in Appendix B to avoid confusion.

D. FUEL OPTIMAL ANALYSIS FOR THE PROPOSED CONFIGURATION

The proposed configuration was simulated using the weighted-time-fuel optimal switching curves with a weighting factor $\lambda = 100$ for each axis. The No Target case was simulated and the simulation plots can be seen in Appendix B. The simulation plots for a positive roll about the $\hat{X}$ axis for minimum-time and weighted-time-fuel optimal control are compared in Figure 25 on page 52. The deadzone on the optimal control plot minimizes the maximum angular velocity value attained. The time response to initially drive the system to zero is increased when compared to minimum-time control.

The simulation plots of position versus time for minimum-time and optimal control with $\lambda = 100$ give the time to complete one limit cycle and the thruster "on times" for one limit cycle as follows:

- Time to complete one limit cycle starting from origin for $\lambda = 0$ (minimum-time):

  Roll → 90 sec
  Pitch → 58 sec
  Yaw → 58 sec

- Time to complete one limit cycle starting from origin for $\lambda = 100$ (optimal-fuel):

  Roll → 140 sec
  Pitch → 110 sec
  Yaw → 110 sec

- "On times" for one limit cycle with $\lambda = 0$:

  Roll → 3 sec
  Pitch → 2 sec
  Yaw → 2 sec

- "On times" for one limit cycle with $\lambda = 100$:

  Roll → 1 sec
  Pitch → 0.4 sec
  Yaw → 0.4 sec

The number of cycles completed during 30 minutes (1800 seconds) of operation is:

- For $\lambda = 0$:

CASE	MAX OVERSHOOT FROM I.C. = 2°/0.2 °/sec & TIME TO ZERO (sec)	MOMENT OF INERTIA TENSOR
NO TARGET	R 2.1 / 2.9 / 1.5 P 2.1 / 2.3 / 1.5 Y 2.1 / 2.9 / 1.5	$[I] = \begin{bmatrix} 39.6 & 0 & \\ 0 & 55 & 0 \\ 0 & 0 & 55 \end{bmatrix}$
CASE1A (Xmax)	R 2.0 / 2.9 / 1.3 P 2.2 / 0.5 / 8.0 Y 2.1 / 0.7 / 6.7	$[I] = \begin{bmatrix} 39.6 & 0 & 0 \\ 0 & 1124 & 0 \\ 0 & 0 & 1124 \end{bmatrix}$
CASE1B(Ymax)	R 2.0 / 2.7 / 1.5 P ∞ ⇐ Y 2.1 / 1.0 / 4.3	$[I] = \begin{bmatrix} 69.3 & -110.5 & 0 \\ -110.5 & 466.4 & 0 \\ 0 & 0 & 496 \end{bmatrix}$
CASE1C (Zmax=3.5')	R 2.1 / 1.7 / 2.7 P 2.2 / 0.8 / 5.5 Y 2.3 / 0.6 / 11	$[I] = \begin{bmatrix} 201.3 & 0 & -257.9 \\ 0 & 628.1 & 0 \\ -257.9 & 0 & 466.4 \end{bmatrix}$
CASE1D (X=Z,Y=1)	R 2.0 / 2.5 / 1.6 P ∞ ⇐ Y ∞ ⇐	$[I] = \begin{bmatrix} 83 & -93.7 & -141.8 \\ -93.7 & 750 & -19.9 \\ -141.8 & -19.9 & 732.9 \end{bmatrix}$
CASE2 (MAN+MMU)	R 2.0 / 1.9 / 2.3 P 2.1 / 0.9 / 5.0 Y 2.1 / 1.0 / 4.3	$[I] = \begin{bmatrix} 110.4 & 2.4 & -1.4 \\ 2.4 & 549.9 & 6.4 \\ -1.4 & 6.4 & 539.2 \end{bmatrix}$

Figure 24. Proposed Configuration Simulation Results Using 1.0 lbf Thrusters

$$\text{Roll} \rightarrow \frac{1800 \text{ sec}}{90 \text{ sec cycle}} = 20 \text{ cycles}$$

$$\text{Pitch and Yaw} \rightarrow \frac{1800 \text{ sec}}{58 \text{ sec/cycle}} = 31 \text{ cycles}$$

- For $\lambda = 100$:

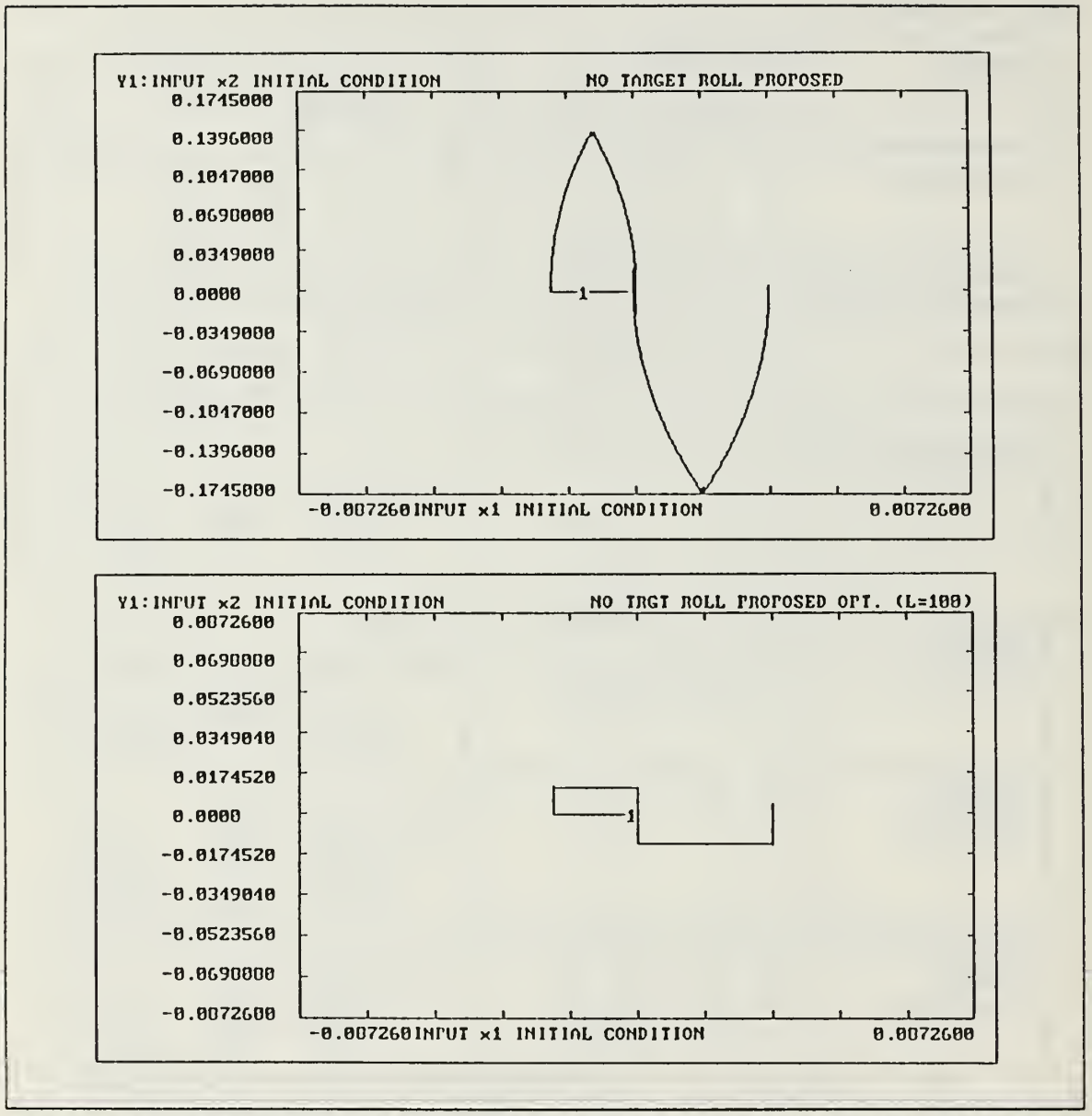

Figure 25. Comparison of Minimum-Time and Optimal Fuel (Lambda = 100) Roll Axis Control for "No Target"

$$\text{Roll} \rightarrow \frac{1800 \text{ sec}}{140 \text{ sec/cycle}} = 12.9 \text{ cycles}$$

$$\text{Pitch and Yaw} \rightarrow \frac{1800 \text{ sec}}{110 \text{ sec/cycle}} = 16.4 \text{ cycles}$$

Total "on time" for one thruster is found by multiplying the number of cycles by the on time per cycle to yield

- For $\lambda = 0$:

  Roll → 60 sec
  Pitch and Yaw → 62 sec

- For $\lambda = 100$:

  Roll → 12.9 sec
  Pitch and Yaw → 6.6 sec

Two thrusters fire per axis or six thrusters total fire as needed for three-axis control. The thruster flow rate is chosen for analysis to be 0.5 pounds/second of nitrogen (N_2). Fuel-optimal analysis for the proposed configuration is summarized in Figure 26 on page 54.

E. END-OF-MISSION ANALYSIS FOR THE PROPOSED CONFIGURATION

The CER mass will decrease by approximately 150 pounds at the end of its mission when the total nitrogen propellant is used up. The CER mass is reduced to 700 pounds and when a worst-case 850 pound target is captured the center of gravity is closer to the target than at the beginning of the mission. The shift in the center of gravity does not effect the summation of torques about the axes since the thrusters are fired in pairs. The decrease in the CER mass (M_1) reduces the total moment of inertia tensors for all target capture cases as shown in equation (2.36). The moment of inertia tensor for the CER without a target at the end of the mission is reduced to:

$$I_{CER} = \begin{bmatrix} 32.6 & 0 & 0 \\ 0 & 45 & 0 \\ 0 & 0 & 45 \end{bmatrix}$$

and the reduction improves minimum-time control. The reduction of the moment of inertia tensors improves the minimum-time control for all target capture cases as shown in Figure 27 on page 55.

FUEL OPTIMAL ANALYSIS FOR PROPOSED CONFIG. OF CER WITHOUT TARGET	LAMBDA = 0 (MIN TIME)	LAMBDA = 100 (OPT. FUEL)
TOTAL "ON" TIME DURING 30 MINUTES OPERATION WITH 6 THRUSTERS	368 SECONDS	52 SECONDS
TOTAL N2 USED DURING 30 MINUTES OPERATION	18.4 LBS	2.6 LBS
"TIME TO ZERO" FROM I.C.: 2° / 0.2°/ SEC	R, P, Y } 0.3 SECONDS	R, P, Y } 3 SECONDS

Figure 26. Fuel Optimal Analysis for Proposed Configuration

CASE (END OF MISSION)	MAX OVERSHOOT FROM I.C. = 2°/0.2°/sec & TIME TO ZERO (sec)	MOMENT OF INERTIA TENSOR
CASE1A (Xmax)	R 2.0 / 9.9 / 0.4 P 2.0 / 3.4 / 1.1 Y 2.0 / 3.4 / 1.1	$[I] = \begin{bmatrix} 39.6 & 0 & 0 \\ 0 & 1124 & 0 \\ 0 & 0 & 1124 \end{bmatrix}$
CASE1B(Ymax)	R 2.0 / 6.7 / 0.8 P 2.0 / 5.1 / 0.8 Y 2.0 / 5.0 / 0.8	$[I] = \begin{bmatrix} 69.3 & -110.5 & 0 \\ -110.5 & 466.4 & 0 \\ 0 & 0 & 496 \end{bmatrix}$
CASE1C.1 (Zmax=2')	R 2.0 / 3.7 / 1.1 P 2.0 / 5.0 / 0.5 Y 2.0 / 5.9 / 0.4	$[I] = \begin{bmatrix} 92.4 & 0 & -147.4 \\ 0 & 519.2 & 0 \\ -147.4 & 0 & 466.4 \end{bmatrix}$
CASE1D (X=Z,Y=1)	R 2.0 / 2.9 / 1.5 P 2.0 / 2.1 / 2.1 Y 2.0 / 2.2 / 2.0	$[I] = \begin{bmatrix} 83 & -93.7 & -141.8 \\ -93.7 & 750 & -19.9 \\ -141.8 & -19.9 & 732.9 \end{bmatrix}$
CASE2 (MAN+MMU)	R 2.0 / 6.9 / 0.5 P 2.1 / 5.0 / 0.7 Y 2.1 / 5.0 / 0.7	$[I] = \begin{bmatrix} 110.4 & 2.4 & -1.4 \\ 2.4 & 549.9 & 6.4 \\ -1.4 & 6.4 & 539.2 \end{bmatrix}$

Figure 27. End-of-Mission Simulation Results for the Proposed Configuration

V. CONCLUSIONS AND RECOMMENDATIONS

A. CONCLUSIONS

The CER baseline configuration of 1.0 lbf thrusters and capture mechanism attached at the bottom of the CER did not provide effective control during capture of a worst-case 850 pound target. Changing the thruster size and location to increase the summation of torques about the axes did not provide effective control during target capture. The unstable control cases were shown to be caused by the acceleration components generated from the cross-products of inertia.

The CER proposed configuration with increased summation of torques about the axes and capture mechanism attached along the $\hat{X}$ axis provides an effective control during all cases of target capture except for Case 1C (+- roll). The unstable control became stable when the target distance from the center of the net was reduced from 3.5 feet to 2 feet on the $\hat{Z}$ axis. Control stability was dramatically improved by moving the capture mechanism closer to the CER center of gravity resulting in a reduction of the cross-products of inertia for target capture operation.

Weighted-time-fuel optimal control with $\lambda = 100$ reduced propellant use by 85% for the selected example but increased the time response to drive the system to zero by a factor of 10. The maximum angular velocity values attained are minimized by the dead zone of the optimal control. Weighted-time-fuel optimal control could be used during coasting periods between orbits when a minimum-time response is not required or for slow commanded rotations (slewing) since the angular velocities are minimized.

Control performance is improved at the end of the mission due to the decrease in mass of the CER. The center of gravity shift, as the mass of the CER is reduced, does not effect the summation of control torques about the axes for the CER with target.

B. RECOMMENDATIONS

The capture mechanism should be attached *along the* $\hat{X}$ *axis* to reduce the distance between the CER center of gravity and the target center of gravity. The cross-products of inertia will be reduced and control stability will be improved.

The baseline thruster configuration should be changed to provide control torques as follows if the CER model used is similar to the model presented in this research:

$$\sum T_x = 34 \text{ ft-lbf}$$
$$\sum T_y = 100 \text{ ft-lbf}$$
$$\sum T_z = 100 \text{ ft-lbf}$$

The baseline thruster *location* could be used to facilitate storage of the CER and to minimize changes in the baseline configuration if the thruster size is increased to

$$F_x = 11.3 \text{ lbf}$$
$$F_y = 33.3 \text{ lbf}$$
$$F_z = 25 \text{ lbf}$$

Weighted-time-fuel optimal control could be used during coasting periods, between orbits or for slow or small commanded rotations, when a minimum-time response is not required. Operation of the CER with target may require immediate minimum-time response and probably should not use weighted-time-fuel optimal control.

The proposed attitude control scheme is simple and effective but is sensitive to target capture location in the capture net. Ensuring the target is captured *as close as possible* to the CER center of gravity will reduce the cross-products of inertia and improve the design and operational attitude control performance.

The control laws used to implement simulation of the CER model are in terms of the control accelerations generated from the principal moments of inertia and of the angular position and velocity for each of the axes. A *more complicated control law* could be used in terms of the control accelerations, angular positions, and angular velocities for the three axes in combination. A switching surface or volume corresponding to the control law would be less sensitive to the cross-product of inertia effects as opposed to the simple switching curves used in these analyses.

The research presented should assist the CER preliminary design phase team in completing some of the attitude control trade-off analyses. Ultimately, this will result in a more practical and safe crew and equipment retriever for space station.

APPENDIX A. TUTSIM SIMULATION PROGRAM

The TUTSIM simulation program will simulate three-axis stabilization for a model described in terms of the sum of the torques applied and the system moment of inertia tensor including non-zero cross-product terms. The program is shown in Figure 28 on page 59, and continued in Figure 29 on page 60, and Figure 30 on page 61. The first 199 block numbers are reserved for the Roll axis, blocks 200 through 399 are for the Pitch axis, and blocks 400 through 599 are for the Yaw axis. The interconnecting inverse moment of inertia terms are interspersed throughout the program. The inputs to the simulation program are listed in Section IV.2 on page 41. The simulation is sensitive to the step-size used since the inner or zero deadband boundries are small. A step-size of .001 worked nicely most of the time. If the simulation chatters at the origin, reduce the step-size. The specific example to follow is for the CER baseline configuration with no target.

```
PROFESSIONAL VERSION OF TUTSIM

Model File: cerbsnt
Date:     2 /    28 /  1989
Time:    13 :    45
Timing:   0.0400000  ,DELTA  ;  10.000E+03  ,RANGE
PlotBlocks and Scales:
Format:
     BlockNo,  Plot-MINimum,  Plot-MAXimum;  Comment
Horz:     I ,  -5.0000     ,   5.0000     ; INPUT x1 INITIAL CONDITION
  Y1:     2 ,  -5.0000     ,   5.0000     ; INPUT x2 INITIAL CONDITION
  Y2:       ,              ,              ;
  Y3:       ,              ,              ;
  Y4:       ,              ,              ;


   0.0350000       1 INT     2                ;INPUT x1 INITIAL CONDITION
   0.0035000       2 INT    67                ;INPUT x2 INITIAL CONDITION
                   3 SUM     1     10         ;x1+(0.5/Ucx)x2[x2]
   0.0000          4 REL     8     -8     -8  ;sign(xI)
                             1
   0.5000000       5 CON
   1.0000          6 CON
   0.0000          7 CON
                   8 MUL    70     73         ;(a/j)Tx-Ucx
                  10 MUL     2     11     66  ;(0.5/Ucx)x2[x2]
                  11 ABS     2                ;[x2]
                  12 SUM     1     13         ;x1+((1+4LUcx)/(2Ucx))x2[x2]
                  13 MUL     2     11     22  ;((1+4LUcx)/(2Ucx))x2[x2]
   4.0000         14 CON
   0.0000         15 CON                      ;INPUT lambda(-L),(optimal wtng)
                  16 MUL    14     15      8  ;4LUcx
                  17 SUM     6     16         ;1+4LUcx
   2.0000         18 CON
                  19 MUL    18      8         ;2Ucx
                  20 IFE    44     47     21  ;begin dead zone
                  21 IFE    43      7    -47  ;leave dead zone
                  22 DIV    17     19         ;(1+4LUcx)/(2Ucx)
                  37 INV    38                ;true if outside zero rect.
                  38 AND    48     41         ;inside zero rect.
 350.000E-06      39 CON                      ;INPUT zero rect. velocity (x2)
                  40 ABS     1                ;[x1]
                  41 SUM    39    -11         ;0.001-[x2]
                  42 IFE    38      7     46  ;inside zero rect.?
                  43 MUL     4      3         ;(x1+(0.5/Ucx)x2[x2])sign(x1)
                  44 MUL     4     12         ;(Block #12)sign(x1)
                  45 MUL     1      2         ;x1*x2
                  46 IFE    45     -4     20  ;set U for 1st&3rd quad
   0.0000         47 REL     8     -8     -8  ;sign(x2)
                             2
                  48 SUM    49    -40         ;0.01-[x1]
 175.000E-06      49 CON                      ;INPUT zero rect. position (x1)
                  56 ORR    59     61         ;outside outer rect.?
                  57 INV    56                ;true if inside outer rect.
   0.0218000      58 CON                      ;INPUT outer rect. position
                  59 SUM   -58     40         ;[x1]-1.25
 872.000E-06      60 CON                      ;INPUT outer rect. velocity
                  61 SUM   -60     11         ;[x2]-.01
```

Figure 28. TUTSIM Simulation Program (First Page)

```
                62 IFE     38      7     42  ;U=0 if inside zero rect.
    1.0000      63 SRS     37     57         ;I.D. and loop thru regions
                64 AND     63     37         ;compare loop and location
                65 IFE     64     62      7  ;U=0 until outside
                66 DIV      5      8         ;0.5/Ucx
                67 SUM     65    241    440  ;sum of control inputs
    0.0000      68 CON                      ;INPUT d/j
                69 MUL    -68     73         ;(-d/j)Tx
    0.0252640   70 CON                      ;INPUT a/j
    0.0000      71 CON                      ;INPUT g/j
                72 MUL     71     73         ;(g/j)Tx
    3.0000      73 CON                      ;INPUT Tx
    0.0035000  200 INT    242              ;INPUT y2 INITIAL CONDITION
    0.0350000  201 INT    200              ;INPUT y1 INITIAL CONDITION
               202 SUM    201    207         ;y1+(0.5/Ucy)y2[y2]
    0.0000     203 REL    204   -204   -204  ;sign(y1)
                          201
               204 MUL    239    249         ;(e/j)Ty=Ucy
    0.5000000  205 CON
               206 DIV    205    204         ;0.5/Ucy
               207 MUL    200    208    206  ;(0.5/Ucy)y2[y2]
               208 ABS    200               ;[y2]
    0.0000     209 CON
    0.0000     210 REL    204   -204   -204  ;sign(y2)
                          200
               211 IFE    212    209   -210  ;leave deadzone
               212 MUL    203    202         ;(y1+(0.5/Ucy)y2[y2])sign(y1)
    0.0000     213 CON                      ;INPUT lambda=L,(opt. fuel wtng)
               214 MUL    200    208    248  ;((1+4LUcy)/(2Ucy))y2[y2]
               215 SUM    201    214         ;y1+((1+4LUcy)/(2Lcy))y2[y2]
               216 MUL    203    215         ;(Block #215)sign(y1)
               217 IFE    216    210    211  ;begin deadzone
               218 MUL    201    200         ;y1*y2
               219 IFE    218   -203    217  ;set Uy for 1st&3rd quadrants
               220 IFE    222    209    219  ;inside zero rectangle?
               221 IFE    222    209    220  ;Uy=0 if inside zero rectangle
               222 AND    225    223         ;inside zero rectangle?
               223 SUM    224   -208         ;0.001-[y2]
  350.000E-06  224 CON                      ;INPUT zero rect. velocity (y2)
               225 SUM    226   -227         ;0.01-[y1]
  175.000E-06  226 CON                      ;INPUT zero rect. position (y1)
               227 ABS    201               ;[y1]
    0.0218000  228 CON                      ;INPUT outer rectangle position
  872.000E-06  229 CON                      ;INPUT outer rectangle velocity
               230 SUM   -228    227         ;[y1]-1.25
               231 SUM   -229    208         ;[y2]-.01
               232 ORR    230    231         ;outside outer rectangle?
               233 INV    232               ;true if inside outer rectangle
               234 INV    222               ;true if outside zero rectangle
    1.0000     235 SRS    234    233         ;Identify and loop thru regions
               236 AND    235    234         ;compare loop and location
               237 IFE    236    221    209  ;Uy=0 until outside
    0.0181843  239 CON                      ;INPUT (e/j)
    0.0000     240 CON                      ;INPUT (b/j)
               241 MUL   -240    249         ;(-b/j)Ty
               242 SUM     69    237    444  ;sum of control torques
    0.0000     243 CON                      ;INPUT (h/j)
               244 MUL   -243    249         ;(-h/j)Ty
               245 MUL     14    213    204  ;4LUcy
               246 SUM      6    245         ;1+4LUcy
```

Figure 29. TUTSIM Simulation Program (Second Page)

```
                247 MUL     18    204          ;2Ucy
                248 DIV    246    247          ;(1+4LUcy)/(2Ucy)
  3.0000        249 CON                        ;INPUT Ty
  0.0035000     400 INT    445                 ;INPUT z2 INITIAL CONDITION
  0.0350000     401 INT    400                 ;INPUT z1 INITIAL CONDITION
                402 SUM    401    407          ;z1+(0.5/Ucz)z2[z2]
  0.0000        403 REL    404   -404   -404   ;sign(z1)
                           401
                404 MUL    441    450          ;(i/j)Tz-Ucz
  0.5000000     405 CON
                406 DIV    405    404          ;0.5/Ucz
                407 MUL    400    408    406   ;(0.5/Ucz)z2[z2]
                408 ABS    400                 ;[z2]
  0.0000        409 CON
  0.0000        410 REL    404   -404   -404   ;sign(z2)
                           400
                411 IFE    412    409   -410   ;leave deadzone
                412 MUL    403    402          ;(z1+(0.5/Ucz)z2[z2])sign(z1)
  0.0000        413 CON                        ;INPUT lambda=L,(opt. fuel wtng)
                414 MUL    400    408    449   ;((1+4LUcz)/(2Ucz))z2[z2]
                415 SUM    401    414          ;z1+((1+4LUcz)/(2Ucz))z2[z2]
                416 MUL    403    415          ;(Block #415)sign(z1)
                417 IFE    416    410    411   ;begin deadzone
                418 MUL    401    400          ;z1*z2
                419 IFE    418   -403    417   ;set Uz for 1st&3rd quadrants
                420 IFE    422    409    419   ;inside zero rectangle?
                421 IFE    422    409    420   ;Uz=0 if inside zero rectangle
                422 AND    425    423          ;inside zero rectangle?
                423 SUM    424   -408          ;0.001-[z2]
350.000E-06     424 CON                        ;INPUT zero rect. velocity (z2)
                425 SUM    426   -427          ;0.01-[z1]
175.000E-06     426 CON                        ;INPUT zero rect. position (z1)
                427 ABS    401
  0.0218000     428 CON                        ;INPUT outer rectangle position
872.000E-06     429 CON                        ;INPUT outer rect. velocity
                430 SUM   -428    427          ;[z1]-1.25
                431 SUM   -429    408          ;[z2]-.01
                432 ORR    430    431          ;outside outer rectangle?
                433 INV    432                 ;true if inside outer rectangle
                434 INV    422                 ;true if outside zero rectangle
  1.0000        435 SRS    434    433          ;Identify and loop thru regions
                436 AND    435    434          ;compare loop and location
                437 IFE    436    421    409   ;Uz=0 until outside
  0.0000        439 CON                        ;INPUT (c/j)
                440 MUL    439    450          ;(c/j)Tz
  0.0181843     441 CON                        ;INPUT (i/j)
  0.0000        443 CON                        ;INPUT (f/j)
                444 MUL   -443    450          ;(-f/j)Tz
                445 SUM     72    244    437   ;sum of control torques
                446 MUL     14    413    404   ;4LUcz
                447 MUL     18    404          ;2Ucz
                448 SUM      6    446          ;1+4LUcz
                449 DIV    448    447          ;(1+4LUcz)/(2Ucz)
  4.0000        450 CON                        ;INPUT Tz
```

Figure 30. TUTSIM Simulation Program (Third Page)

APPENDIX B. SIMULATION PLOTS

	BlockNo,	Plot-MINImum,	Plot-MAXImum;	Comment
Horz:	0 ,	0.0000 ,	10.0000 ;	Time
Y1:	1 ,	-0.0872600 ,	0.0872600 ;	INPUT x1 INITIAL CONDITION
Y2:	201 ,	-0.0872600 ,	0.0872600 ;	INPUT y1 INITIAL CONDITION
Y3:	401 ,	-0.0872600 ,	0.0872600 ;	INPUT z1 INITIAL CONDITION
Y4:	,	,	;	

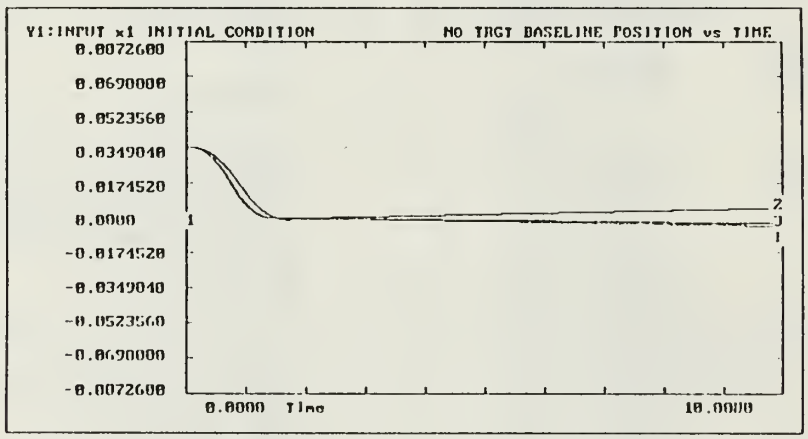

	BlockNo,	Plot-MINImum,	Plot-MAXImum;	Comment
Horz:	1 ,	-0.0872600 ,	0.0872600 ;	INPUT x1 INITIAL CONDITION
Y1:	2 ,	-0.0872600 ,	0.0872600 ;	INPUT x2 INITIAL CONDITION
Y2:	,	,	;	
Y3:	,	,	;	
Y4:	,	,	;	

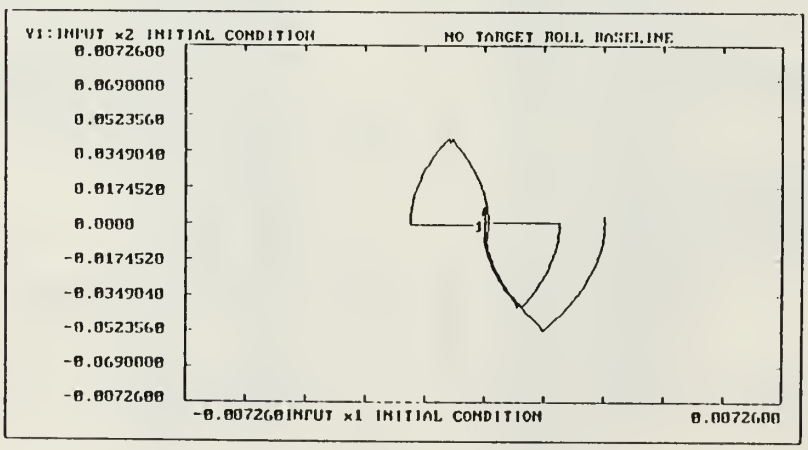

Figure 31. Simulation Plots for Baseline No Target

```
        BlockNo,   Plot-MINimum,   Plot-MAXimum;   Comment
Horz:     201 ,    -0.0872600   ,    0.0872600   ; INPUT y1 INITIAL CONDITION
  Y1:     200 ,    -0.0872600   ,    0.0872600   ; INPUT y2 INITIAL CONDITION
  Y2:         ,                 ,                ;
  Y3:         ,                 ,                ;
  Y4:         ,                 ,                ;
```

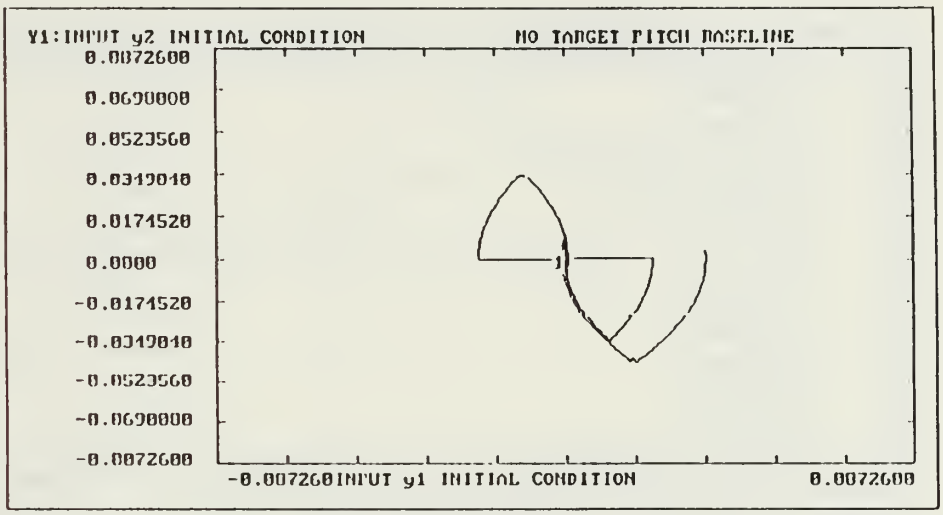


```
        BlockNo,   Plot-MINimum,   Plot-MAXimum;   Comment
Horz:     401 ,    -0.0872600   ,    0.0872600   ; INPUT z1 INITIAL CONDITION
  Y1:     400 ,    -0.0872600   ,    0.0872600   ; INPUT z2 INITIAL CONDITION
  Y2:         ,                 ,                ;
  Y3:         ,                 ,                ;
  Y4:         ,                 ,                ;
```

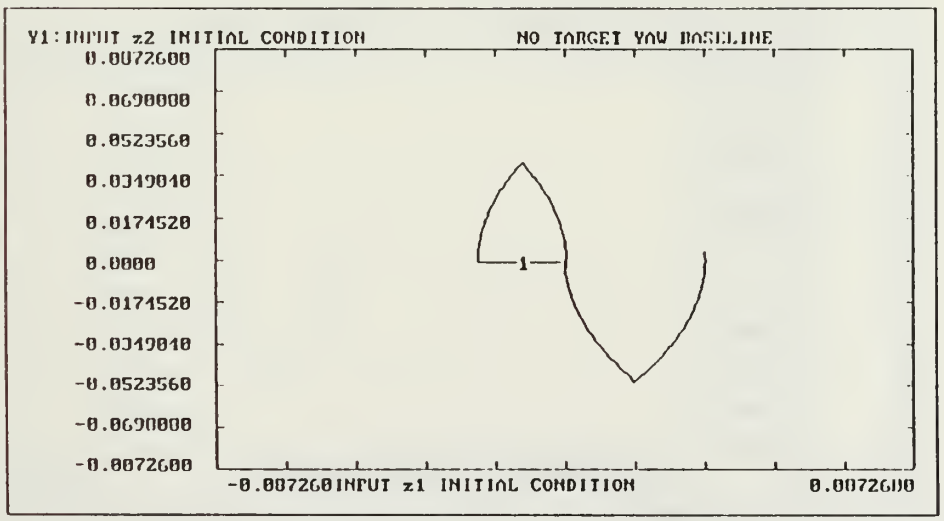

Figure 32. Baseline No Target

```
      BlockNo,   Plot-MINimum,   Plot-MAXimum;  Comment
Horz:      0 ,    0.0000      ,  10.0000      ; Time
  Y1:      1 ,   -0.0872600   ,   0.0872600   ; INPUT x1 INITIAL CONDITION
  Y2:    201 ,   -0.0872600   ,   0.0872600   ; INPUT y1 INITIAL CONDITION
  Y3:    401 ,   -0.0872600   ,   0.0872600   ; INPUT z1 INITIAL CONDITION
  Y4:        ,                ,               ;
```

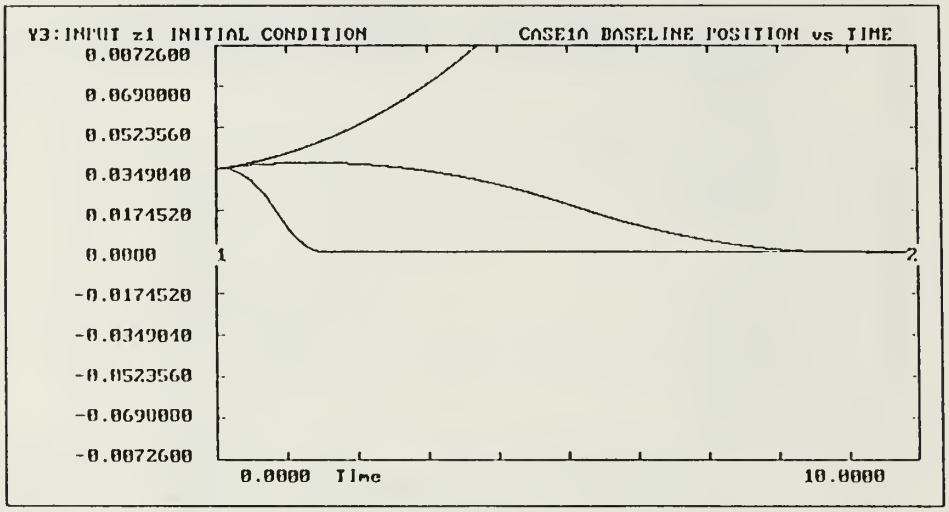


```
      BlockNo,   Plot-MINimum,   Plot-MAXimum;  Comment
Horz:      1 ,   -0.0872600   ,   0.0872600   ; INPUT x1 INITIAL CONDITION
  Y1:      2 ,   -0.0872600   ,   0.0872600   ; INPUT x2 INITIAL CONDITION
  Y2:        ,                ,               ;
  Y3:        ,                ,               ;
  Y4:        ,                ,               ;
```

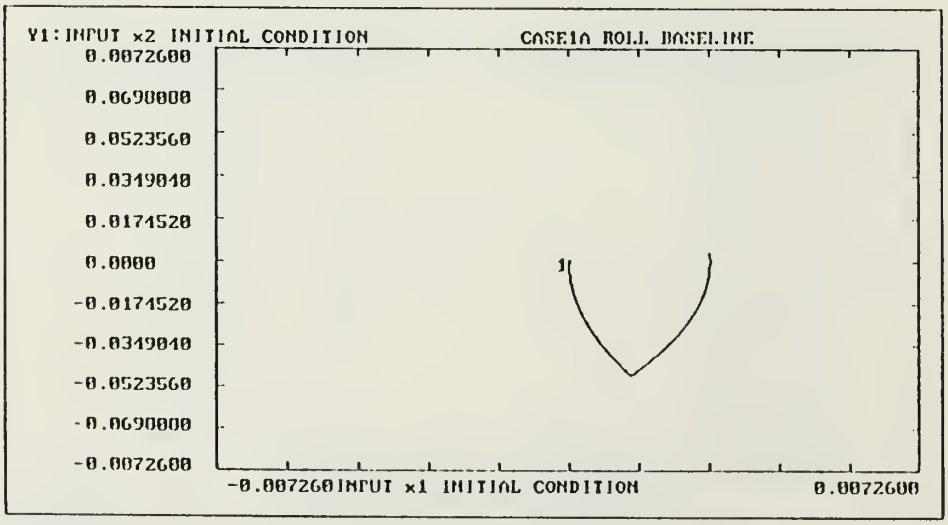

Figure 33. Baseline Case 1A

```
        BlockNo,   Plot-MINimum,   Plot-MAXimum;   Comment
Horz:    201 ,    -0.0872600  ,     0.0872600  ;  INPUT y1 INITIAL CONDITION
  Y1:    200 ,    -0.0872600  ,     0.0872600  ;  INPUT y2 INITIAL CONDITION
  Y2:        ,                ,                ;
  Y3:        ,                ,                ;
  Y4:        ,                ,                ;
```

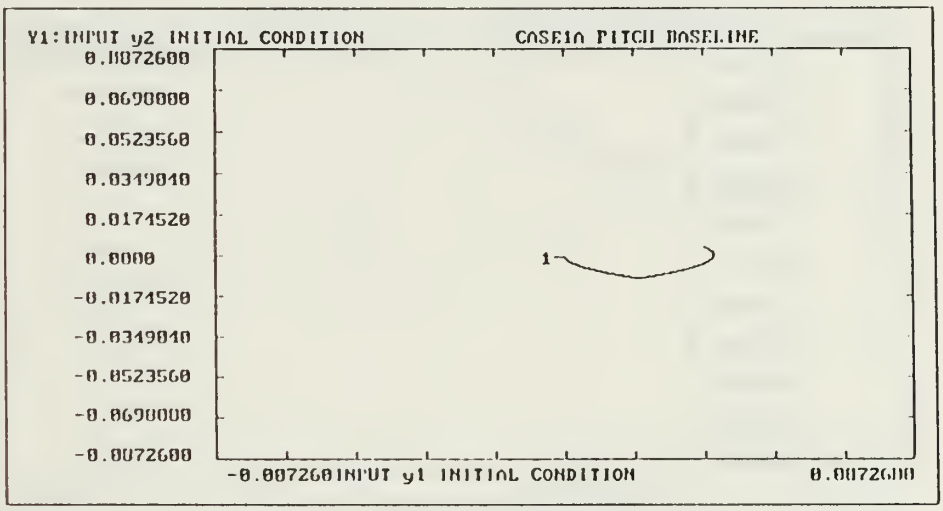


```
        BlockNo,   Plot-MINimum,   Plot-MAXimum;   Comment
Horz:    401 ,    -0.0872600  ,     0.0872600  ;  INPUT z1 INITIAL CONDITION
  Y1:    400 ,    -0.0872600  ,     0.0872600  ;  INPUT z2 INITIAL CONDITION
  Y2:        ,                ,                ;
  Y3:        ,                ,                ;
  Y4:        ,                ,                ;
```

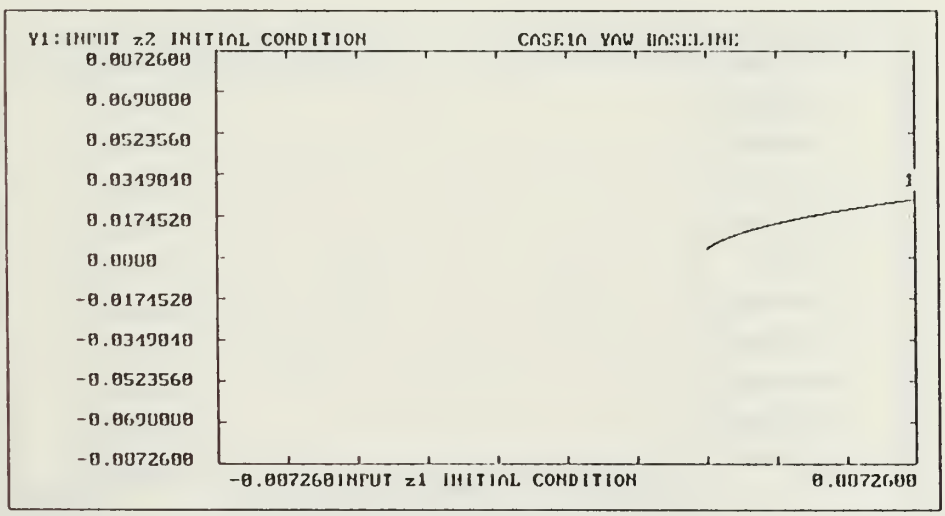

Figure 34. Baseline Case 1A

```
        BlockNo,   Plot-MINImum,   Plot-MAXImum;  Comment
Horz:       0 ,     0.0000     ,   10.0000      ; Time
  Y1:       1 ,    -0.0870000  ,    0.0870000   ; INPUT x1 INITIAL CONDITION
  Y2:     201 ,    -0.0870000  ,    0.0870000   ; INPUT y1 INITIAL CONDITION
  Y3:     401 ,    -0.0870000  ,    0.0870000   ; INPUT z1 INITIAL CONDITION
  Y4:         ,                ,                ;
```

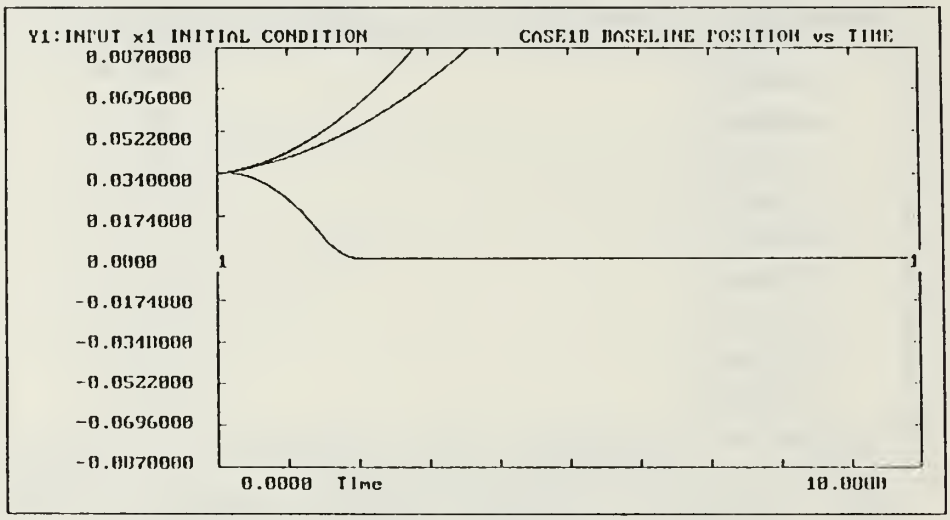


```
        BlockNo,   Plot-MINImum,   Plot-MAXImum;  Comment
Horz:       1 ,    -0.0870000  ,    0.0870000   ; INPUT x1 INITIAL CONDITION
  Y1:       2 ,    -0.0870000  ,    0.0870000   ; INPUT x2 INITIAL CONDITION
  Y2:         ,                ,                ;
  Y3:         ,                ,                ;
  Y4:         ,                ,                ;
```

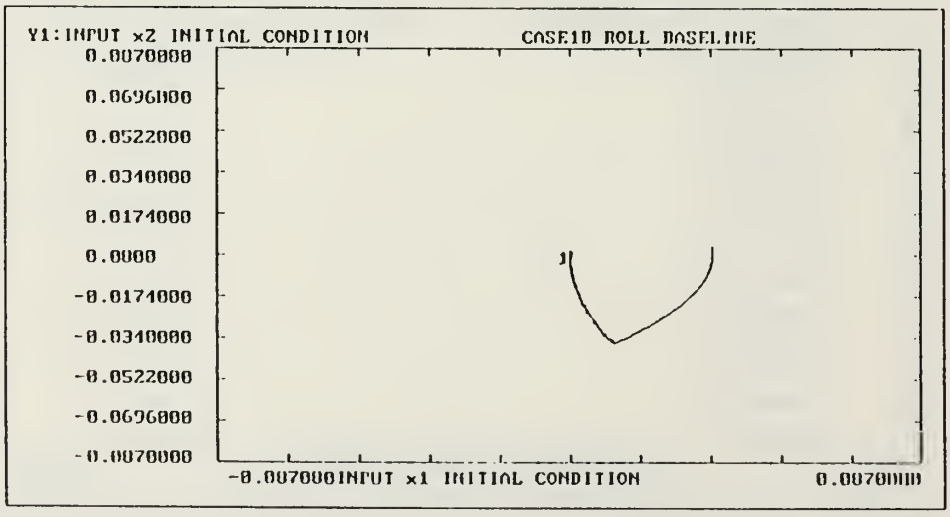

Figure 35. Baseline Case 1B

```
      BlockNo,   Plot-MINimum,   Plot-MAXimum;   Comment
Horz:   201 ,   -0.0870000   ,    0.0870000   ; INPUT y1 INITIAL CONDITION
  Y1:   200 ,   -0.0870000   ,    0.0870000   ; INPUT y2 INITIAL CONDITION
  Y2:       ,                ,                ;
  Y3:       ,                ,                ;
  Y4:       ,                ,                ;
```

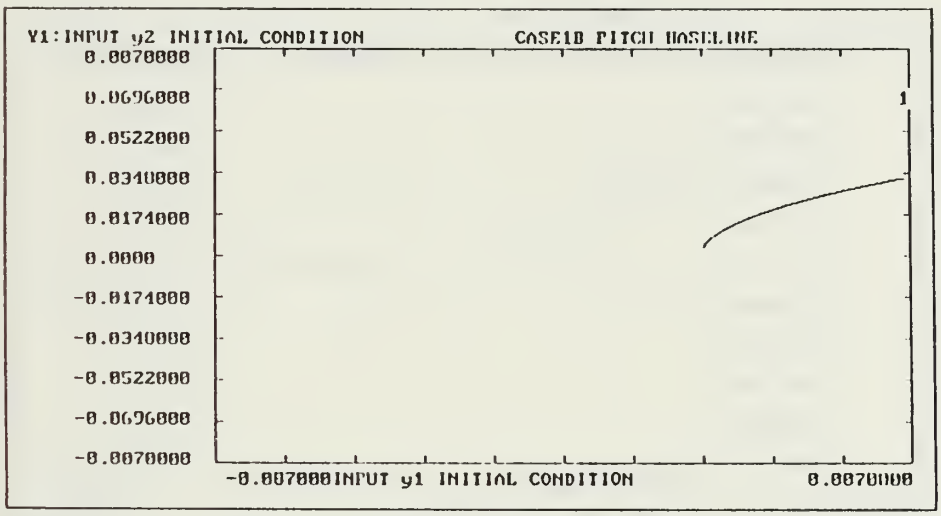


```
      BlockNo,   Plot-MINimum,   Plot-MAXimum;   Comment
Horz:   401 ,   -0.0870000   ,    0.0870000   ; INPUT z1 INITIAL CONDITION
  Y1:   400 ,   -0.0870000   ,    0.0870000   ; INPUT z2 INITIAL CONDITION
  Y2:       ,                ,                ;
  Y3:       ,                ,                ;
  Y4:       ,                ,                ;
```

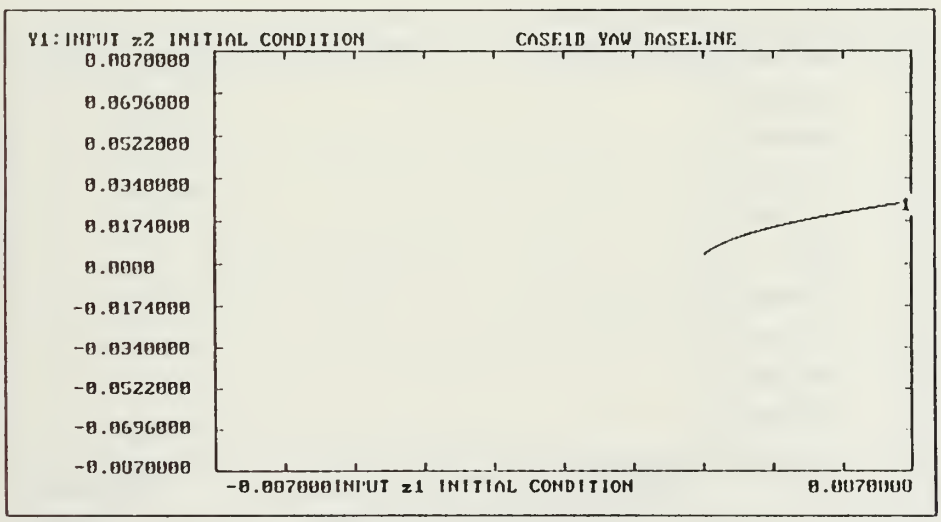

Figure 36. Baseline Case 1B

```
      BlockNo,   Plot-MINImum,   Plot-MAXImum;   Comment
Horz:     0 ,    0.0000      ,  20.0000      ; Time
  Y1:     1 ,   -0.0870000   ,   0.0870000   ; INPUT x1 INITIAL CONDITION
  Y2:   201 ,   -0.0870000   ,   0.0870000   ; INPUT y1 INITIAL CONDITION
  Y3:   401 ,   -0.0870000   ,   0.0870000   ; INPUT z1 INITIAL CONDITION
  Y4:       ,                ,              ;
```

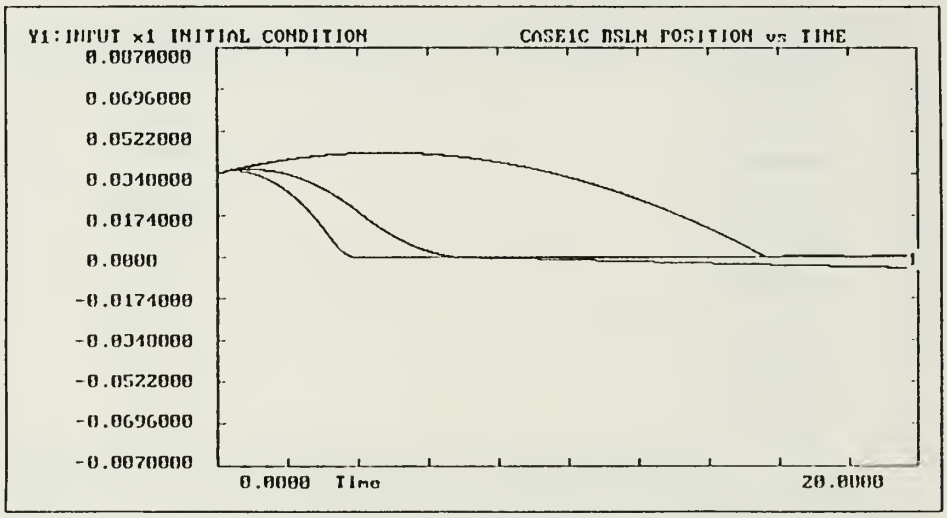


```
      BlockNo,   Plot-MINImum,   Plot-MAXImum;   Comment
Horz:     1 ,   -0.0870000   ,   0.0870000   ; INPUT x1 INITIAL CONDITION
  Y1:     2 ,   -0.0870000   ,   0.0870000   ; INPUT x2 INITIAL CONDITION
  Y2:       ,                ,              ;
  Y3:       ,                ,              ;
  Y4:       ,                ,              ;
```

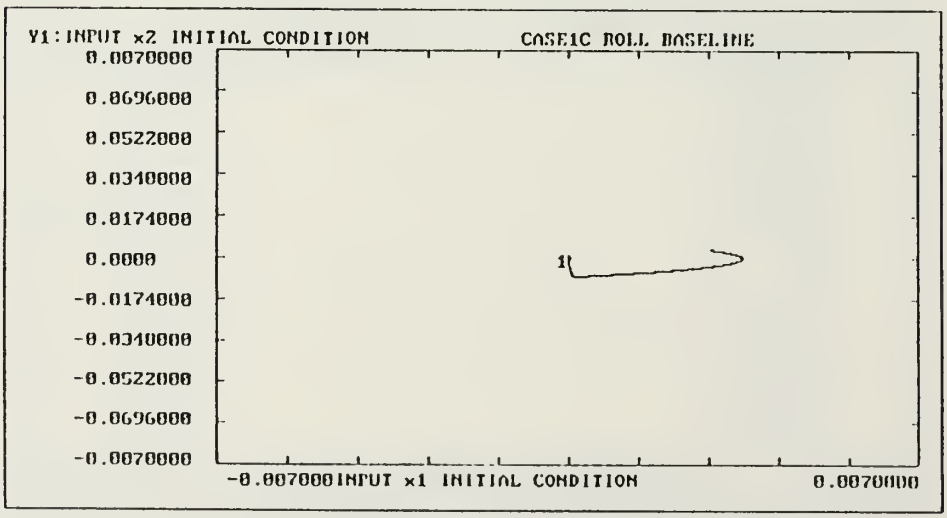

Figure 37. Baseline Case 1C

```
      BlockNo,   Plot-MINimum,   Plot-MAXimum;  Comment
Horz:   201 ,   -0.0870000   ,    0.0870000   ; INPUT y1 INITIAL CONDITION
  Y1:   200 ,   -0.0870000   ,    0.0870000   ; INPUT y2 INITIAL CONDITION
  Y2:       ,                ,                ;
  Y3:       ,                ,                ;
  Y4:       ,                ,                ;
```

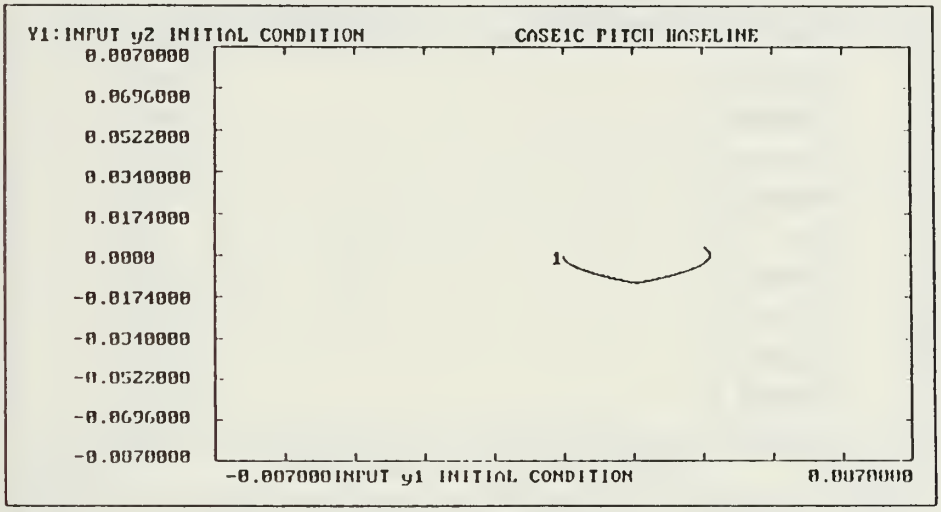


```
      BlockNo,   Plot-MINimum,   Plot-MAXimum;  Comment
Horz:   401 ,   -0.0870000   ,    0.0870000   ; INPUT z1 INITIAL CONDITION
  Y1:   400 ,   -0.0870000   ,    0.0870000   ; INPUT z2 INITIAL CONDITION
  Y2:       ,                ,                ;
  Y3:       ,                ,                ;
  Y4:       ,                ,                ;
```

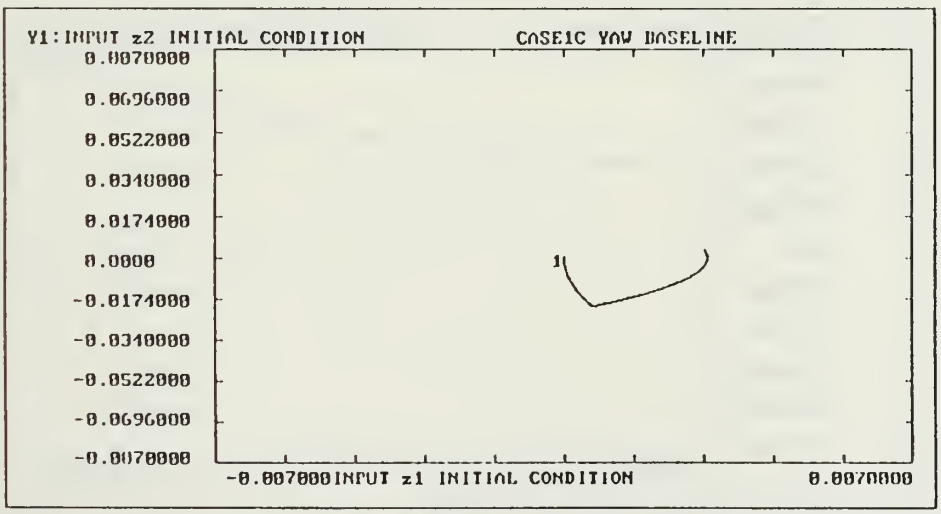

Figure 38. Baseline Case 1C

```
      BlockNo,   Plot-MINimum,   Plot-MAXimum;  Comment
Horz:     1 ,   -0.0870000   ,    0.0870000   ; INPUT x1 INITIAL CONDITION
  Y1:     2 ,   -0.0870000   ,    0.0870000   ; INPUT x2 INITIAL CONDITION
  Y2:       ,                ,                ;
  Y3:       ,                ,                ;
  Y4:       ,                ,                ;
```

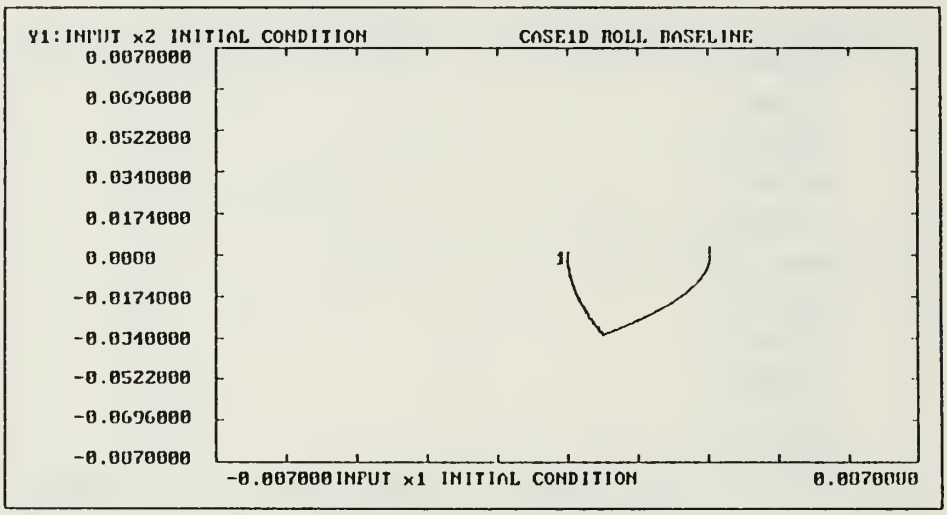


```
      BlockNo,   Plot-MINimum,   Plot-MAXimum;  Comment
Horz:     0 ,     0.0000     ,    3.0000     ; Time
  Y1:     1 ,   -0.0870000   ,    0.0870000   ; INPUT x1 INITIAL CONDITION
  Y2:   201 ,   -0.0870000   ,    0.0870000   ; INPUT y1 INITIAL CONDITION
  Y3:   401 ,   -0.0870000   ,    0.0870000   ; INPUT z1 INITIAL CONDITION
  Y4:       ,                ,                ;
```

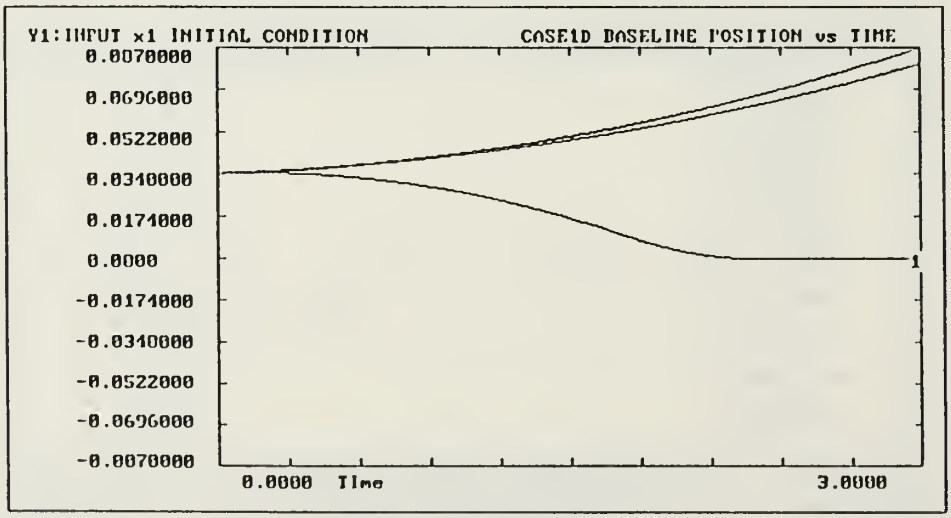

Figure 39. Baseline Case 1D

```
      BlockNo,   Plot-MINimum,   Plot-MAXimum;   Comment
Horz:   201 ,   -0.0870000   ,    0.0870000   ; INPUT y1 INITIAL CONDITION
  Y1:   200 ,   -0.0870000   ,    0.0870000   ; INPUT y2 INITIAL CONDITION
  Y2:       ,                ,                ;
  Y3:       ,                ,                ;
  Y4:       ,                ,                ;
```

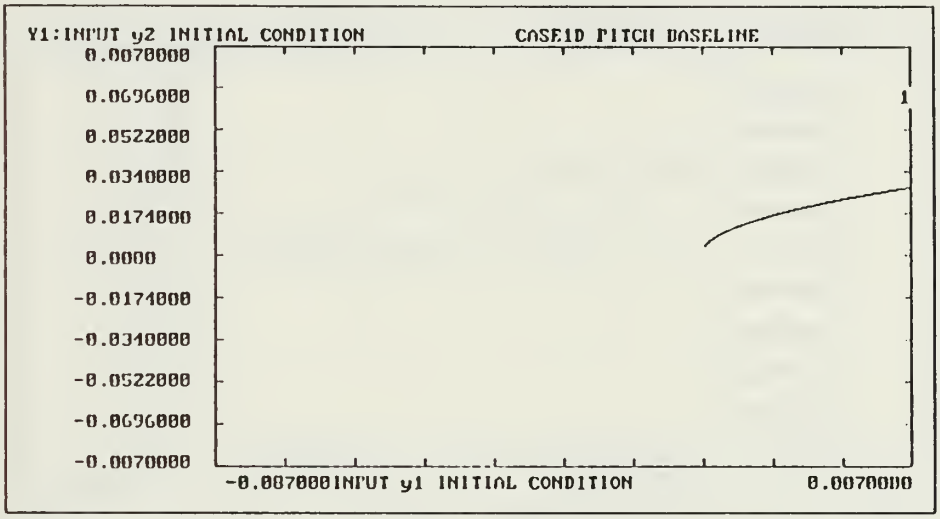


```
      BlockNo,   Plot-MINimum,   Plot-MAXimum;   Comment
Horz:   401 ,   -0.0870000   ,    0.0870000   ; INPUT z1 INITIAL CONDITION
  Y1:   400 ,   -0.0870000   ,    0.0870000   ; INPUT z2 INITIAL CONDITION
  Y2:       ,                ,                ;
  Y3:       ,                ,                ;
  Y4:       ,                ,                ;
```

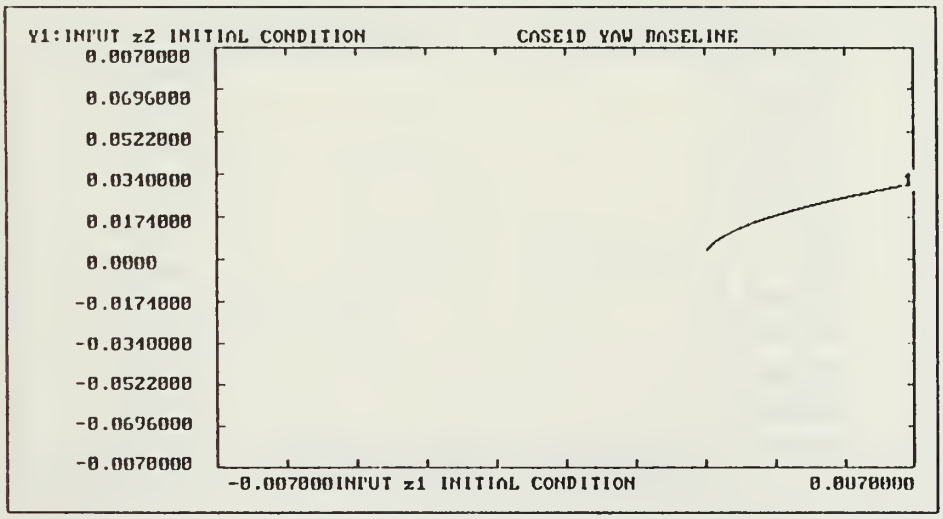

Figure 40. Baseline Case 1D

```
      BlockNo,   Plot-MINimum,   Plot-MAXimum;  Comment
Horz:     0 ,    0.0000      ,  10.0000      ; Time
  Y1:     1 ,   -0.0870000   ,   0.0870000   ; INPUT x1 INITIAL CONDITION
  Y2:   201 ,   -0.0870000   ,   0.0870000   ; INPUT y1 INITIAL CONDITION
  Y3:   401 ,   -0.0870000   ,   0.0870000   ; INPUT z1 INITIAL CONDITION
  Y4:       ,                ,               ;
```

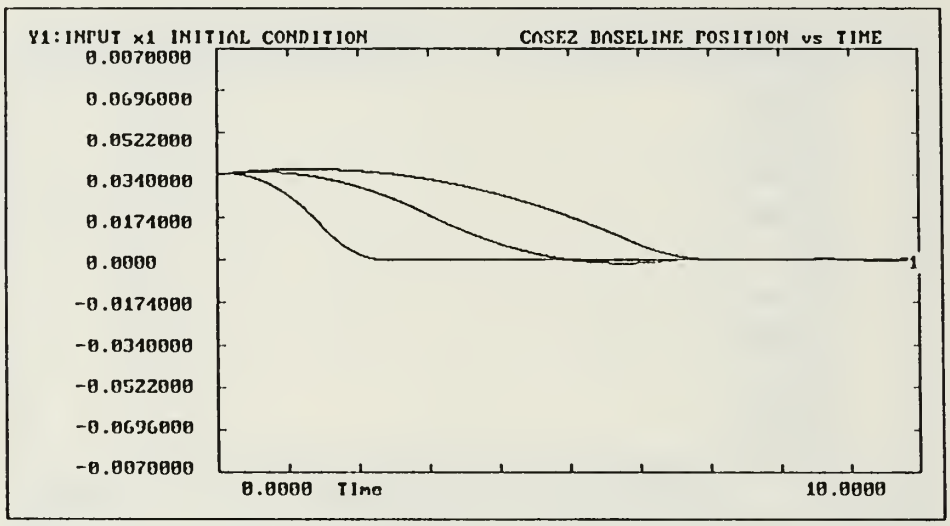


```
      BlockNo,   Plot-MINimum,   Plot-MAXimum;  Comment
Horz:     1 ,   -0.0870000   ,   0.0870000   ; INPUT x1 INITIAL CONDITION
  Y1:     2 ,   -0.0870000   ,   0.0870000   ; INPUT x2 INITIAL CONDITION
  Y2:       ,                ,               ;
  Y3:       ,                ,               ;
  Y4:       ,                ,               ;
```

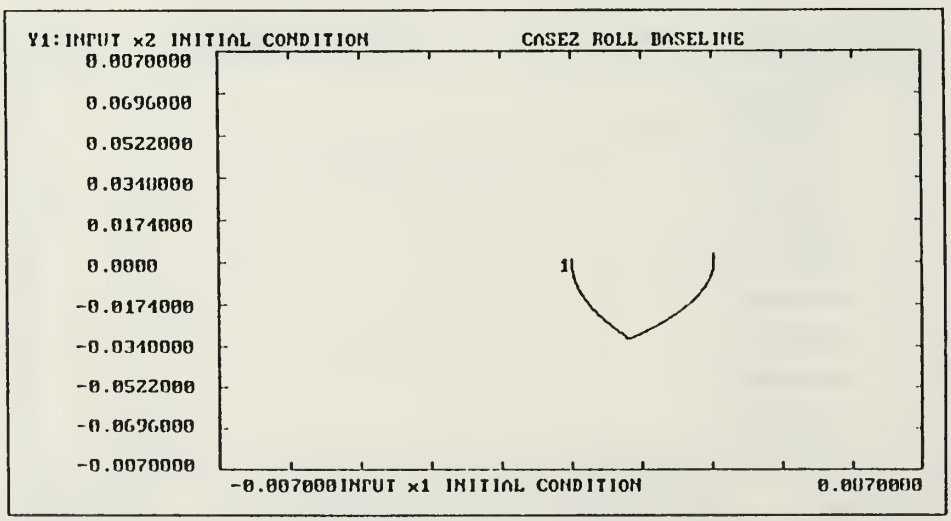

Figure 41. Baseline Case 2

```
      BlockNo,   Plot-MINimum,   Plot-MAXimum;  Comment
Horz:   201 ,   -0.0870000   ,    0.0870000   ; INPUT y1 INITIAL CONDITION
  Y1:   200 ,   -0.0870000   ,    0.0870000   ; INPUT y2 INITIAL CONDITION
  Y2:       ,                ,                ;
  Y3:       ,                ,                ;
  Y4:       ,                ,                ;
```

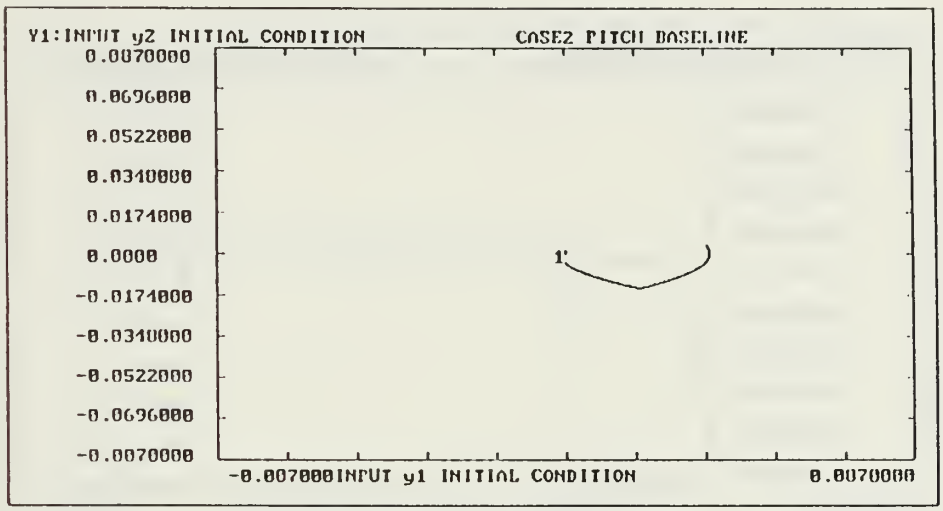


```
      BlockNo,   Plot-MINimum,   Plot-MAXimum;  Comment
Horz:   401 ,   -0.0870000   ,    0.0870000   ; INPUT z1 INITIAL CONDITION
  Y1:   400 ,   -0.0870000   ,    0.0870000   ; INPUT z2 INITIAL CONDITION
  Y2:       ,                ,                ;
  Y3:       ,                ,                ;
  Y4:       ,                ,                ;
```

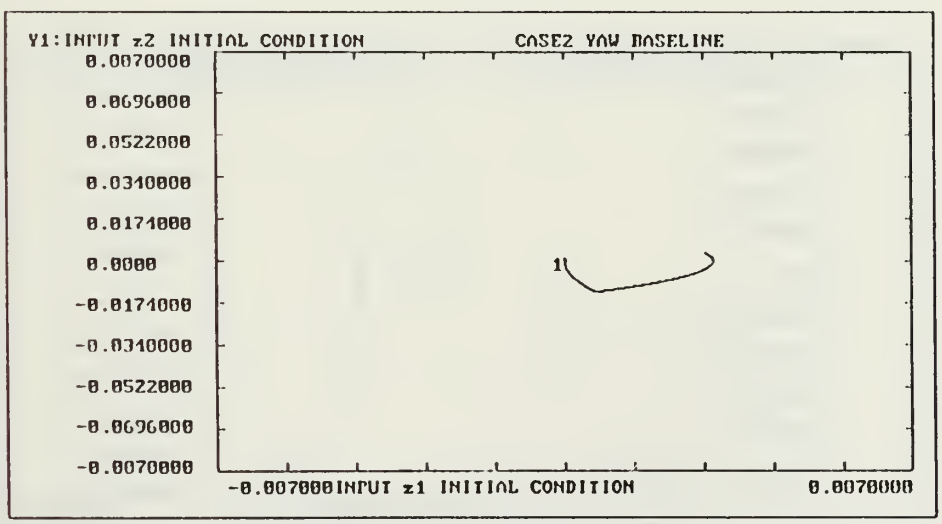

Figure 42. Baseline Case 2

```
      BlockNo,   Plot-MINimum,   Plot-MAXimum;   Comment
Horz:     0 ,     0.0000      ,   60.0000      ; Time
  Y1:     1 ,    -0.0872600   ,    0.0872600   ; INPUT x1 INITIAL CONDITION
  Y2:   201 ,    -0.0872600   ,    0.0872600   ; INPUT y1 INITIAL CONDITION
  Y3:   401 ,    -0.0872600   ,    0.0872600   ; INPUT z1 INITIAL CONDITION
  Y4:       ,                 ,                ;
```

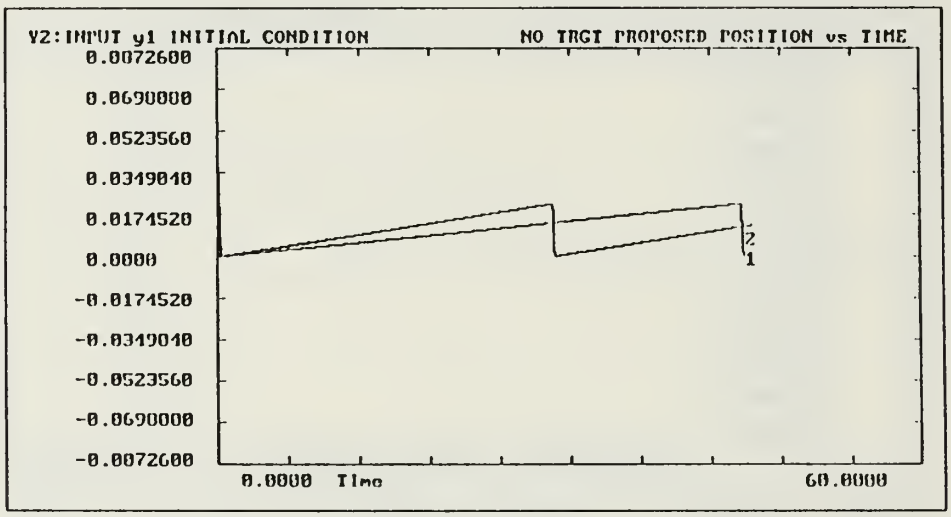


```
      BlockNo,   Plot-MINimum,   Plot-MAXimum;   Comment
Horz:     1 ,    -0.0872600   ,    0.0872600   ; INPUT x1 INITIAL CONDITION
  Y1:     2 ,    -0.1745000   ,    0.1745000   ; INPUT x2 INITIAL CONDITION
  Y2:       ,                 ,                ;
  Y3:       ,                 ,                ;
  Y4:       ,                 ,                ;
```

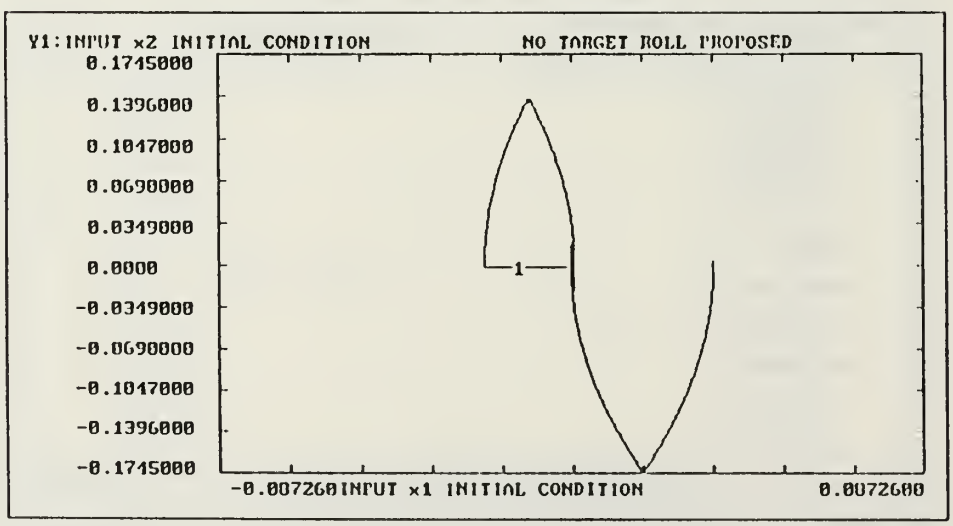

Figure 43. Proposed No Target

```
      BlockNo,   Plot-MINimum,   Plot-MAXimum;  Comment
Horz:    201 ,   -0.0872600   ,    0.0872600  ; INPUT y1 INITIAL CONDITION
  Y1:    200 ,   -0.2600000   ,    0.2600000  ; INPUT y2 INITIAL CONDITION
  Y2:        ,                ,               ;
  Y3:        ,                ,               ;
  Y4:        ,                ,               ;
```

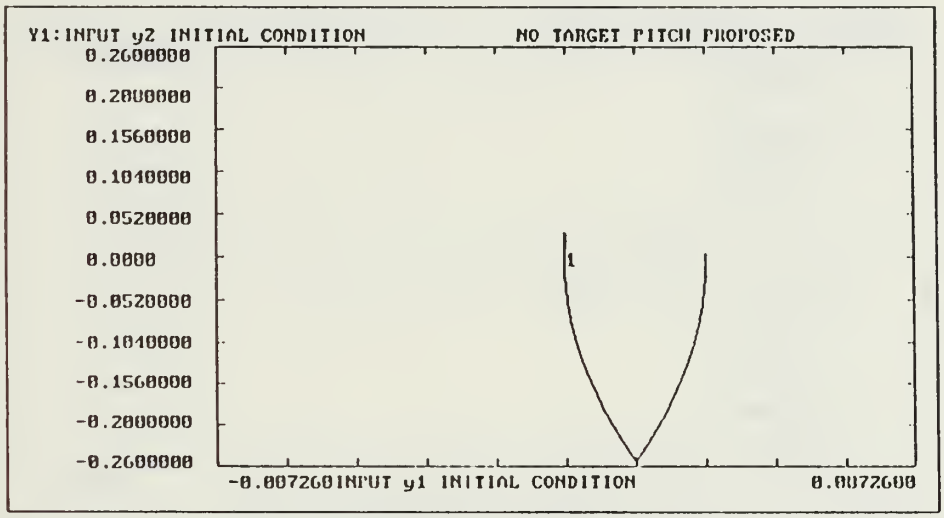


```
      BlockNo,   Plot-MINimum,   Plot-MAXimum;  Comment
Horz:    401 ,   -0.0872600   ,    0.0872600  ; INPUT z1 INITIAL CONDITION
  Y1:    400 ,   -0.2600000   ,    0.2600000  ; INPUT z2 INITIAL CONDITION
  Y2:        ,                ,               ;
  Y3:        ,                ,               ;
  Y4:        ,                ,               ;
```

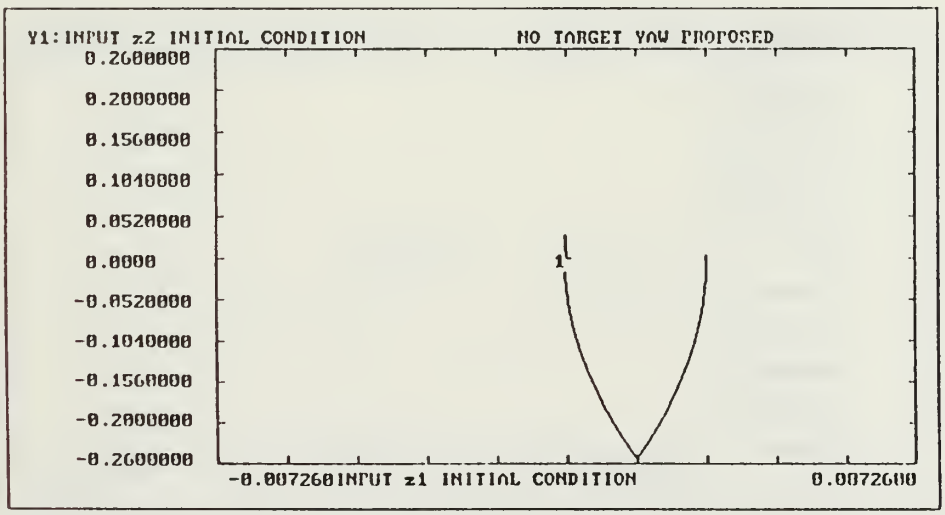

Figure 44. Proposed No Target

```
      BlockNo,  Plot-MINimum,  Plot-MAXimum;  Comment
Horz:     0 ,    0.0000     ,  90.0000     ; Time
  Y1:     1 ,   -0.0872600  ,   0.0872600  ; INPUT x1 INITIAL CONDITION
  Y2:   201 ,   -0.0872600  ,   0.0872600  ; INPUT y1 INITIAL CONDITION
  Y3:   401 ,   -0.0872600  ,   0.0872600  ; INPUT z1 INITIAL CONDITION
  Y4:       ,               ,              ;
```

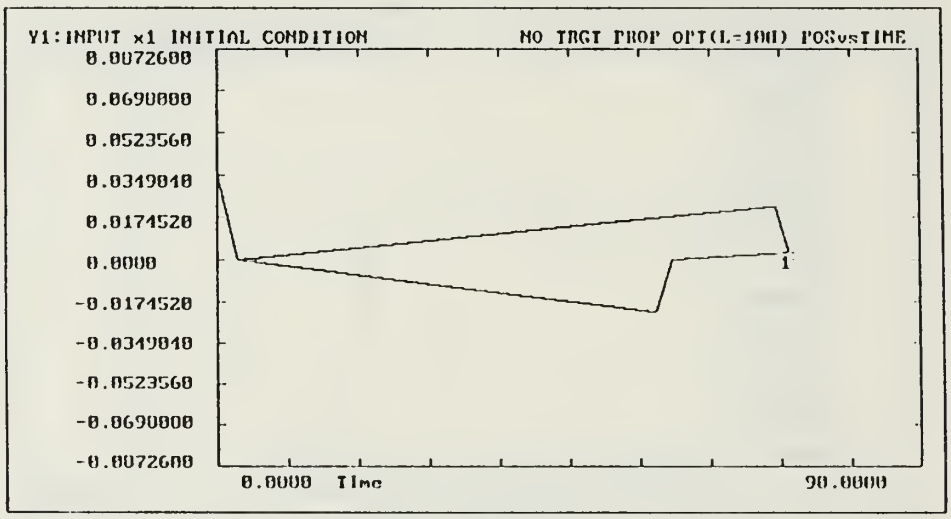


```
      BlockNo,  Plot-MINimum,  Plot-MAXimum;  Comment
Horz:     1 ,   -0.0872600  ,   0.0872600  ; INPUT x1 INITIAL CONDITION
  Y1:     2 ,   -0.0872600  ,   0.0872600  ; INPUT x2 INITIAL CONDITION
  Y2:       ,               ,              ;
  Y3:       ,               ,              ;
  Y4:       ,               ,              ;
```

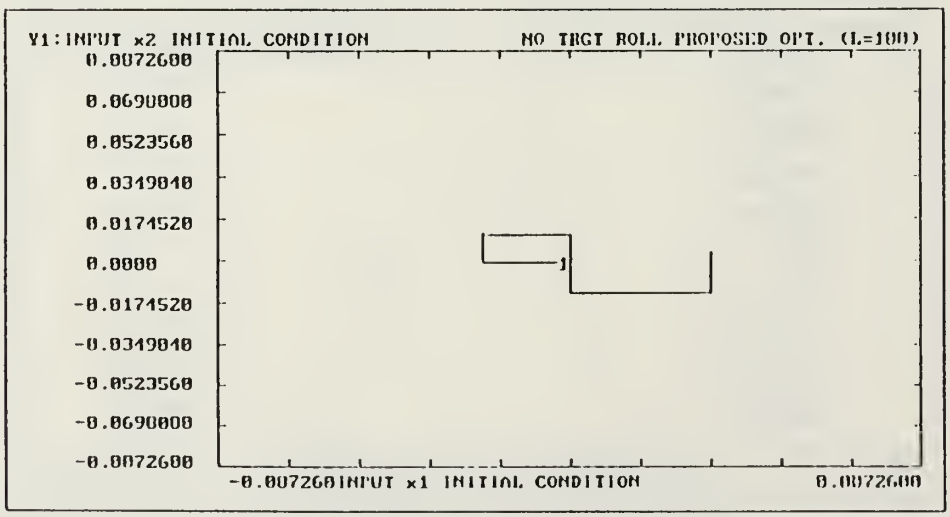

Figure 45. Proposed Optimal (L = 100) No Target

```
      BlockNo,   Plot-MINImum,   Plot-MAXImum;  Comment
Horz:   201 ,   -0.0872600  ,    0.0872600  ; INPUT y1 INITIAL CONDITION
  Y1:   200 ,   -0.0872600  ,    0.0872600  ; INPUT y2 INITIAL CONDITION
  Y2:       ,               ,               ;
  Y3:       ,               ,               ;
  Y4:       ,               ,               ;
```

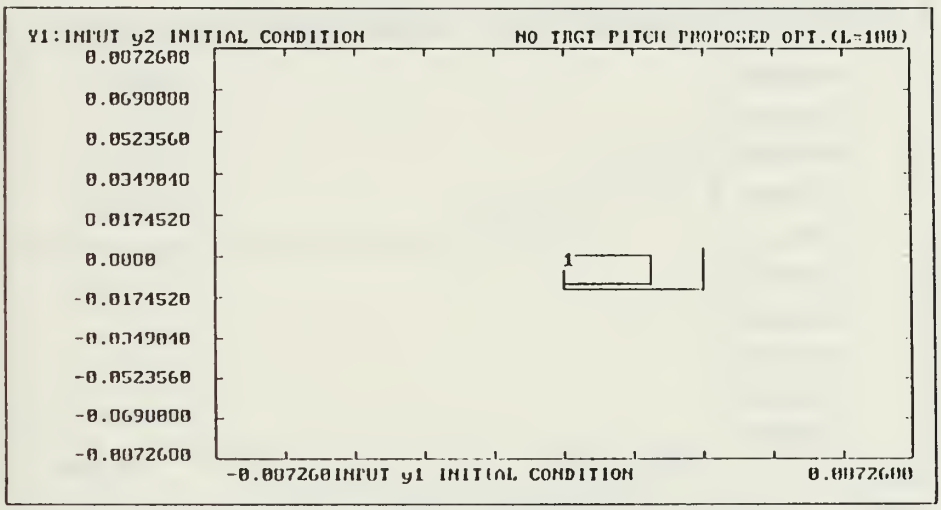


```
      BlockNo,   Plot-MINImum,   Plot-MAXImum;  Comment
Horz:   401 ,   -0.0872600  ,    0.0872600  ; INPUT z1 INITIAL CONDITION
  Y1:   400 ,   -0.0872600  ,    0.0872600  ; INPUT z2 INITIAL CONDITION
  Y2:       ,               ,               ;
  Y3:       ,               ,               ;
  Y4:       ,               ,               ;
```

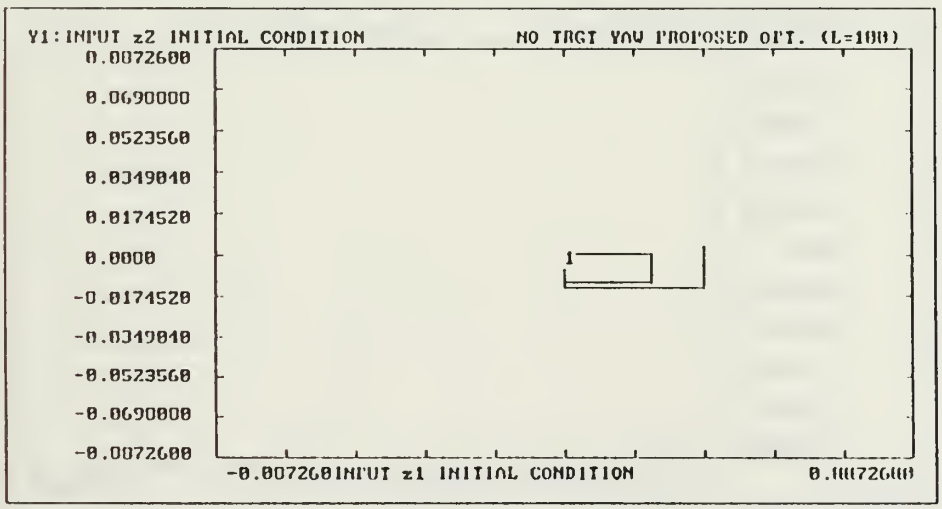

Figure 46. Proposed Optimal (L = 100) No Target

```
        BlockNo,   Plot-MINimum,   Plot-MAXimum;  Comment
Horz:       0 ,     0.0000      ,     3.0000     ; Time
  Y1:       1 ,    -0.0870000   ,     0.0870000  ; INPUT x1 INITIAL CONDITION
  Y2:     201 ,    -0.0870000   ,     0.0870000  ; INPUT y1 INITIAL CONDITION
  Y3:     401 ,    -0.0870000   ,     0.0870000  ; INPUT z1 INITIAL CONDITION
  Y4:         ,                ,                ;
```

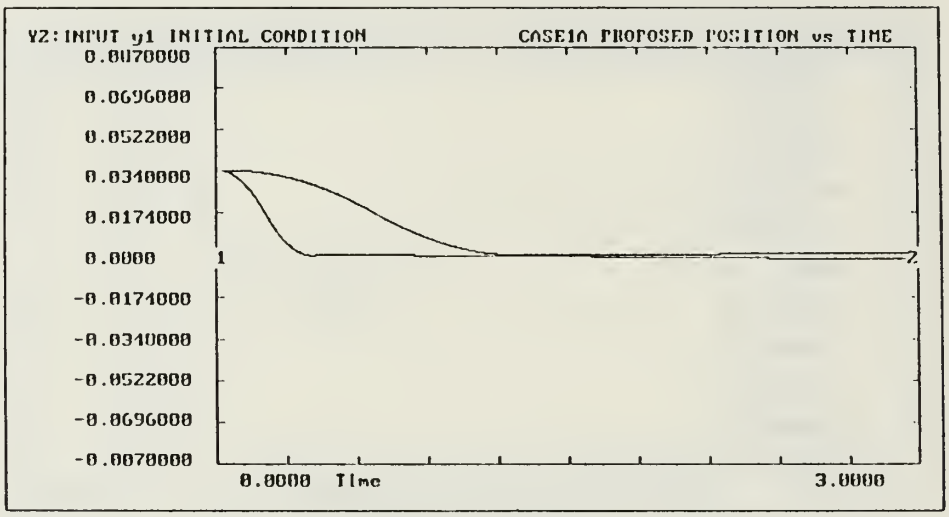


```
        BlockNo,   Plot-MINimum,   Plot-MAXimum;  Comment
Horz:       1 ,    -0.0870000   ,     0.0870000  ; INPUT x1 INITIAL CONDITION
  Y1:       2 ,    -0.1750000   ,     0.1750000  ; INPUT x2 INITIAL CONDITION
  Y2:         ,                ,                ;
  Y3:         ,                ,                ;
  Y4:         ,                ,                ;
```

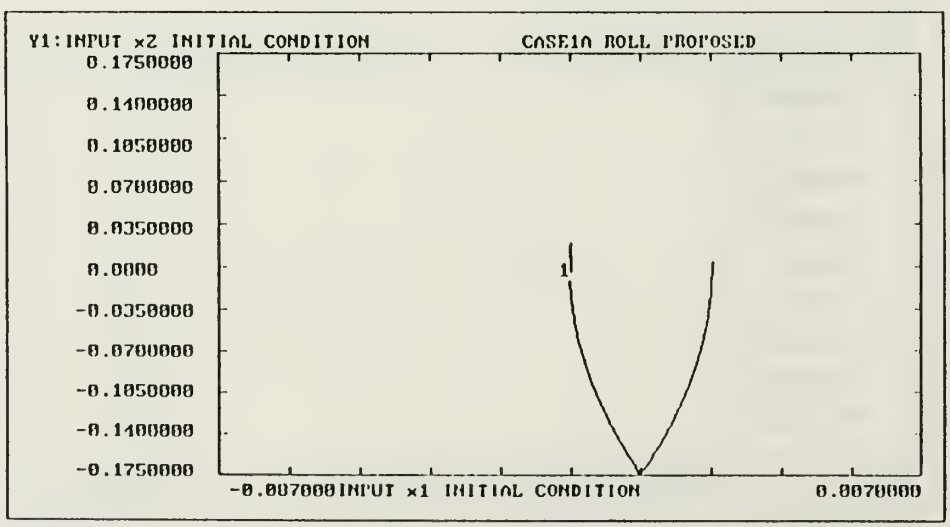

Figure 47. Proposed Case 1A

```
      BlockNo,   Plot-MINImum,   Plot-MAXImum;   Comment
Horz:   201 ,   -0.0870000   ,    0.0870000   ; INPUT y1 INITIAL CONDITION
  Y1:   200 ,   -0.1750000   ,    0.1750000   ; INPUT y2 INITIAL CONDITION
  Y2:       ,                ,                ;
  Y3:       ,                ,                ;
  Y4:       ,                ,                ;
```

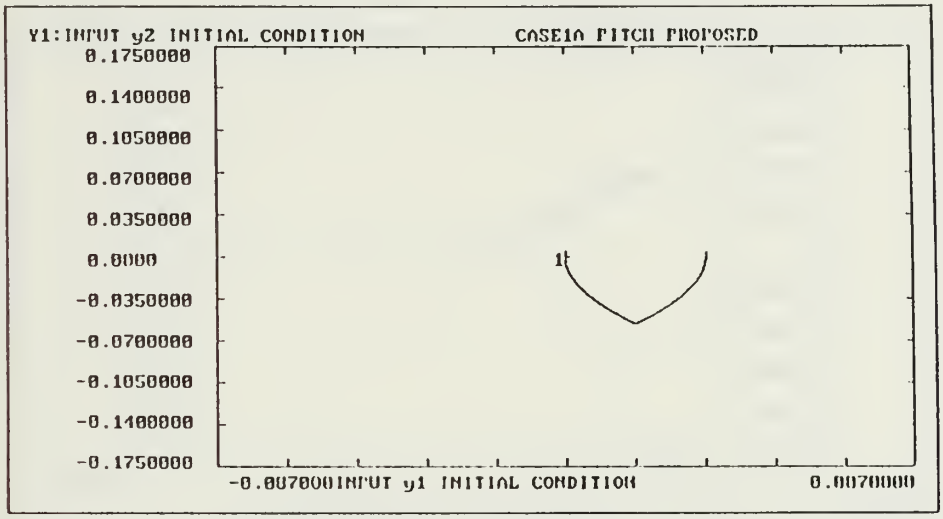


```
      BlockNo,   Plot-MINImum,   Plot-MAXImum;   Comment
Horz:   401 ,   -0.0870000   ,    0.0870000   ; INPUT z1 INITIAL CONDITION
  Y1:   400 ,   -0.1750000   ,    0.1750000   ; INPUT z2 INITIAL CONDITION
  Y2:       ,                ,                ;
  Y3:       ,                ,                ;
  Y4:       ,                ,                ;
```

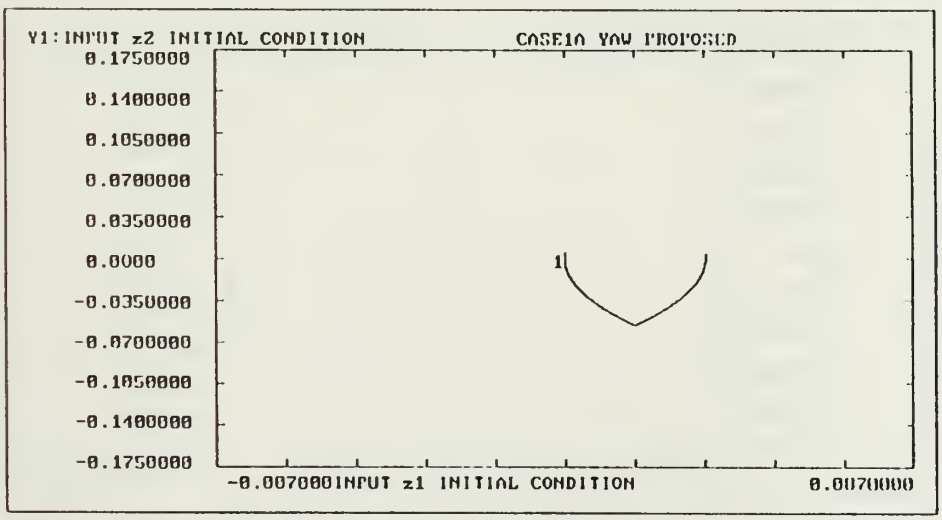

Figure 48. Proposed Case 1A

```
      BlockNo,   Plot-MINimum,   Plot-MAXimum;   Comment
Horz:      0 ,     0.0000     ,     2.0000     ; Time
  Y1:      1 ,   -0.0870000   ,    0.0870000   ; INPUT x1 INITIAL CONDITION
  Y2:    201 ,   -0.0870000   ,    0.0870000   ; INPUT y1 INITIAL CONDITION
  Y3:    401 ,   -0.0870000   ,    0.0870000   ; INPUT z1 INITIAL CONDITION
  Y4:        ,                ,                ;
```

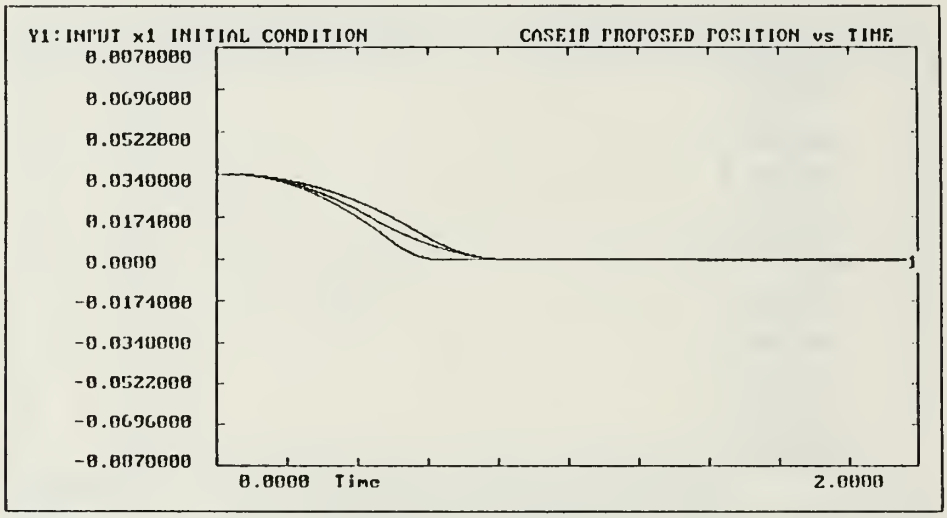


```
      BlockNo,   Plot-MINimum,   Plot-MAXimum;   Comment
Horz:      1 ,   -0.0870000   ,    0.0870000   ; INPUT x1 INITIAL CONDITION
  Y1:      2 ,   -0.1750000   ,    0.1750000   ; INPUT x2 INITIAL CONDITION
  Y2:        ,                ,                ;
  Y3:        ,                ,                ;
  Y4:        ,                ,                ;
```

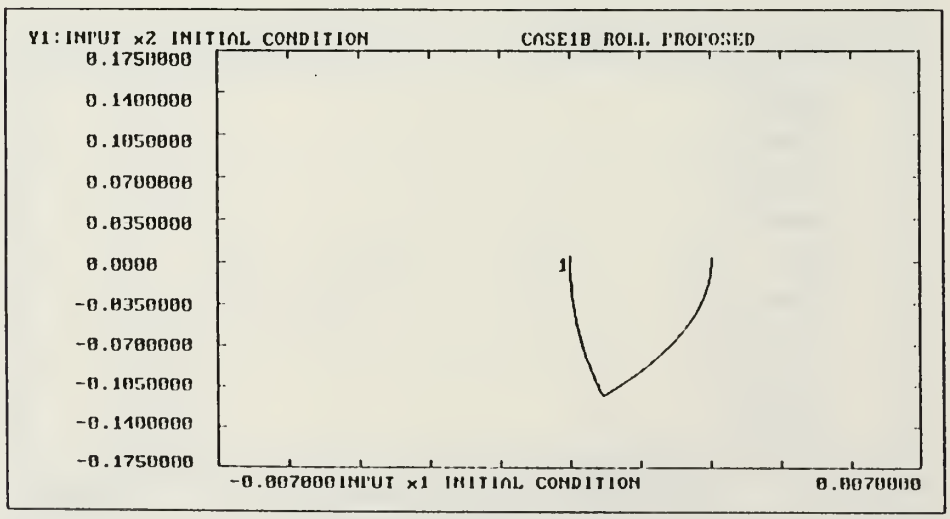

Figure 49. Proposed Case 1B

```
      BlockNo,   Plot-MINImum,   Plot-MAXimum;  Comment
Horz:   201 ,   -0.0870000   ,    0.0870000   ; INPUT y1 INITIAL CONDITION
  Y1:   200 ,   -0.1750000   ,    0.1750000   ; INPUT y2 INITIAL CONDITION
  Y2:       ,                ,                ;
  Y3:       ,                ,                ;
  Y4:       ,                ,                ;
```

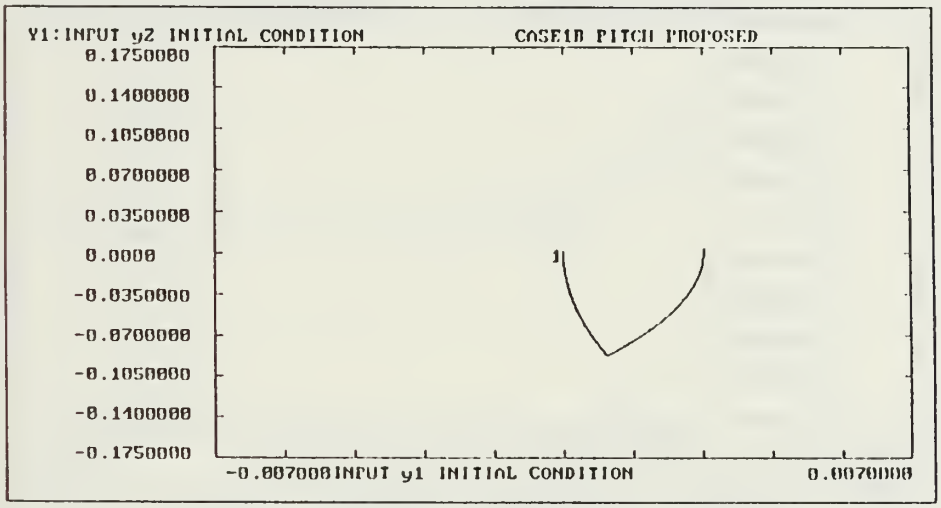


```
      BlockNo,   Plot-MINImum,   Plot-MAXimum;  Comment
Horz:   401 ,   -0.0870000   ,    0.0870000   ; INPUT z1 INITIAL CONDITION
  Y1:   400 ,   -0.0870000   ,    0.0870000   ; INPUT z2 INITIAL CONDITION
  Y2:       ,                ,                ;
  Y3:       ,                ,                ;
  Y4:       ,                ,                ;
```

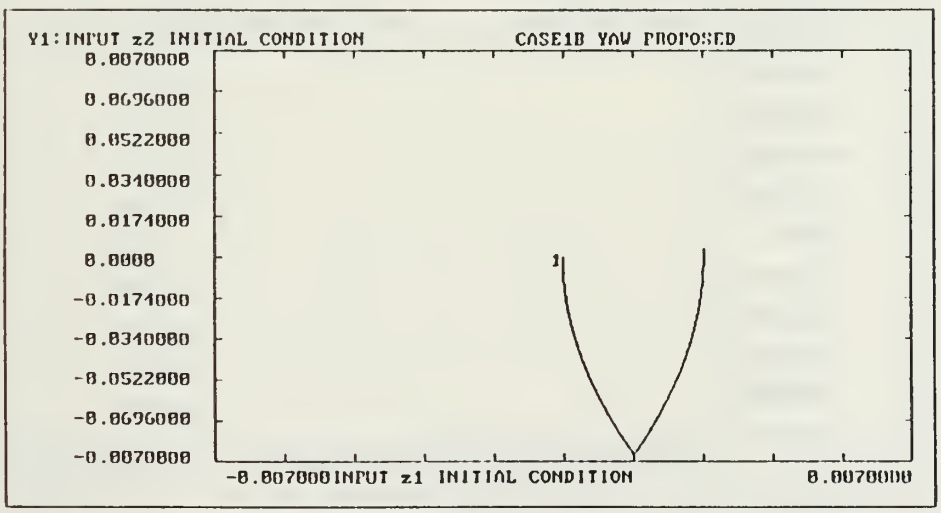

Figure 50. Proposed Case 1B

```
      BlockNo,   Plot-MINimum,   Plot-MAXimum;  Comment
Horz:     0 ,    0.0000      ,    3.0000      ; Time
  Y1:     1 ,   -0.0870000   ,    0.0870000   ; INPUT x1 INITIAL CONDITION
  Y2:   201 ,   -0.0870000   ,    0.0870000   ; INPUT y1 INITIAL CONDITION
  Y3:   401 ,   -0.0870000   ,    0.0870000   ; INPUT z1 INITIAL CONDITION
  Y4:       ,                ,                ;
```

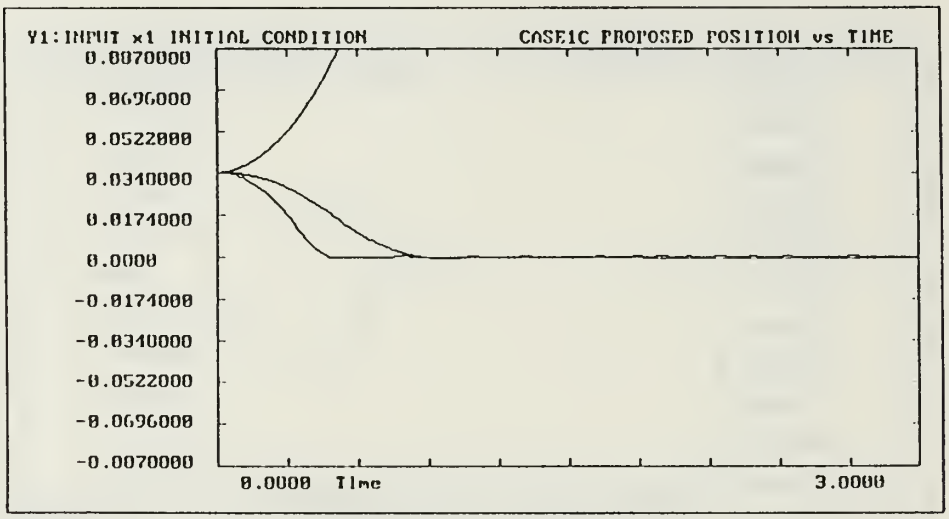


```
      BlockNo,   Plot-MINimum,   Plot-MAXimum;  Comment
Horz:     1 ,   -0.0870000   ,    0.0870000   ; INPUT x1 INITIAL CONDITION
  Y1:     2 ,   -0.0870000   ,    0.0870000   ; INPUT x2 INITIAL CONDITION
  Y2:       ,                ,                ;
  Y3:       ,                ,                ;
  Y4:       ,                ,                ;
```

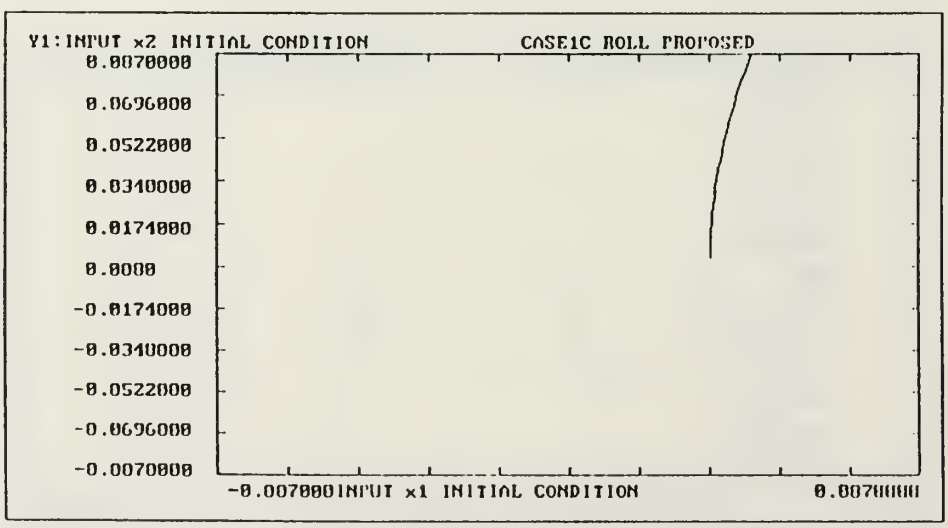

Figure 51. Proposed Case 1C

```
      BlockNo,   Plot-MINimum,   Plot-MAXimum;   Comment
Horz:   201 ,   -0.0870000   ,    0.0870000   ; INPUT y1 INITIAL CONDITION
  Y1:   200 ,   -0.0870000   ,    0.0870000   ; INPUT y2 INITIAL CONDITION
  Y2:       ,                ,                ;
  Y3:       ,                ,                ;
  Y4:       ,                ,                ;
```

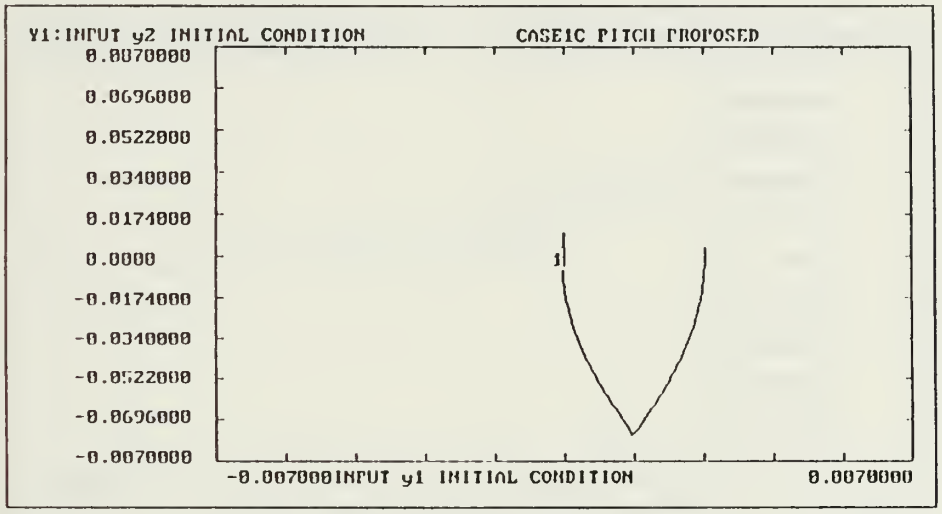


```
      BlockNo,   Plot-MINimum,   Plot-MAXimum;   Comment
Horz:   401 ,   -0.0870000   ,    0.0870000   ; INPUT z1 INITIAL CONDITION
  Y1:   400 ,   -0.1750000   ,    0.1750000   ; INPUT z2 INITIAL CONDITION
  Y2:       ,                ,                ;
  Y3:       ,                ,                ;
  Y4:       ,                ,                ;
```

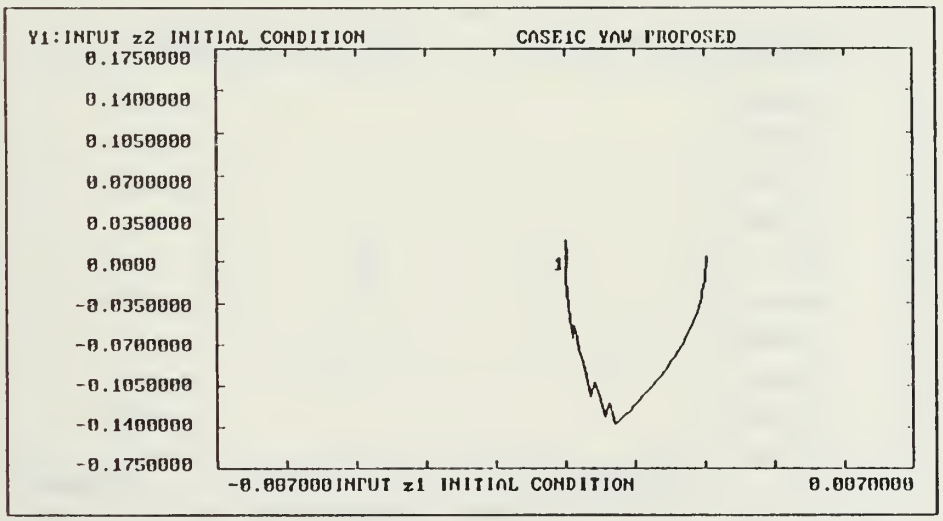

Figure 52. Proposed Case 1C

```
      BlockNo,   Plot-MINimum,   Plot-MAXimum;  Comment
Horz:      0 ,    0.0000      ,    2.0000      ; Time
  Y1:      1 ,   -0.0870000   ,    0.0870000   ; INPUT x1 INITIAL CONDITION
  Y2:    201 ,   -0.0870000   ,    0.0870000   ; INPUT y1 INITIAL CONDITION
  Y3:    401 ,   -0.0870000   ,    0.0870000   ; INPUT z1 INITIAL CONDITION
  Y4:        ,                ,                ;
```

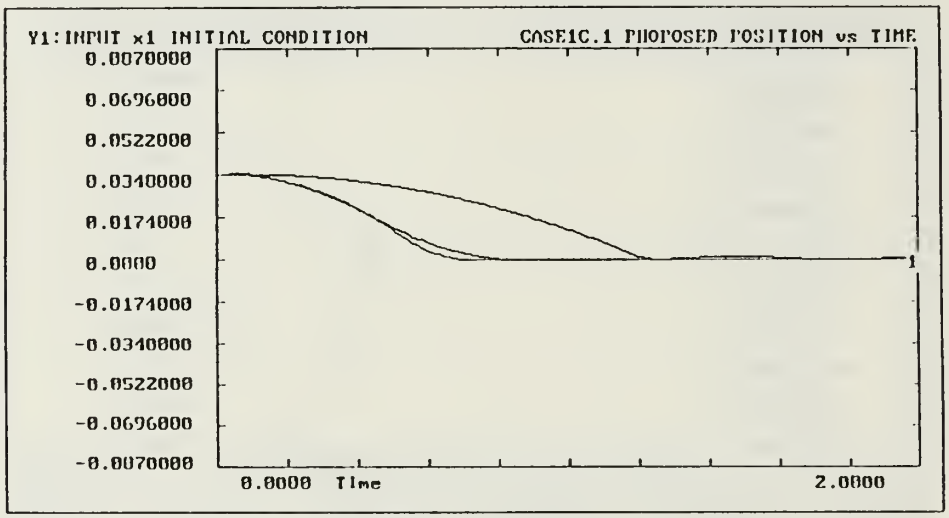


```
      BlockNo,   Plot-MINimum,   Plot-MAXimum;  Comment
Horz:      1 ,   -0.0870000   ,    0.0870000   ; INPUT x1 INITIAL CONDITION
  Y1:      2 ,   -0.0870000   ,    0.0870000   ; INPUT x2 INITIAL CONDITION
  Y2:        ,                ,                ;
  Y3:        ,                ,                ;
  Y4:        ,                ,                ;
```

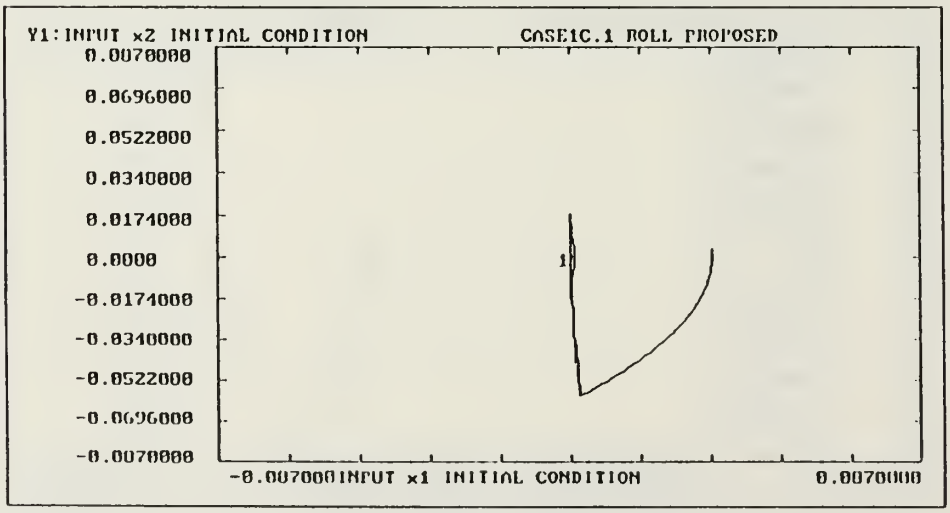

Figure 53. Proposed Case 1C.1

	BlockNo,	Plot-MINImum,	Plot-MAXImum;	Comment
Horz:	201 ,	-0.0870000 ,	0.0870000 ;	INPUT y1 INITIAL CONDITION
Y1:	200 ,	-0.0870000 ,	0.0870000 ;	INPUT y2 INITIAL CONDITION
Y2:	,	,	;	
Y3:	,	,	;	
Y4:	,	,	;	

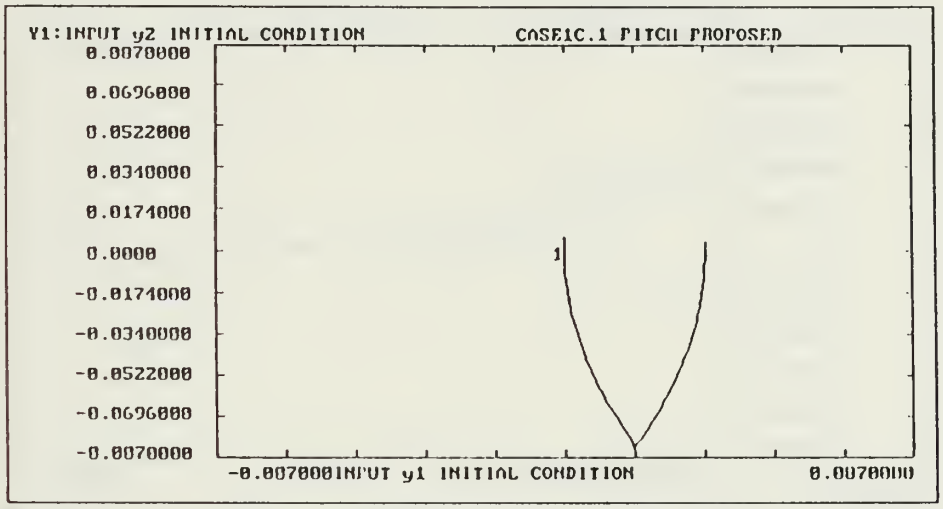

	BlockNo,	Plot-MINImum,	Plot-MAXImum;	Comment
Horz:	401 ,	-0.0870000 ,	0.0870000 ;	INPUT z1 INITIAL CONDITION
Y1:	400 ,	-0.1750000 ,	0.1750000 ;	INPUT z2 INITIAL CONDITION
Y2:	,	,	;	
Y3:	,	,	;	
Y4:	,	,	;	

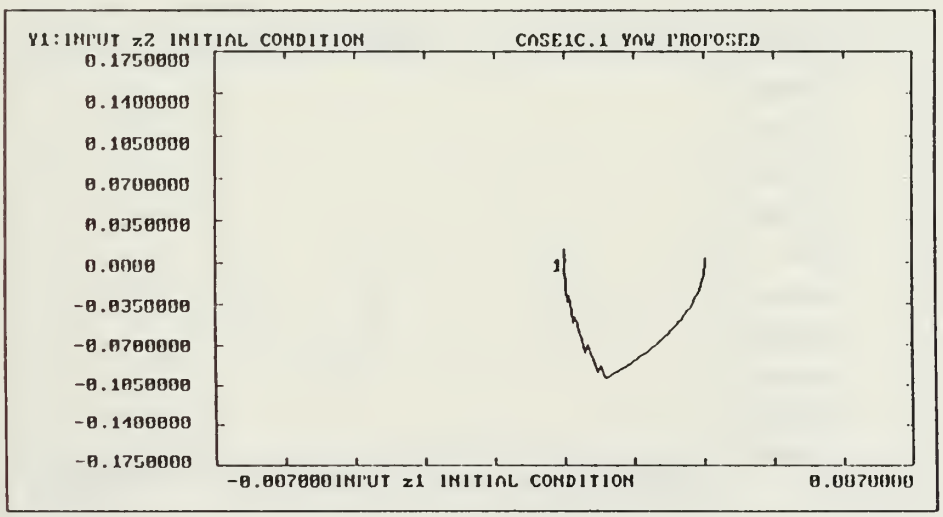

Figure 54. Proposed Case 1C.1

```
      BlockNo,   Plot-MINImum,   Plot-MAXImum;  Comment
Horz:      0 ,    0.0000      ,  10.0000      ; Time
  Y1:      1 ,   -0.0870000   ,   0.0870000   ; INPUT x1 INITIAL CONDITION
  Y2:    201 ,   -0.0870000   ,   0.0870000   ; INPUT y1 INITIAL CONDITION
  Y3:    401 ,   -0.0870000   ,   0.0870000   ; INPUT z1 INITIAL CONDITION
  Y4:        ,                ,               ;
```

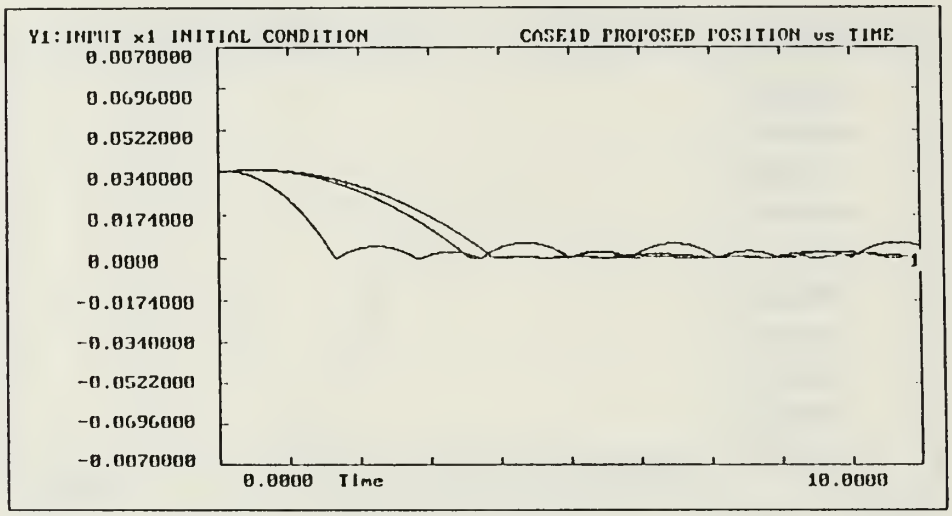


```
      BlockNo,   Plot-MINImum,   Plot-MAXImum;  Comment
Horz:      1 ,   -0.0870000   ,   0.0870000   ; INPUT x1 INITIAL CONDITION
  Y1:      2 ,   -0.0870000   ,   0.0870000   ; INPUT x2 INITIAL CONDITION
  Y2:        ,                ,               ;
  Y3:        ,                ,               ;
  Y4:        ,                ,               ;
```

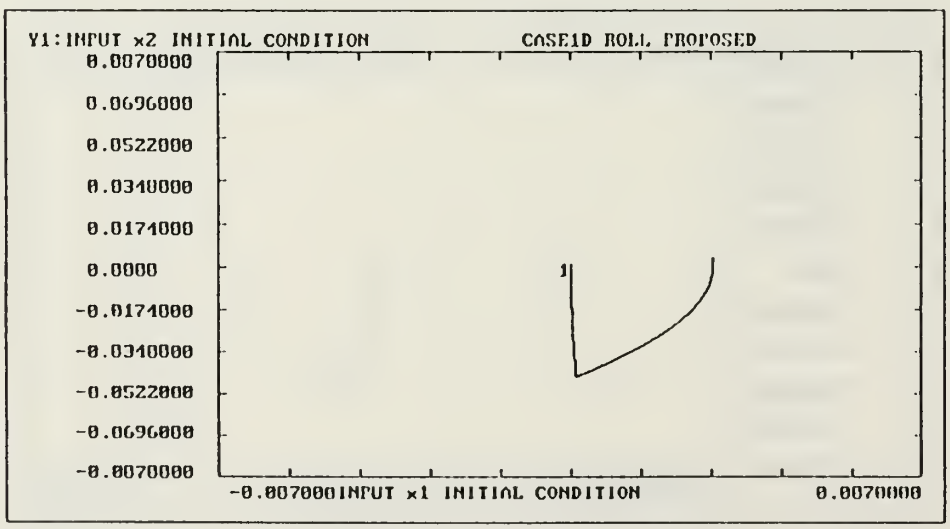

Figure 55. Proposed Case 1D

```
      BlockNo,   Plot-MINimum,   Plot-MAXimum;   Comment
Horz:   201 ,   -0.0870000   ,    0.0870000   ; INPUT y1 INITIAL CONDITION
  Y1:   200 ,   -0.0870000   ,    0.0870000   ; INPUT y2 INITIAL CONDITION
  Y2:       ,                ,                ;
  Y3:       ,                ,                ;
  Y4:       ,                ,                ;
```

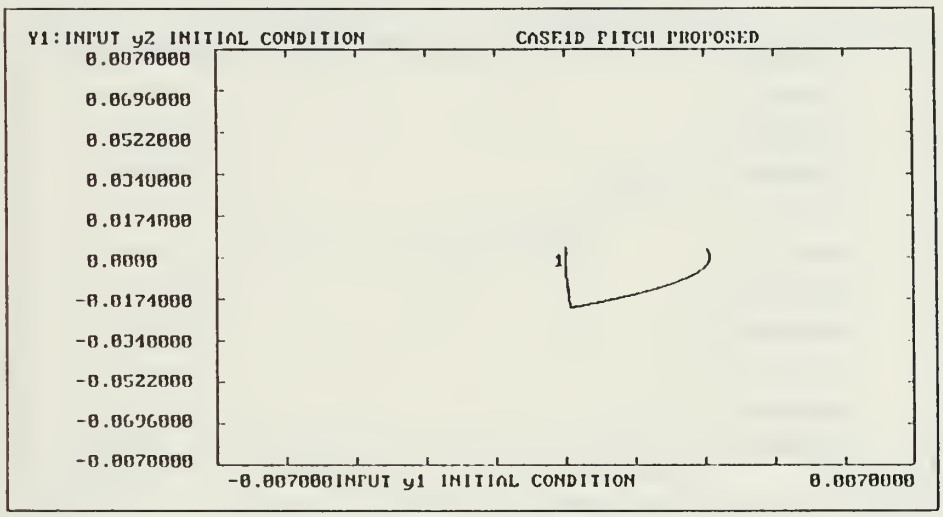


```
      BlockNo,   Plot-MINimum,   Plot-MAXimum;   Comment
Horz:   401 ,   -0.0870000   ,    0.0870000   ; INPUT z1 INITIAL CONDITION
  Y1:   400 ,   -0.0870000   ,    0.0870000   ; INPUT z2 INITIAL CONDITION
  Y2:       ,                ,                ;
  Y3:       ,                ,                ;
  Y4:       ,                ,                ;
```

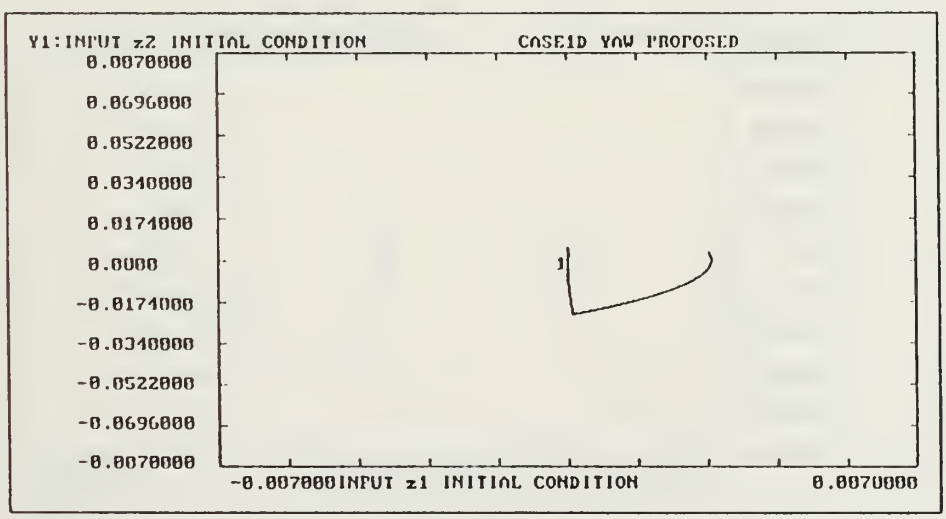

Figure 56. Proposed Case 1D

```
      BlockNo,   Plot-MINimum,   Plot-MAXimum;  Comment
Horz:      0 ,    0.0000      ,    2.0000      ; Time
  Y1:      1 ,   -0.0870000   ,    0.0870000   ; INPUT x1 INITIAL CONDITION
  Y2:    201 ,   -0.0870000   ,    0.0870000   ; INPUT y1 INITIAL CONDITION
  Y3:    401 ,   -0.0870000   ,    0.0870000   ; INPUT z1 INITIAL CONDITION
  Y4:        ,                ,                ;
```

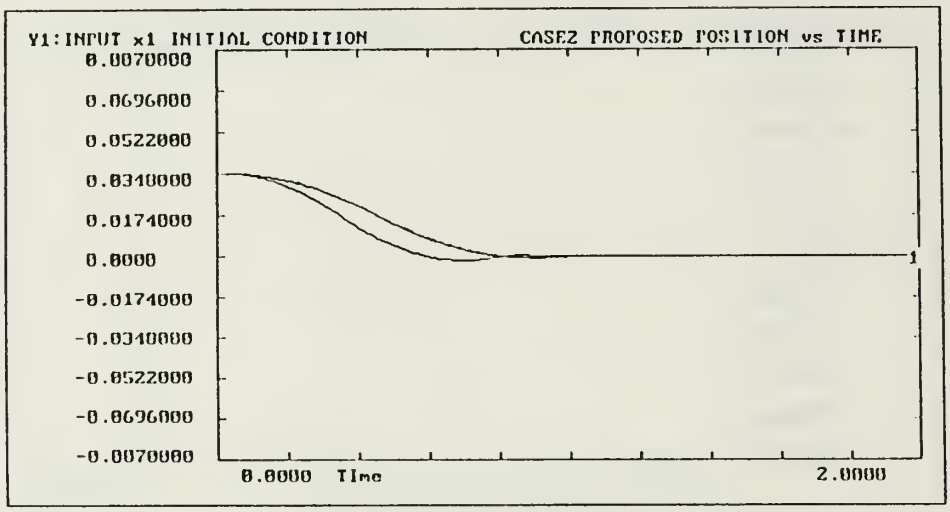


```
      BlockNo,   Plot-MINimum,   Plot-MAXimum;  Comment
Horz:      1 ,   -0.0870000   ,    0.0870000   ; INPUT x1 INITIAL CONDITION
  Y1:      2 ,   -0.1750000   ,    0.1750000   ; INPUT x2 INITIAL CONDITION
  Y2:        ,                ,                ;
  Y3:        ,                ,                ;
  Y4:        ,                ,                ;
```

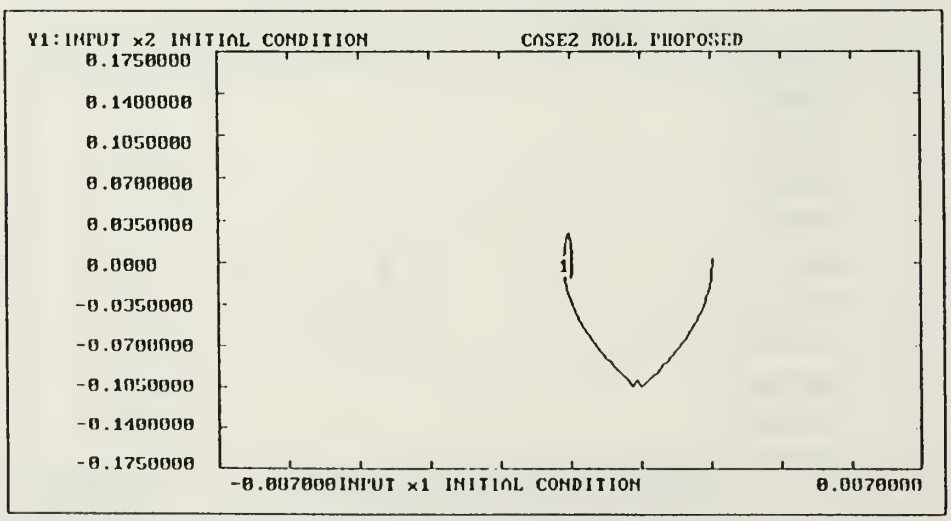

Figure 57. Proposed Case 2

```
      BlockNo,   Plot-MINimum,   Plot-MAXimum;   Comment
Horz:   201 ,   -0.0870000   ,    0.0870000   ; INPUT y1 INITIAL CONDITION
  Y1:   200 ,   -0.0870000   ,    0.0870000   ; INPUT y2 INITIAL CONDITION
  Y2:       ,                ,                ;
  Y3:       ,                ,                ;
  Y4:       ,                ,                ;
```

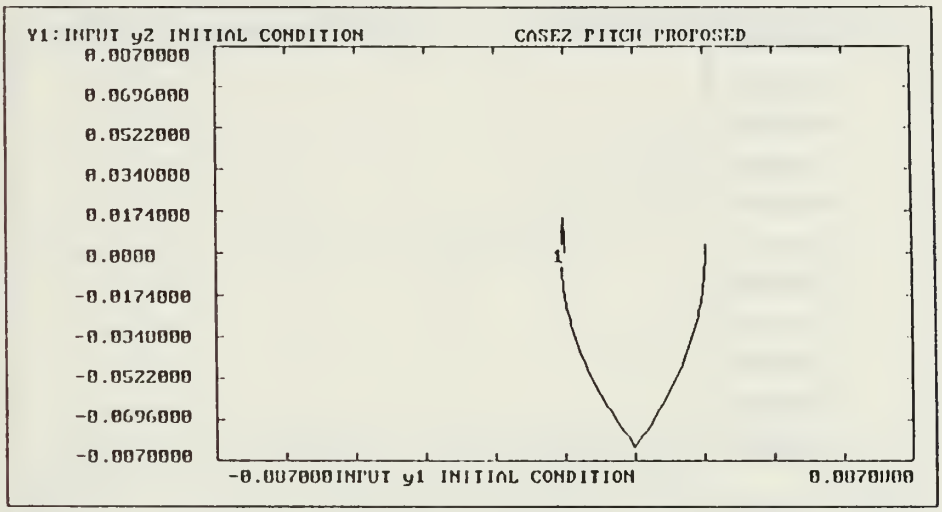


```
      BlockNo,   Plot-MINimum,   Plot-MAXimum;   Comment
Horz:   401 ,   -0.0870000   ,    0.0870000   ; INPUT z1 INITIAL CONDITION
  Y1:   400 ,   -0.0870000   ,    0.0870000   ; INPUT z2 INITIAL CONDITION
  Y2:       ,                ,                ;
  Y3:       ,                ,                ;
  Y4:       ,                ,                ;
```

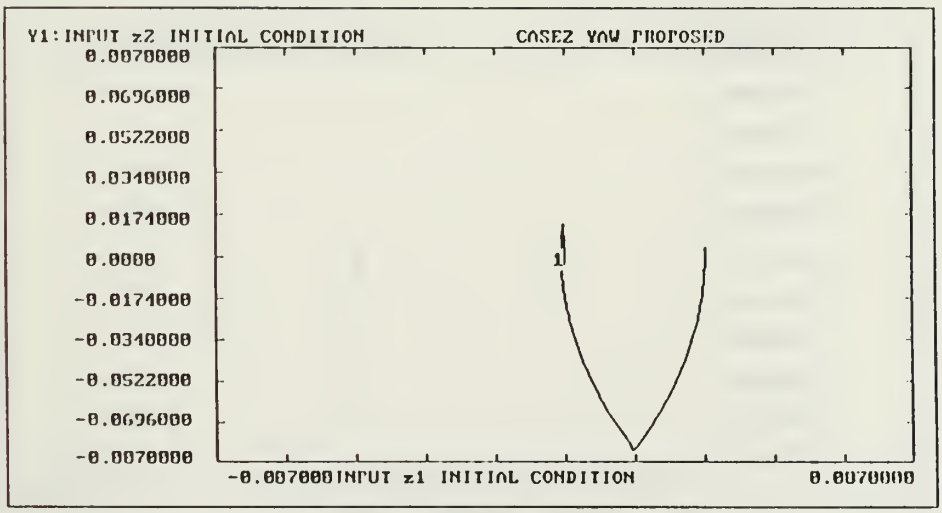

Figure 58. Proposed Case 2

```
      BlockNo,   Plot-MINimum,   Plot-MAXimum;  Comment
Horz:     0 ,    0.0000      ,    3.0000      ; Time
  Y1:     1 ,   -0.0870000   ,    0.0870000   ; INPUT x1 INITIAL CONDITION
  Y2:   201 ,   -0.0870000   ,    0.0870000   ; INPUT y1 INITIAL CONDITION
  Y3:   401 ,   -0.0870000   ,    0.0870000   ; INPUT z1 INITIAL CONDITION
  Y4:       ,                ,                ;
```

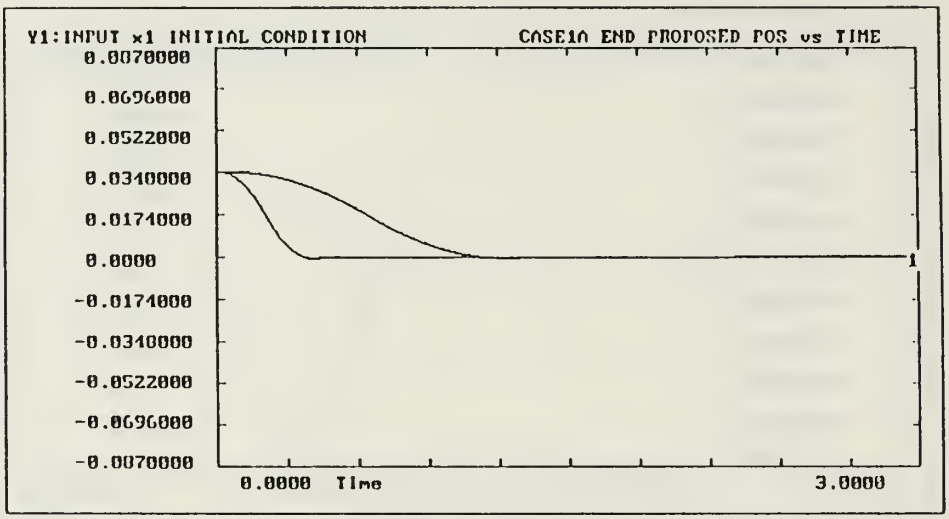


```
      BlockNo,   Plot-MINimum,   Plot-MAXimum;  Comment
Horz:     1 ,   -0.0870000   ,    0.0870000   ; INPUT x1 INITIAL CONDITION
  Y1:     2 ,   -0.1750000   ,    0.1750000   ; INPUT x2 INITIAL CONDITION
  Y2:       ,                ,                ;
  Y3:       ,                ,                ;
  Y4:       ,                ,                ;
```

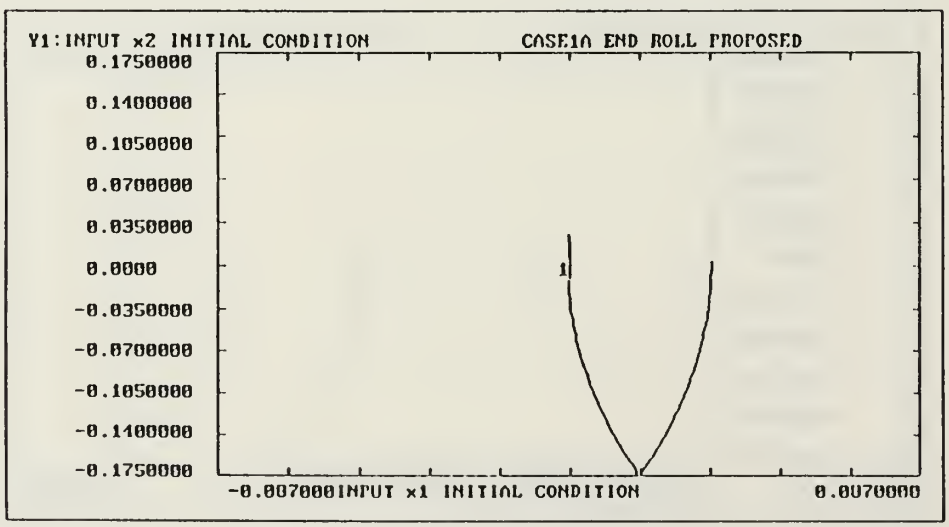

Figure 59. Proposed Case 1A End of mission

```
      BlockNo,   Plot-MINimum,   Plot-MAXimum;  Comment
Horz:   201 ,   -0.0870000   ,    0.0870000   ; INPUT y1 INITIAL CONDITION
  Y1:   200 ,   -0.0870000   ,    0.0870000   ; INPUT y2 INITIAL CONDITION
  Y2:       ,                ,                ;
  Y3:       ,                ,                ;
  Y4:       ,                ,                ;
```

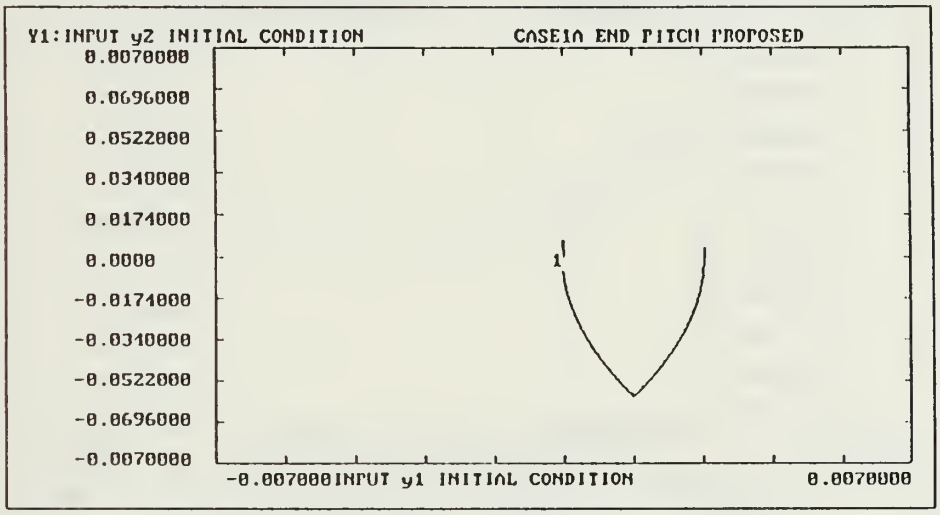


```
      BlockNo,   Plot-MINimum,   Plot-MAXimum;  Comment
Horz:   401 ,   -0.0870000   ,    0.0870000   ; INPUT z1 INITIAL CONDITION
  Y1:   400 ,   -0.0870000   ,    0.0870000   ; INPUT z2 INITIAL CONDITION
  Y2:       ,                ,                ;
  Y3:       ,                ,                ;
  Y4:       ,                ,                ;
```

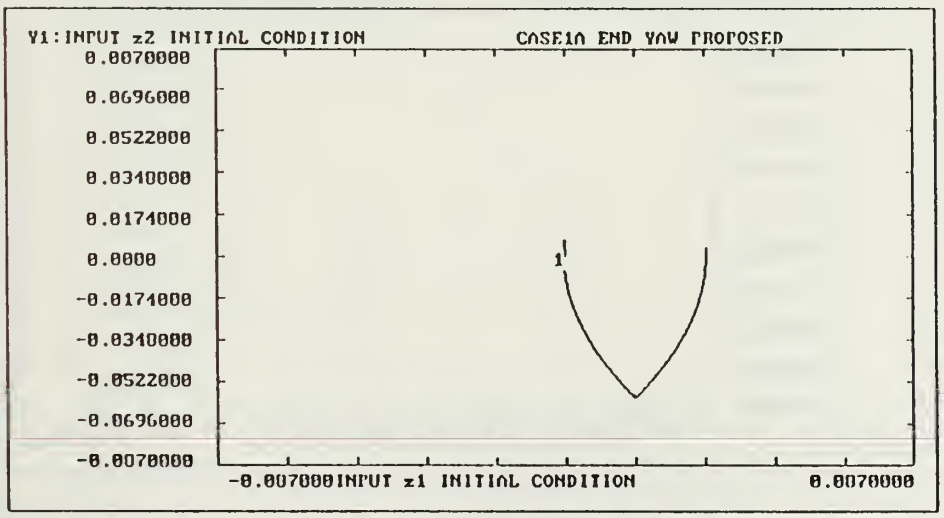

Figure 60. Proposed Case 1A End of Mission

```
      BlockNo,   Plot-MINimum,   Plot-MAXimum;   Comment
Horz:     0 ,     0.0000     ,     3.0000     ; Time
  Y1:     1 ,    -0.0870000  ,     0.0870000  ; INPUT x1 INITIAL CONDITION
  Y2:   201 ,    -0.0870000  ,     0.0870000  ; INPUT y1 INITIAL CONDITION
  Y3:   401 ,    -0.0870000  ,     0.0870000  ; INPUT z1 INITIAL CONDITION
  Y4:       ,                ,                ;
```

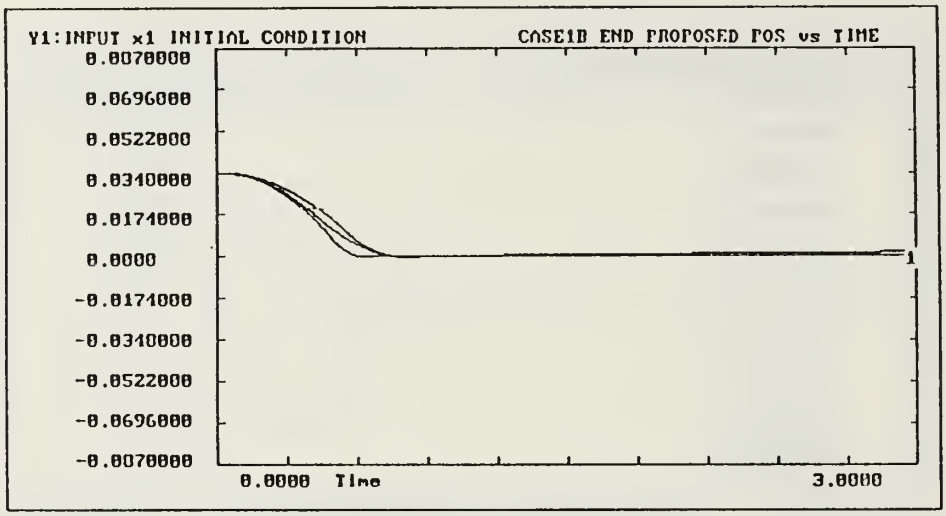


```
      BlockNo,   Plot-MINimum,   Plot-MAXimum;   Comment
Horz:     1 ,    -0.0870000  ,     0.0870000  ; INPUT x1 INITIAL CONDITION
  Y1:     2 ,    -0.1750000  ,     0.1750000  ; INPUT x2 INITIAL CONDITION
  Y2:       ,                ,                ;
  Y3:       ,                ,                ;
  Y4:       ,                ,                ;
```

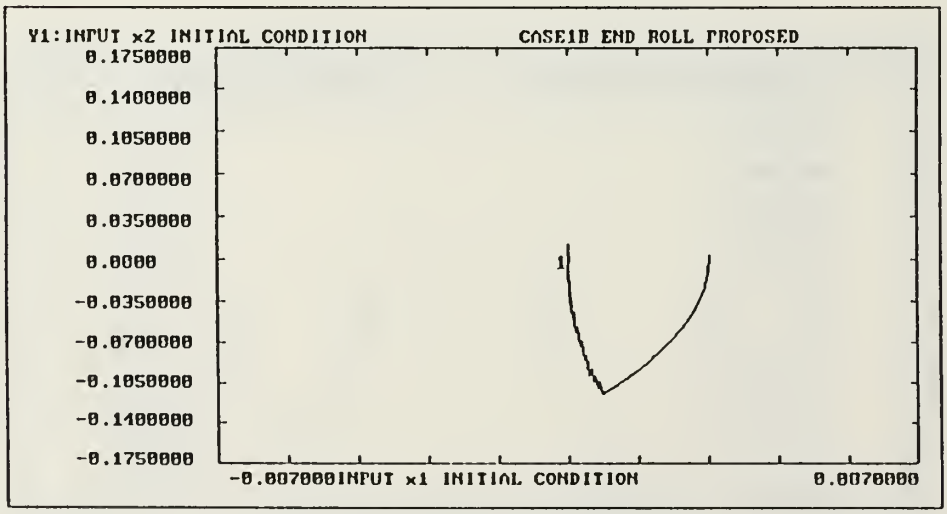

Figure 61. Proposed Case 1B End of Mission

```
      BlockNo,  Plot-MINimum,  Plot-MAXimum;  Comment
Horz:   201 ,  -0.0870000  ,   0.0870000  ; INPUT y1 INITIAL CONDITION
  Y1:   200 ,  -0.0870000  ,   0.0870000  ; INPUT y2 INITIAL CONDITION
  Y2:       ,              ,               ;
  Y3:       ,              ,               ;
  Y4:       ,              ,               ;
```

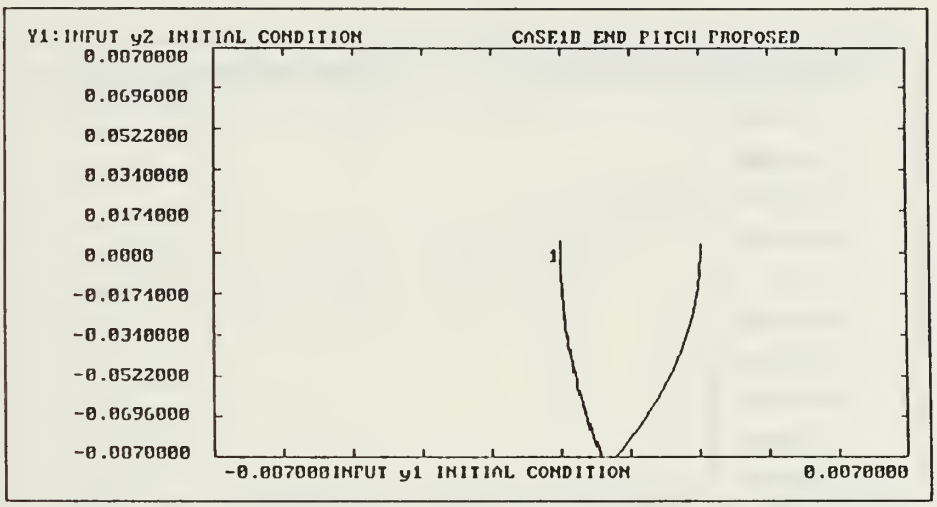


```
      BlockNo,  Plot-MINimum,  Plot-MAXimum;  Comment
Horz:   401 ,  -0.0870000  ,   0.0870000  ; INPUT z1 INITIAL CONDITION
  Y1:   400 ,  -0.0870000  ,   0.0870000  ; INPUT z2 INITIAL CONDITION
  Y2:       ,              ,               ;
  Y3:       ,              ,               ;
  Y4:       ,              ,               ;
```

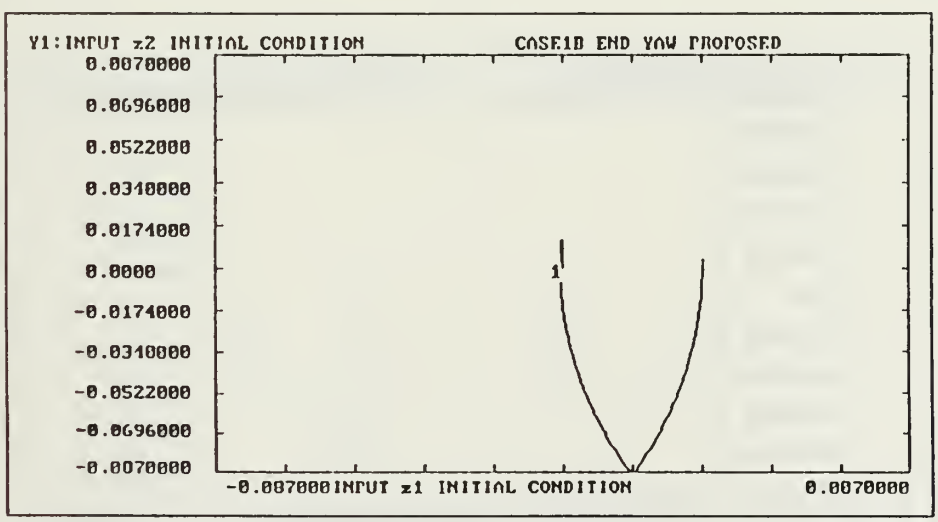

Figure 62. Proposed Case 1B End of Mission

```
      BlockNo,  Plot-MINimum,  Plot-MAXimum;  Comment
Horz:     0 ,    0.0000     ,    3.0000     ; Time
  Y1:     1 ,   -0.0870000  ,    0.0870000  ; INPUT x1 INITIAL CONDITION
  Y2:   201 ,   -0.0870000  ,    0.0870000  ; INPUT y1 INITIAL CONDITION
  Y3:   401 ,   -0.0870000  ,    0.0870000  ; INPUT z1 INITIAL CONDITION
  Y4:       ,               ,               ;
```

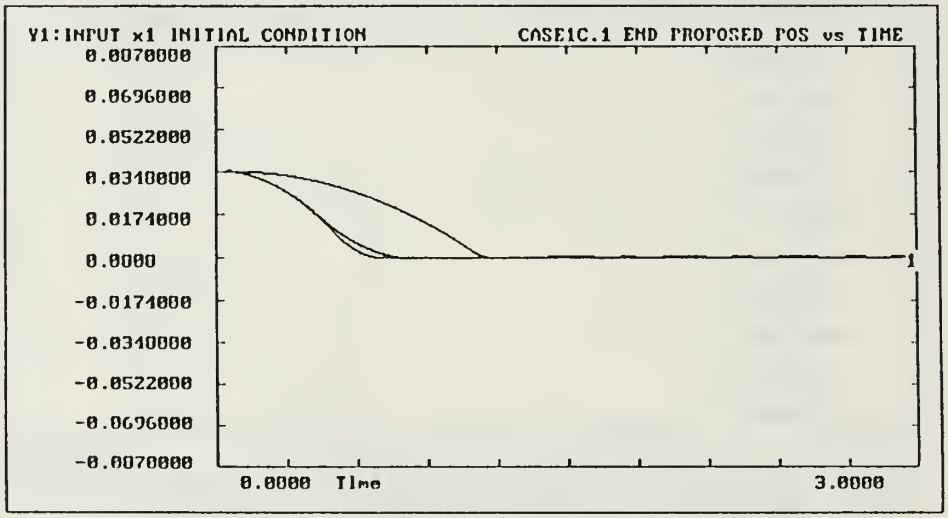


```
      BlockNo,  Plot-MINimum,  Plot-MAXimum;  Comment
Horz:     1 ,   -0.0870000  ,    0.0870000  ; INPUT x1 INITIAL CONDITION
  Y1:     2 ,   -0.0870000  ,    0.0870000  ; INPUT x2 INITIAL CONDITION
  Y2:       ,               ,               ;
  Y3:       ,               ,               ;
  Y4:       ,               ,               ;
```

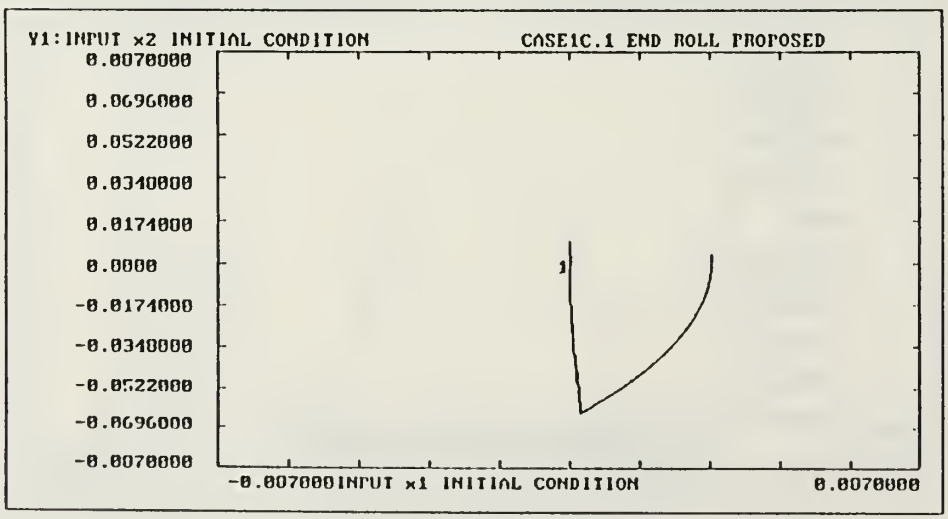

Figure 63. Proposed Case 1C.1 End of Mission

```
      BlockNo,  Plot-MINimum,  Plot-MAXimum;  Comment
Horz:   201 ,  -0.0870000  ,   0.0870000  ; INPUT y1 INITIAL CONDITION
  Y1:   200 ,  -0.0870000  ,   0.0870000  ; INPUT y2 INITIAL CONDITION
  Y2:       ,              ,              ;
  Y3:       ,              ,              ;
  Y4:       ,              ,              ;
```

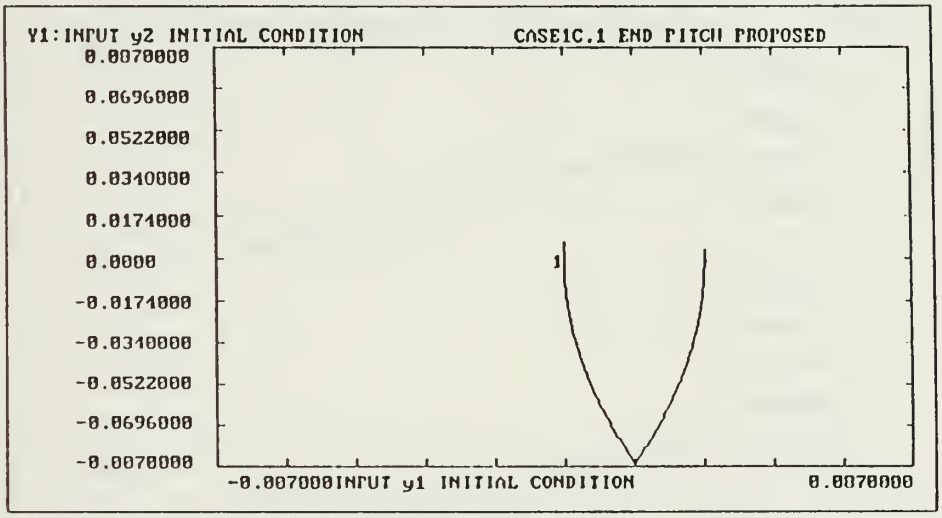


```
      BlockNo,  Plot-MINimum,  Plot-MAXimum;  Comment
Horz:   401 ,  -0.0870000  ,   0.0870000  ; INPUT z1 INITIAL CONDITION
  Y1:   400 ,  -0.1750000  ,   0.1750000  ; INPUT z2 INITIAL CONDITION
  Y2:       ,              ,              ;
  Y3:       ,              ,              ;
  Y4:       ,              ,              ;
```

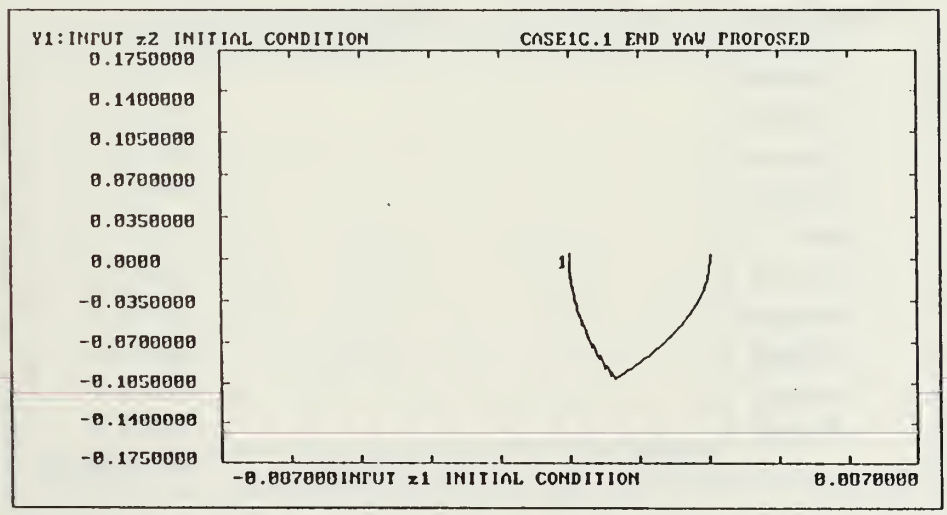

Figure 64. Proposed Case 1C.1 End of Mission

```
      BlockNo,   Plot-MINimum,   Plot-MAXimum;   Comment
Horz:     0 ,     0.0000      ,    3.0000      ; Time
  Y1:     1 ,    -0.0870000   ,    0.0870000   ; INPUT x1 INITIAL CONDITION
  Y2:   201 ,    -0.0870000   ,    0.0870000   ; INPUT y1 INITIAL CONDITION
  Y3:   401 ,    -0.0870000   ,    0.0870000   ; INPUT z1 INITIAL CONDITION
  Y4:       ,                 ,                ;
```

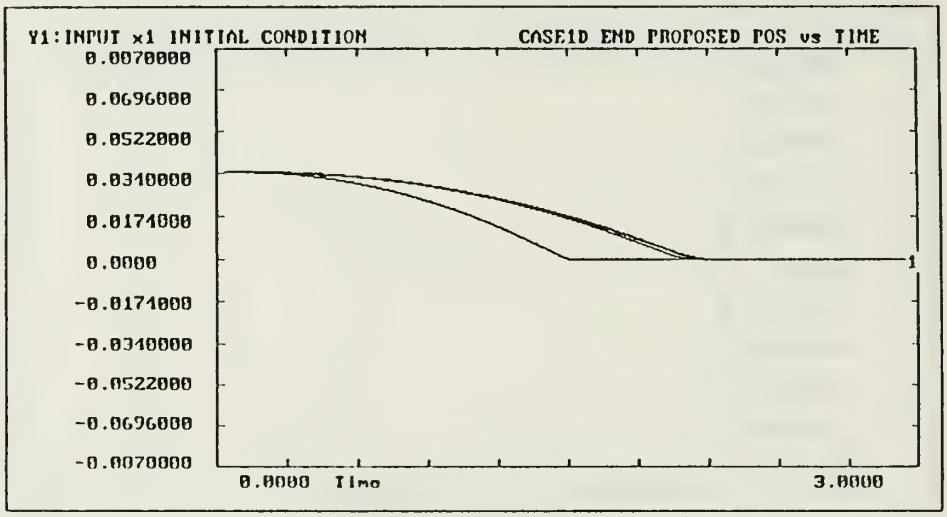


```
      BlockNo,   Plot-MINimum,   Plot-MAXimum;   Comment
Horz:     1 ,    -0.0870000   ,    0.0870000   ; INPUT x1 INITIAL CONDITION
  Y1:     2 ,    -0.0870000   ,    0.0870000   ; INPUT x2 INITIAL CONDITION
  Y2:       ,                 ,                ;
  Y3:       ,                 ,                ;
  Y4:       ,                 ,                ;
```

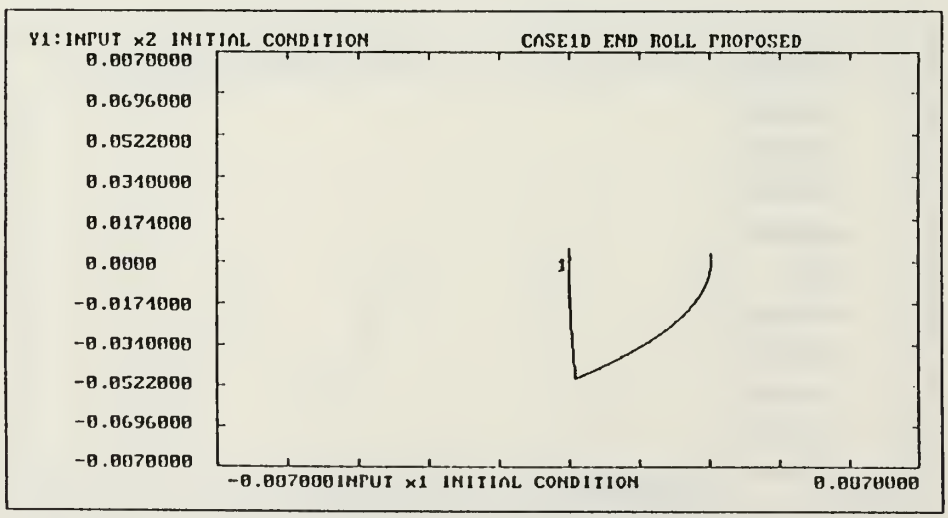

Figure 65. Proposed Case 1D End of Mission

```
      BlockNo,   Plot-MINimum,   Plot-MAXimum;   Comment
Horz:   201 ,   -0.0870000   ,    0.0870000   ; INPUT y1 INITIAL CONDITION
  Y1:   200 ,   -0.0870000   ,    0.0870000   ; INPUT y2 INITIAL CONDITION
  Y2:       ,                ,                ;
  Y3:       ,                ,                ;
  Y4:       ,                ,                ;
```

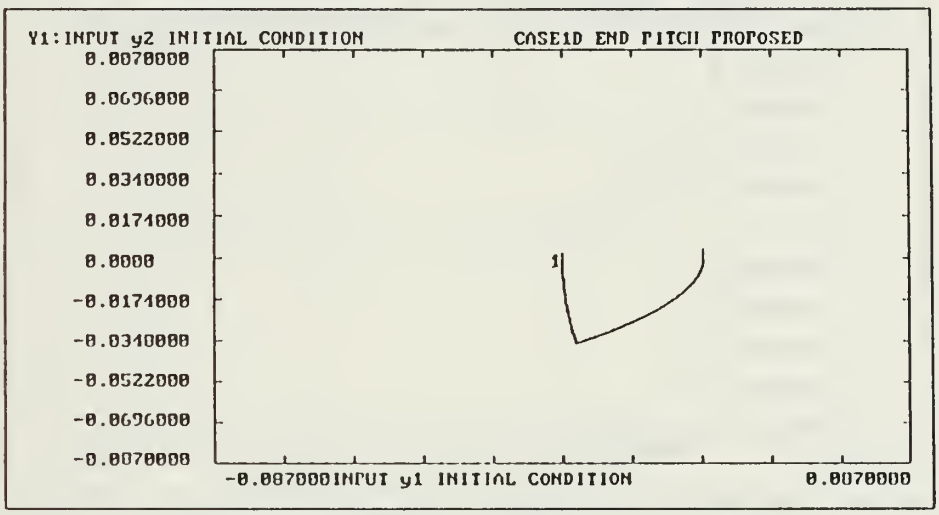


```
      BlockNo,   Plot-MINimum,   Plot-MAXimum;   Comment
Horz:   401 ,   -0.0870000   ,    0.0870000   ; INPUT z1 INITIAL CONDITION
  Y1:   400 ,   -0.0870000   ,    0.0870000   ; INPUT z2 INITIAL CONDITION
  Y2:       ,                ,                ;
  Y3:       ,                ,                ;
  Y4:       ,                ,                ;
```

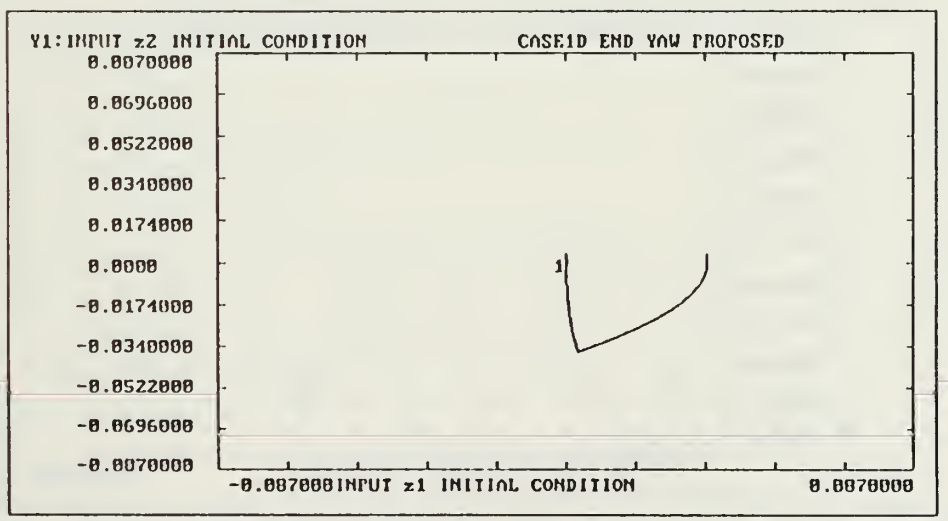

Figure 66. Proposed Case 1D End of Mission

```
      BlockNo,   Plot-MINimum,   Plot-MAXimum;   Comment
Horz:     0 ,     0.0000     ,     3.0000     ; Time
  Y1:     1 ,    -0.0870000  ,     0.0870000  ; INPUT x1 INITIAL CONDITION
  Y2:   201 ,    -0.0870000  ,     0.0870000  ; INPUT y1 INITIAL CONDITION
  Y3:   401 ,    -0.0870000  ,     0.0870000  ; INPUT z1 INITIAL CONDITION
  Y4:       ,                ,                ;
```

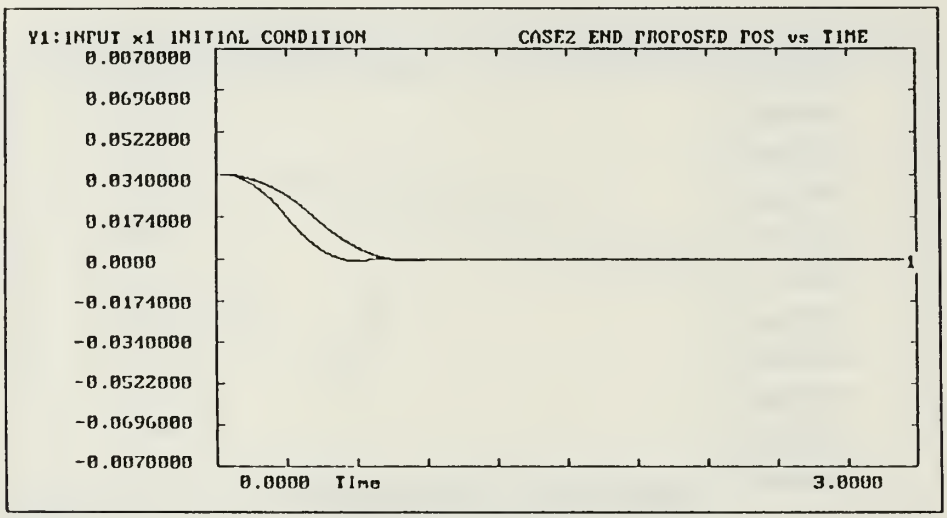


```
      BlockNo,   Plot-MINimum,   Plot-MAXimum;   Comment
Horz:     1 ,    -0.0870000  ,     0.0870000  ; INPUT x1 INITIAL CONDITION
  Y1:     2 ,    -0.1750000  ,     0.1750000  ; INPUT x2 INITIAL CONDITION
  Y2:       ,                ,                ;
  Y3:       ,                ,                ;
  Y4:       ,                ,                ;
```

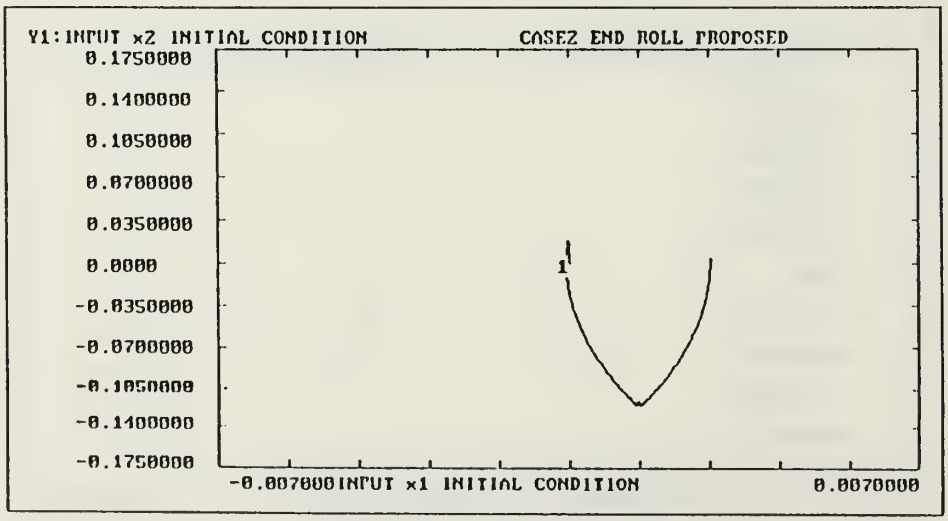

Figure 67. Proposed Case 2 End of Mission

```
     BlockNo,  Plot-MINimum,  Plot-MAXimum;  Comment
Horz:   201 ,  -0.0870000  ,   0.0870000  ; INPUT y1 INITIAL CONDITION
  Y1:   200 ,  -0.0870000  ,   0.0870000  ; INPUT y2 INITIAL CONDITION
  Y2:       ,              ,              ;
  Y3:       ,              ,              ;
  Y4:       ,              ,              ;
```

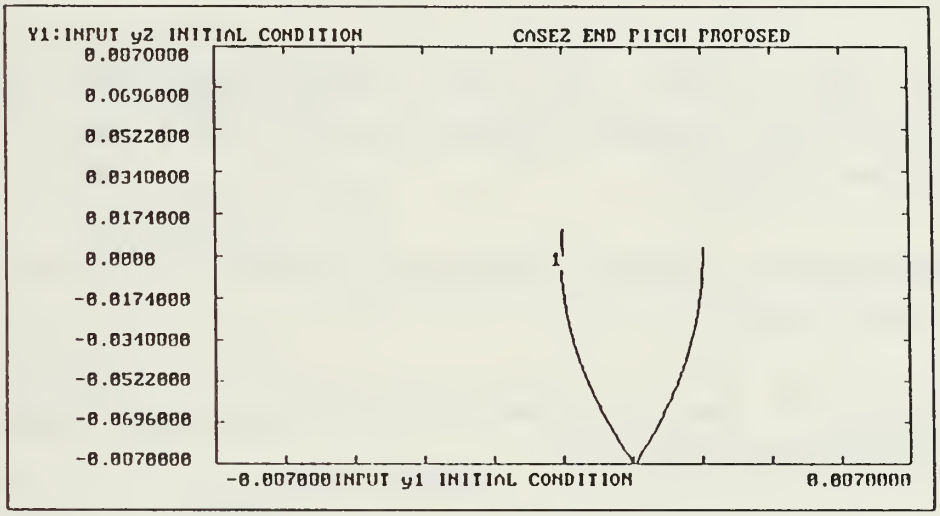


```
     BlockNo,  Plot-MINimum,  Plot-MAXimum;  Comment
Horz:   401 ,  -0.0870000  ,   0.0870000  ; INPUT z1 INITIAL CONDITION
  Y1:   400 ,  -0.0870000  ,   0.0870000  ; INPUT z2 INITIAL CONDITION
  Y2:       ,              ,              ;
  Y3:       ,              ,              ;
  Y4:       ,              ,              ;
```

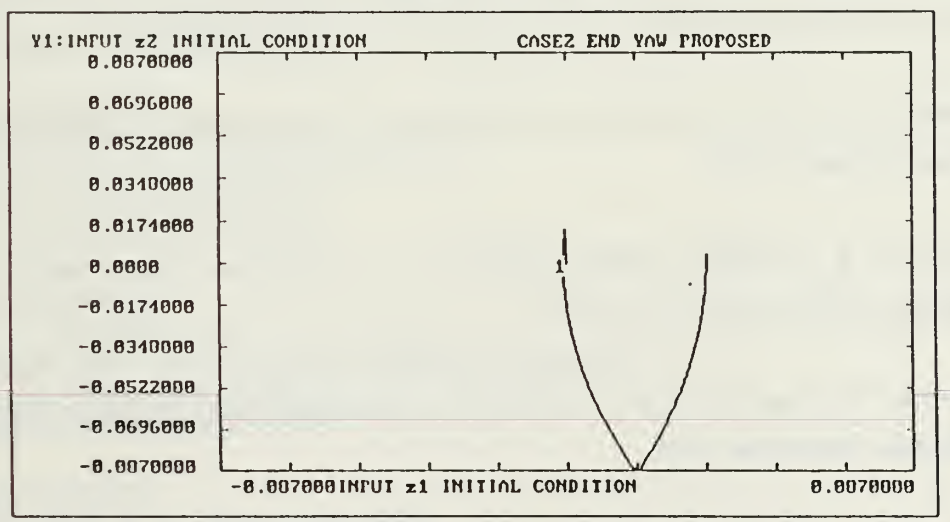

Figure 68. Proposed Case 2 End of Mission

LIST OF REFERENCES

1. *Best and Final Offer; Responses to Questions and RFP Amendment 7 Book 2*, McDonnell Douglas Astronautics Company-Space Station Division, 25 September 1987.

2. *Space Station Projects Office Work Package 2 Request for Proposal (9-BF2-51-7-1P-P01)*, National Aeronautics and Space Administration, Johnson Space Center, May 1987.

3. Hamilton, Sir W.R., *Elements of Quaternions*, pp.113-114, London: Longmans, Green and Co., 1866.

4. Wertz, James R., *Spacecraft Attitude Determination and Control*, Holland: D. Reidel Publishing Company, 1986.

5. Halliday, D. and Resnick, R., *Fundamentals of Physics* 3rd ed., pp. 236-240, Canada: John Wiley & Sons, Inc., 1988.

6. Martin Marietta Aerospace Report MMU-SE-17-46,REV A., *Manned Manuevering Unit, Space Shuttle Program User's Guide*, pp. 54-59, July 1985.

7. Goldstein. H., *Classical Mechanics*, 2nd ed., pp. 197-198, Reading, Massachusetts: Addison-Wesley, 1981.

8. Kirk, D. E., *Optimal Control Theory: An Introduction*, Prentice-Hall Inc., Englewood Cliffs, New Jersey, 1970.

9. Reynolds, W.E., and Wolf, J., *TUTSIM Users Manual*, Tutsim Products, Palo Alto, California, September 1988.

INITIAL DISTRIBUTION LIST

		No. Copies
1.	Defense Technical Information Center Cameron Station Alexandria, VA 22304-6145	2
2.	Library, Code 0142 Naval Postgraduate School Monterey, CA 93943-5002	2
3.	Commander United States Space Command Attn: Technical Library Peterson AFB, Colorado 80914	2
4.	Commander Naval Space Command Attn: Code N3 Dahlgren, Virginia 22448	2
5.	Director, Navy Space Systems Division Chief of Naval Operations (OP-943) Washington, DC 20350-2000	1
6.	Superintendent Attn: Chairman, Code 62 Department of Electrical and Computer Engineering Naval Postgraduate School Monterey, California 93943	1
7.	Superintendent Attn: Professor R. Panholzer, Code 72 Space Systems Academic Group Naval Postgraduate School Monterey, California 93943	4
8.	Superintendent Attn: Prof. Jeff B. Burl, Code 62Bl Department of Electrical and Computer Engineering Naval Postgraduate School Monterey, California 93943	2
9.	Superintendent Attn: Prof. H. A. Titus, Code 62Ts Department of Electrical and Computer Engineering Naval Postgraduate School Monterey, California 93943	1

10. Superintendent 1
Attn: Dr. George J. Thaler, Code 62Tr
Department of Electrical and Computer Engineering
Naval Postgraduate School
Monterey, California 93943

11. McDonnell Douglas Space Systems Company 1
Attn: Mr. John Harduvel
A95-J845; M S 11-3
5301 Bolsa Avenue
Huntington Beach, California 92647-2048

12. Mr C. E. Whitsett 1
NASA, Johnson Space Center
EC5
Houston, Texas 77058

13. Commander 1
Naval Air Force, U.S. Atlantic Fleet
Attn: CAPT T.C. Lackey, Code 03
Norfolk, Virginia 23511

14. Commander 1
VMFAT-101
Attn: LT Jeffrey W. Hansen
MCAS El Toro, California 92630

15. Commander 2
Helicopter Combat Support Squadron Six, LP4
Attn: LCDR Daniel L. Hansen
NAS Norfolk, Virginia 23511

NAVAL POSTGRADUATE SCHOOL
MONTEREY, CALIFORNIA 93943-5002

Thesis
H201233 Hansen
c.1 Modeling, simulation, and analyses of attitude control for the Crew/Equipment Retriever (CER) proposed for Space Station.

AMERICAN BINDERY
TOPEKA KANSAS

thesH201233
Modeling, simulation, and analyses of at
3 2768 000 81897 5
DUDLEY KNOX LIBRARY